
Bachelorarbeit

zur Erlangung des akademischen Grades Bachelor of Engineering Elektrotechnik

DESIGN AND MODELLING OF RING RESONATORS USED AS OPTICAL FILTERS FOR COMMUNICATIONS APPLICATIONS

Marcel Elshoff

Author, Hochschule Niederrhein, student register: 704065

Oscar Rautenberg

Author, Hochschule Niederrhein, student register: 696851

Dr. Paul Urquhart

Supervisor, Universidad Pública de Navarra

Prof. Dr. rer. Nat. Georg Schulte (Hochschule Niederrhein)

Tutor, Hochschule Niederrhein

Pamplona, März 2010

Abstract

This project is a theoretical study of multiple coupled ring resonators, which offer potential applications as demultiplexing filters in DWDM optical transmission systems. The rings can be fabricated as integrated optical structures or they can be formed using micro- or nano-optical fibres. Our approach is analytical, which provides detailed predictions with minimal computer resources. The ideal filter spectral profile for most applications is as close as possible to a rectangle (known as “box-like”) and in order to achieve this we design and model multiple ring resonators.

We formulate the compound ring resonator theory with complex field equations to account for phase and amplitude. Then we calculate the transfer functions. We do it in two ways: one way is using linear equations and the other is by matrix theory. We apply both methodologies to one-, two- and three-ring resonators and we show how the matrix formalism can be extended to model arrays of N identical rings.

By using the transfer functions we provide detailed physical interpretations of the spectra which are required to design good filter characteristics. We show that rings of equal circumferences provide the best profiles and we derive simple analytical formulas, called “degeneracy condition”, to predict the required coupler ratios for two- and three-ring resonators. It is thus possible to provide a transfer function with single peaks of equal and unity magnitude and a depth of modulation that we choose. Provided that the couplers within the rings conform to the degeneracy condition, we can predict the finesse of a double-ring transfer function.

We further extend the ring resonator matrix theory to N identical rings by using a method called “diagonal decomposition”. The amplitude transfer function for N rings can thus be derived with this more advanced mathematical technique. The result that we obtain is in a format that can be extended in future more extended studies.

Throughout this project our aim is to provide tangible design guidelines for compound ring resonators, with their potential application to telecommunications networks in mind.

Acknowledgement

First of all, we would like to thank our project supervisor Dr. Paul Urquhart for his support and encouragement during our time at the Universidad Pública de Navarra. We really appreciate his helpful lectures, discussions, guidance and corrections in this thesis.

We wish to thank Prof. Dr. rer. nat. Schulte, who paved the way to this project and his monitoring during the project.

We would also like to thank the European Union (Sokrates/Erasmus scholarship) and the “Förderverein des Fachbereich für Elektrotechnik und Informatik der Hochschule Niederrhein” for supporting us with a scholarship. Without the scholarship we could not have written this thesis in Spain and could not enjoy this new living and working experience.

We thank the Universidad Pública de Navarra for providing a visiting position to complete our work.

Our parents Angelika and Bernd and Monika and Winfried deserve our sincerest gratitude for their support, backup and financial aid. Without them, neither our study of electrical engineering nor this project would have been possible. Thank you for everything you have done for us.

Table of Contents

Abstract	1
Acknowledgement	2
Table of Contents.....	3
Authorship	5
1. Introduction.....	6
2. Theory of Waveguide-Based Resonant Waveguides	11
2.1 Introduction.....	11
2.2 Free Spectral Range.....	12
2.3 Optical Waveguides and Directional Couplers	13
2.4 Analysis Using Complex Fields.....	15
2.5 Matrix Formulation of Ring Resonators.....	18
2.6 Extension to Multiple Rings.....	21
2.7 Diagonal Decomposition	21
2.8 Figures of Merit: Finesse and Modulation Depth.....	25
3. Matrix Theory of Two- and Three-Ring Resonator.....	27
3.1 Introduction.....	27
3.2 Matrix Formulation	28
3.3 Matrix Formulation of a Two-Ring Resonator.....	35
3.4 Matrix Formulation of a Three-Ring Resonator	38
4. Ring Transfer Functions and Their Interpretation	41
4.1 Introduction.....	41
4.2 Single-Ring Resonator: Transfer Function	42
4.3 Single-Ring Resonator: Finesse	45
4.4 Two-Ring Resonator: Transfer Function	47
4.5 Two-Ring Resonator: Equal Circumferences	50
4.6 Two-Ring Resonator: Degeneracy Condition	57
4.7 Two-Ring Resonator: Depth of Modulation	60
4.8 Two-Ring Resonator: Finesse	65
4.9 Two-Ring Resonator: Influence of Loss	69
4.10 Three-Ring Resonator	72
4.11 Comparison of Optimised Ring Transfer Functions.....	77

5. Extension to N-Ring Resonators.....	81
6. Conclusion	89
7. Appendix A: Q-Coefficients for the Transfer Matrix	92
7.1 One-Ring Resonator.....	92
7.2 Two-Ring Resonator.....	93
7.3 Three-Ring Resonator	95
7.4 N-Ring Resonator.....	99
8. Appendix B: Derivation of Intensity Transfer Functions	101
8.1 Two-Ring Resonator.....	101
8.2 Three-Ring Resonator	104
List of References	107

Authorship

- | | |
|---|------------------|
| 1. Introduction | Marcel Elshoff |
| 2. Theory | Marcel Elshoff |
| 3. Matrix Theory of Two- and Three-Ring Resonator | Marcel Elshoff |
| 4. Ring Transfer Functions and Their Interpretation | Oscar Rautenberg |
| 5. Extension to N-Ring Resonators | Marcel Elshoff |
| 6. Conclusion | Oscar Rautenberg |
| 7. Appendix A: Q-Coefficients for the Transfer Matrix | Marcel Elshoff |
| 8. Appendix B | Oscar Rautenberg |

1 Introduction

Optical filters are crucial passive components for modern optical communications systems [1]. Micro-waveguide and fibre-based ring resonators are of great interest due to their versatile functionalities and compactness. They are being designed for different applications, such as wavelength filtering, multiplexing, switching and modulation. The most important performance characteristics of these resonators are their free spectral range (FSR), finesse (which is related to the Q-factor), depth of modulation and throughput loss. Their main design characteristics are the circumference of the rings and the coupling ratios of the couplers that they include (equivalent to the reflectivities of a Fabry-Pérot resonator).

This project is a theoretical study of multiple compound ring resonators, which are used as demultiplexing filters with optimised pass-bands for wavelength division multiplexed (WDM) transmission systems [2][3]. Our studies are specifically for dense wavelength division multiplexed (DWDM) systems [4]. The rings can be either in an integrated optical format or in a micro-/ nano- fibre format. Either one channel or a predetermined group of channels can be selected. The channels are modulated, which means each one has a spectrum and the filter must be able to cope with this; the filter profile must therefore be adapted to the intended application and its centre wavelength must coincide with the target channel. Specifically, we need a pass band that does not disturb the signal. To this end, the ideal filter spectral profile for most applications would be a rectangle (known as being “box-like”) and in order to achieve such a function we design and model multiple ring resonators. We know that in reality such a filter function is not achievable but the bell-shaped curves which are provided by single-cavity resonators could possibly truncate the propagating channel. Therefore, we require rather more advanced filter designs; a more complicated filter is needed. For this reason we have to make a compromise: A simple filter structure gives unsuitable spectra but a more complicated structure gives us better pass-bands with the disadvantage of greater physical complexity. We believe that the designs proposed in this project are a good balance between these extremes.

The work reported here is based on ring resonators. They provide periodic pass bands in the frequency domain, with a periodicity that is inversely proportional to the ring circumferences. To satisfy the needs of DWDM filtering the rings must be

miniature structures with a circumference in the range of about 100 to 1000 μm . They must be acceptably simple designs and to this end they can be fabricated in two different ways. One possibility is an integrated optical single-mode waveguide on top of a substrate, as shown in Figure 1-1, and the other is micro-/ nano- optical fibres bent to a tight coil, as shown in Figure 1-2. The outer fibres shown in Figure 1-2 might seem bizarre. Their outer diameters are comparable to the wavelength, yet they can guide light. The terminologies used are micro-fibres, when the outer diameter is similar to one wavelength and nano-fibres when they are significantly smaller.

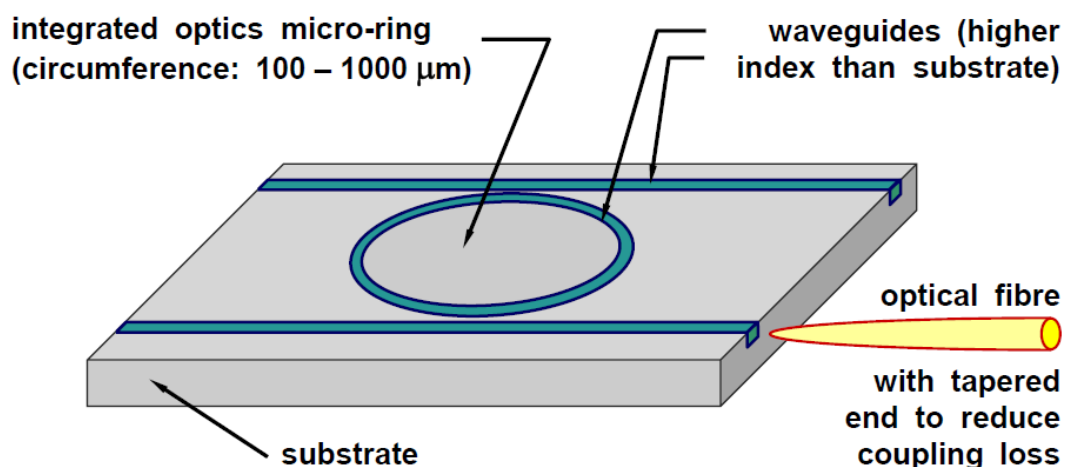


Figure 1-1 *Integrated optical single-mode waveguide ring resonator. One of the fibre connections is shown. Up to four fibres can be coupled, depending on the filter's intended application.*

Whether they are waveguide- or fibre-based, the resonators demonstrate periodic pass-bands and this determines how they are designed and applied. We could have, for example 40 DWDM channels, with the aim of accepting every tenth one and rejecting the others. Alternatively, we may require a filter that passes only channel number 7 out of a group of sixteen.

For our purposes the use of a single ring resonator is problematical. Its main difficulty is that we do not obtain a box-like function. When we consider the spectrum of a digital data stream, such as that of non-return-to-zero (NRZ) pulses, each channel has a complicated structure before it encounters the filter. If the filter provides a spectral profile that deviates significantly from being box-like, it will distort

the signal and thus adversely influence its bit error rate (BER), upon arrival at an optical receiver.

In this report we concentrate on future possible applications of compound rings for DWDM filters. However, other applications for ring structures are also possible. Compound rings can be used for fibre- or waveguide-based sensors, as well as for fibre- or waveguide-based lasers [5]. We do not explore these topics in this report because they are outside the scope of the project. Our aim is to study compound rings with a view to their use in DWDM communications but we suggest speculatively that some of the results that we provide might be of value in other contexts.

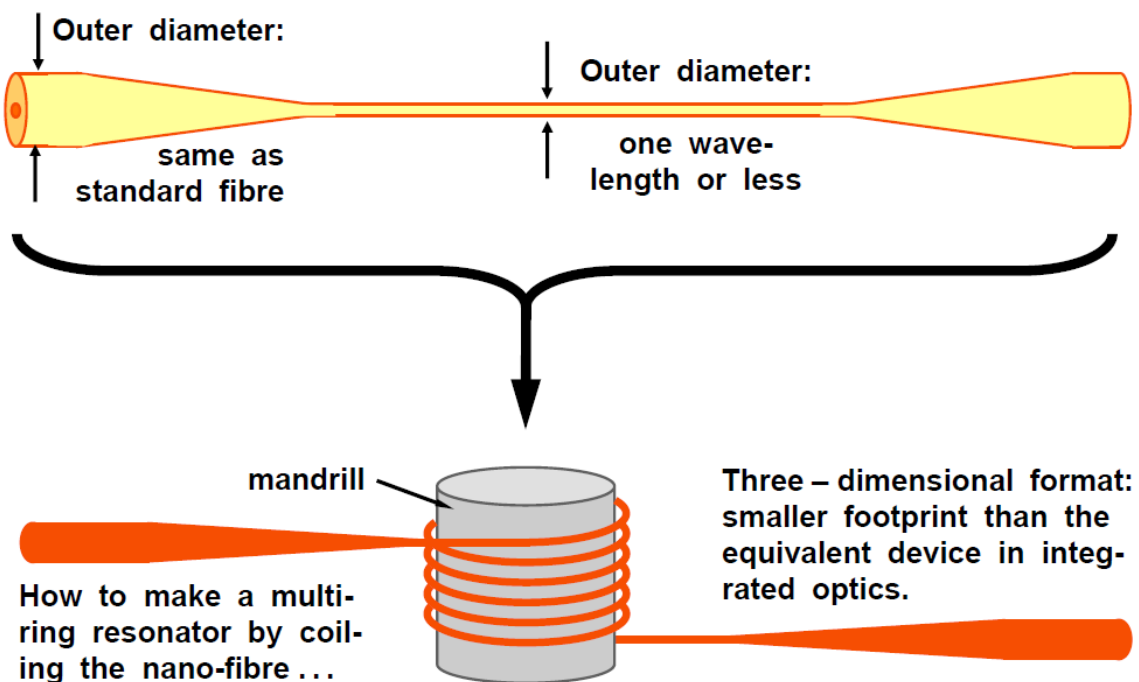


Figure 1-2 *Micro-/ nano-fibres bent to a tight coil, the radius of which determines the pass-band periodicity.*

The main categories of filters used in WDM optical communications are thin film interference filters, arrayed wave gratings (AWGs) and fibre Bragg gratings. These have all benefited from much greater research and development than microring resonators and so it is difficult to make a fair comparison. Indeed, one of the justifications for the present project is that we need a greater knowledge of the potential of compound rings to enable a fair comparison with their competitors. For

this reason we do not attempt to compare what we have achieved with other filter types. That is a task for a future project.

In this report, we develop analytical models based on linear algebra in order to develop transfer functions for compound ring resonators. The equations that we solve are in terms of complex fields because they include phase, as well as amplitude information. Where appropriate, we use matrices because they structure the algebra in a useful manner. Where analytical models are possible in engineering applications, they are particularly beneficial because they remove the need for intensive computation and demanding software. Moreover, they can often provide valuable insight into the physical processes taking place. However, when the equations become large, as in the current project, there is an ever-present risk of algebraic mistakes. For this reason, it is necessary to adopt quality control measures, as would be done in a project where large amounts of computer code is written.

Quality control is important to combat the ever-present risk of miscalculations: the resonators we consider are complicated and therefore the equations to model them are large. In order to minimise the risk, no equation has been derived by a single person without checking firstly by the same person and secondly by another. Our aim was to emulate the best practice of industrial software engineering, where all code is checked by an engineer who did not write it in the first instance. Additionally, many of the equations have been calculated by two different methods. For example, our two- and three-ring resonator algebra has been obtained by matrices and by a non-matrix method, as reported in Chapter 3. Moreover, in Chapter 5 we calculated eigenvalues by two separate ways, giving us a degree of confidence that we would not otherwise have. Although such measures have slowed down our work, we believe that it is a worthwhile sacrifice for the additional assurance that it provides.

Chapter 2 of this report states the overriding assumptions and underlying theory to understand multiple ring resonators. It explains the mathematics and physics to formulate the theory. Chapter 3 then uses the theory to derive the transfer filter functions for one-, two- and three-ring resonators. Afterwards, Chapter 4 is an extensive account with the aim of providing a comprehensive overview of how two- and three-ring resonators can best be designed as DWDM filters. Our objective was

to give an unified overview of the multi-faceted design methodology for the intended application. In addition to that, we have gone further and extend our theory to N-ring resonators. Although we were not able to obtain the intensity response, we achieved the difficult and most demanding part: we used a more advanced matrix method to provide the amplitude transfer function. Our technique is called “diagonal decomposition”, which allows N matrices to be raised to a power in an efficient manner. As a result, our calculation is in a state that can be continued by future workers.

2 Theory of Waveguide-Based Resonant Structures

2.1 Introduction

This chapter is about the physics and mathematics that are indispensable to understand the multiple ring resonator structure; it establishes the underlying theory for use in the following chapters. We describe an optical ring resonator as a filter device and its characteristics. Our formulation of the complete structure uses linear complex equations and we draw analogies with the theory of Fabry-Pérot (FP) resonators [6]. One key issue is the nature of the couplers between each ring. We discuss these by considering their characteristics, equations, losses and scattering effects and we cross-refer them to the action of the mirrors in Fabry-Pérot theory. The mathematics of multiple ring structures requires lengthy equations and so a matrix-method called diagonal decomposition is explained, to be used to extend our theory to N rings. Finally, we illustrate the way to design multi-ring resonators for an arbitrarily large number of rings.

An integrated optical ring resonator is a single transverse mode waveguide-based device formed as a circle (ring). Two couplers enable light to be inserted into and extracted from the ring. Every coupler has a coupling coefficient, which states how effectively the coupler transfers light from one waveguide to another. Commonly integrated optical ring resonators are fabricated as silica waveguides on silicon substrate but all-glass, polymer or all-semiconductor structures are also used. It is not essential that the rings be exact circles, because oval rings are also possible. High precision fabrication technologies are now available, to guarantee the best quality of the integrated waveguide so that it is a high purity material with low surface roughness. They are also fabricated very carefully to control the coupling ratios. The rings can be either in an integrated optical format or in a micro-/ nano-fibre format. A standard single mode silicate telecommunications fibre has a diameter of close to $125\mu\text{m}$. Alternatively, when the outer diameter is comparable to one wavelength, which is about $1\mu\text{m}$, we refer to it as a “micro-fibre”. When the diameter is significantly less than one wavelength, which is down to 10nm , we refer to it as a “nano-fibre”. Whether the rings are in integrated optical or micro/nano-optical format we must be able to take account of bending losses, as we will discuss later in this chapter.

2.2 Free Spectral Range

As stated in Chapter 1, optical resonators provide transmission spectra that are periodic in the frequency domain. They demonstrate narrow peaks followed by broad low transmission minima. We therefore need a measure of the frequency interval between the peaks and this is the free spectral range (FSR). The FSR for any resonator is the reciprocal round trip time of a photon in the cavity. When the resonator is an FP design, that is the time for the photon to travel from one mirror to the second mirror and back again. However, in a ring the time is for the photon to make one circuit of the fibre. The ring circumference relates directly to its FSR by

$$\Delta\nu = \frac{c}{n_{eff} \cdot L_{Ring}} \quad (2.1)$$

L_{Ring} is the circumference, c is the velocity of light in vacuum and n_{eff} is the refractive index of the waveguide, which is commonly about 1.5. As Equation (2.1) states, the FSR is a frequency difference (Hz), which is a reciprocal of time. $\Delta\nu$ is the frequency interval between the intensity maxima of the resonator's periodic transfer function. It is clear from Equation (2.1) that FSR varies inversely with circumference, which means that if we wish to achieve a wide spectral separation between the peaks of the transfer function we must use a ring with a small diameter.

We have calculated the ring circumferences with Equation (2.1). For example, we require a ring circumference of 200 μ m to achieve a FSR of 1000GHz. In a DWDM system, where the channels are commonly positioned every 100GHz (corresponding to about 0.8nm), such a ring would allow us to select every tenth channel [7]. Alternatively, we would need a ring circumference of 400 μ m to obtain a FSR of 500GHz. Hence we can conclude that the larger the FSR becomes, the smaller the circumference required. Unfortunately, from the industrial point of view there is a limit for the ring circumference because very small rings have significant bending loss. For this reason, instead of making the ring smaller, we can use multiple rings to achieve better filtering functions. We can fabricate a multiple-ring resonator, by coiling micro- or nano-fibre on a mandrill or by appropriate patterning of integrated optical waveguides on a substrate.

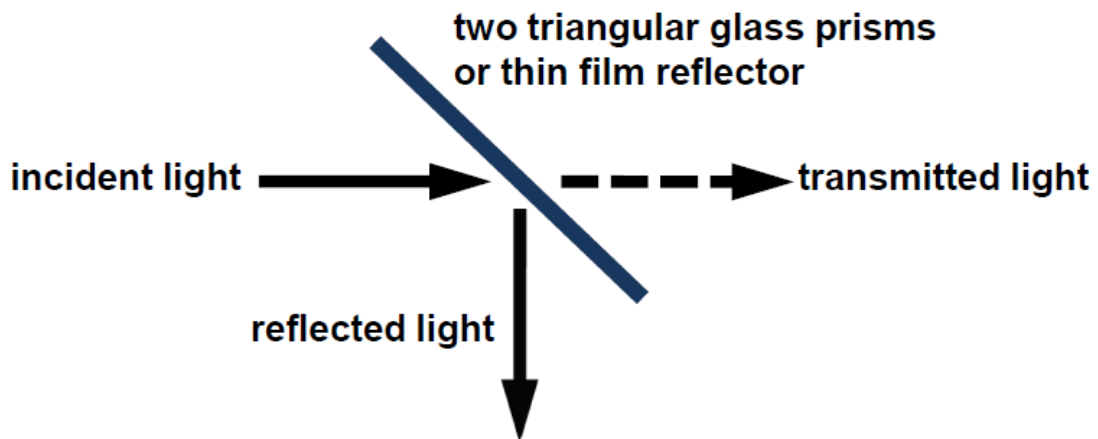


Figure 2-1 Optical device: Beam-splitter.

2.3 Optical Waveguides and Directional Couplers

Every ring considered in this project has two optical directional couplers, where light can be launched or leave the ring. The coupler is the equivalent of the beam splitter, which is depicted in Figure 2-1. The beam splitter is an optical component that splits a beam of light. A part of the incident light is reflected, the other part is transmitted. The coupling-ratio of the reflected and transmitted light is determined by the detailed geometry of the coupling zone of the coupler.

A coupler is a four port device, as illustrated in Figure 2-2. The waveguides shown have a higher refractive index than the substrate, which often consists of glass, but silicon can also be used. Usually light is only launched into one port, but in certain applications, such as optical add-drop multiplexers (OADM), it can be launched into more than one. The waveguides in the drawing are rectangular, but the coupler operation is also valid for the curved waveguides that we consider. As we can see, the only difference between the two is in the coupling zone. The distance between the rectangle waveguides is always the same, while the distance between curved waveguides varies continuously. In a directional coupler there is a transverse overlap of the fields in the coupling zone so that there is transfer of energy from one waveguide to the other. The detailed theory of directional couplers is complicated, especially when the geometry differs from the simple one shown in Figure 2-2. However, a detailed knowledge of the wave interactions that take place within the couplers is not necessary because all of the essential features can be summarised

within two macroscopic parameters: one is the coupling coefficient K and the other is the loss coefficient γ . Both of them are dimensionless and they are obtained from detailed solutions of Maxwell's equations, usually with the aid of computer-based numerical techniques.

In the general case, we have to deal with loss in couplers. Light scattering and small bending within our couplers are the main mechanisms. Furthermore, the waveguides that interconnect our couplers must be curved, and so we have to incorporate bending, scattering and absorption loss of the propagating waves. The bending losses appear because the propagation conditions alter at a bend. The rays of light, which would propagate axially in a straight section, are lost into the cladding (of a fibre) or the substrate (of a planar waveguide). Due to this fact, the bending loss increases markedly with decreasing ring circumferences. Therefore, the best fabrication technologies available are needed to produce good waveguides and couplers. Techniques such as the use of non-step-index profiles and high waveguide-substrate refractive index differences can help in this respect. We achieve the best ring geometry with the lowest loss, when the two bent waveguides have the same arc radius and when there is always the same distance between them. Moreover, the quality of the material, the waveguide is made of, is an important factor. Depending on how pure the material is, we obtain low absorption loss. Any surface roughness of the waveguide as the result of certain fabrication techniques causes unwanted micro-bending and scattering.

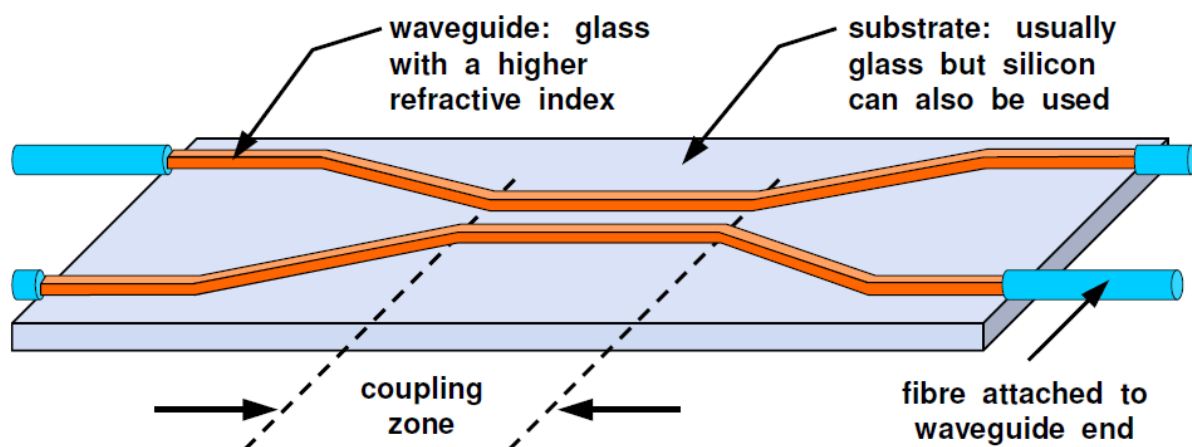


Figure 2-2 *Integrated optical directional coupler shown in simple rectangular geometry. Many other designs are also possible.*

2.4 Analysis Using Complex Fields

The electric field analysis that is used for the coupler and waveguide propagation theory includes phase. We use complex fields because phase characteristics are indispensable to obtain a realistic model of ring resonators. One computational challenge is that the complex field equations require more algebraic manipulation than would be the case with real quantities. In order to explain the waveguide and coupler equations we need some definitions:

$$\delta_{j,k} = \left(\frac{-\alpha}{2} + i \cdot \beta \right) \cdot L_{j,k} \quad (2.2)$$

Bending, scattering and absorption losses of the waveguides are defined in the α -coefficient, called loss-coefficient. Its unit is 1/L (reciprocal meters in the SI usage) and we can also vary it into dB/L because normally loss is specified in dB. The β -coefficient is the propagation constant of the waveguides and we assume that it is the same throughout the entire device. Generally we can say that α and β account for the amplitude and phase changes, respectively. $L_{j,k}$ is one passage in the cavity of a FP resonator. A double passage in the cavity of a FP resonator is the equivalent of one optical circuit in the ring, which is stated in the equation $L_{\text{Ring}} = 2 \cdot L_{\text{Cavity}}$. The definition of the waveguide's propagation constant β , with $n_{\text{effective}}$ as its effective refractive index:

$$\beta = \frac{2 \cdot \pi \cdot n_{\text{effective}}}{\lambda} \quad (2.3)$$

The propagation constant of the free space is the same, except that $n_{\text{effective}} = 1$.

The terms that we use to describe the action of a coupler are:

$$r_m = (1 - K_m)^{\frac{1}{2}} \cdot (1 - \gamma_m)^{\frac{1}{2}} \quad (2.4)$$

$$t_m = i \cdot K_m^{\frac{1}{2}} \cdot (1 - \gamma_m)^{\frac{1}{2}} \quad (2.5)$$

K_m and γ_m are the coupling ratio and the coupler excess loss, respectively. Commonly γ_m is very small and it can be ignored in some circumstances. r_m and t_m are their equivalents in the FP theory, where r_m is the reflectance of the mirror and t_m is its transmittance, as shown in Figure 2-3. They relate to each other as $r_m = 1-t_m$. Based on the FP theory we refer to the “effective” transmittance and reflectance of couplers.

Figure 2-3 shows a single ring resonator and a Fabry-Pérot cavity for comparison. The reference points m and n are marked on the rings in which m is the coupler number and n is the coupler’s input-output point 1,2,3 or 4, going in a clockwise direction. Reference points j and k refer to the length of the equivalent FP cavity in which j is the first mirror number and k is the second mirror number, i.e. the length from mirror “0” to mirror “1” is defined as $L_{0,1}$.

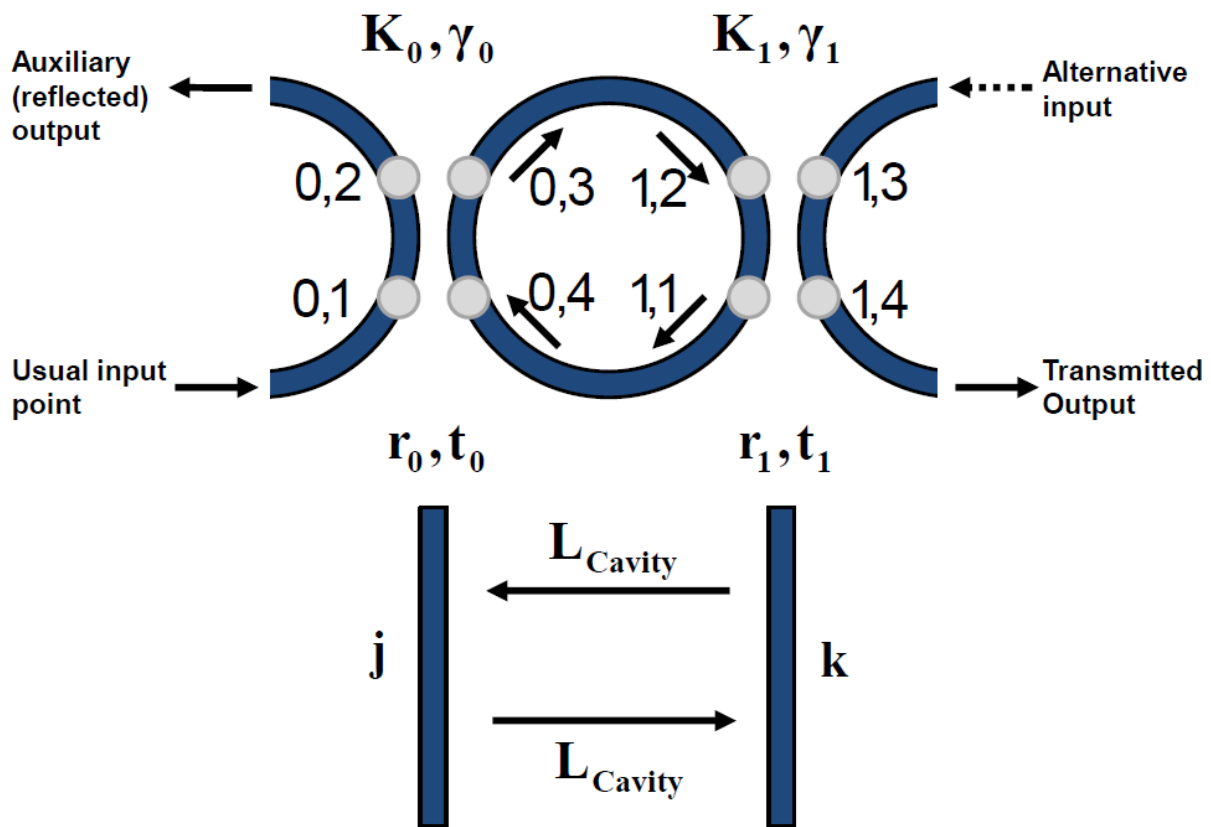


Figure 2-3 One ring resonator (top) and the equivalent two-mirror Fabry-Pérot resonator (below).

As we have seen, we always have four reference points for every coupler. Therefore, in general eight equations are needed because light can propagate in two directions at every point: forwards and backwards. According to this, in the most general circumstances, we have 16 equations for a single ring resonator, 24 equations for a two-ring resonator and 32 equations for a three-ring resonator because we need 2, 3 and 4 couplers, as appropriate. Fortunately, our physical knowledge of light propagation within ring resonators provides some simplification. When light is launched only via the “usual input point”, marked on the bottom left of the ring resonator on Figure 2-3, the waves circulate clockwise within the ring, as shown by the arrows. We can then halve the number of initial field equations so that only 8 are required for a single ring. By similar reasoning, the number needed for two- and three-ring resonators are 12 and 16, respectively.

We now state the four important equations needed to describe a coupler and afterwards a single ring:

$$E_{0,1}^+ = input \quad (2.6)$$

$$E_{0,2}^- = r_0 \cdot E_{0,1}^+ + t_0 \cdot E_{0,4}^- \quad (2.7)$$

$$E_{0,3}^+ = r_0 \cdot E_{0,4}^- + t_0 \cdot E_{0,1}^+ \quad (2.8)$$

$$E_{0,4}^- = E_{1,1}^- \cdot e^{\delta_{1,0}} \quad (2.9)$$

$E_{m,n}$ are the complex field components, where “+” and “-” specify the direction of the light propagation. “+” is the forward propagation from left side to the right, “-” is the backward propagation the right side to the left. $E_{0,1}^+$ is the known input. $E_{0,2}^-$ is a possible output because light from input $E_{0,1}^+$ can be coupled out of the ring at this point, which is the equivalent of a reflection from a FP cavity. In addition, there is transmitted light from $E_{0,4}^-$. $E_{0,3}^+$ is the output of the coupler that propagates towards the right. Light that has made one or more circuits of the ring re-enters the coupler as the field term $E_{0,4}^-$. Equation (2.9) includes an exponential term in $\delta_{1,0}$ and this is needed to account for phase and amplitude changes due to propagation in a

waveguide of length $L_{1,0}$. It should also be noted that, according to Equations (2.4) and (2.5) r_0 is real but t_0 is imaginary.

In order to formulate the complete structure for a single ring resonator, we also need the equations for the second coupler, shown on the top right of Figure 2-3. Additionally to the four Equations (2.6) to (2.9), we obtain the following four Equations to describe a single ring:

$$E_{1,1}^- = r_1 \cdot E_{1,2}^+ + t_1 \cdot E_{1,3}^- \quad (2.10)$$

$$E_{1,2}^+ = E_{0,3}^+ \cdot e^{\delta_{0,1}} \quad (2.11)$$

$$E_{1,3}^- = E_{1,3}^- \quad (2.12)$$

$$E_{1,4}^+ = r_1 \cdot E_{1,3}^- + t_1 \cdot E_{1,2}^+ \quad (2.13)$$

$E_{1,1}^-$ consists of the transmitted light from reference point (1,3) and the reflected light from (1,2). $E_{1,2}^+$ is the light from point (0,3) which propagates in the waveguide in “+” direction and it includes the term $e^{\delta_{0,1}}$ to account for the associated amplitude and phase change. $E_{1,3}^-$ can be another input, but usually it is zero. $E_{1,4}^+$ is the transmitted light from point (1,2) and the reflected light from point (1,3).

2.5 Matrix Formulation of Ring Resonators

As we can see, Equations (2.6) - (2.13) are the 8 equations for a single ring resonator, to which we previously referred. If we want to calculate a two-ring resonator, we need 12 equations, with a corresponding increase in algebraic manipulation. (The theory of a two-ring resonator is formulated in Section 3.3 and the interpretation of the final result is described in Chapter 4.) Therefore, we decided to use matrices because they are able to regiment and organize equations in a structured way that can be handled by well-known techniques. When we started this part of our project we did not know if matrix theory would work or be easier. However,

it seemed a logical approach for a series of linear equations, which model passive optical processes that have no gain.

In order to obtain the matrix for one ring, we use the Equations (2.6) – (2.13) to start our calculation. Equation (2.7) is substituted into Equation (2.9) and (2.10) to give:

$$E_{0,2}^- = t_1 \cdot t_2 \cdot E_{1,3}^- \cdot e^{\delta_{1,0}} + t_1 \cdot r_2 \cdot E_{1,2}^+ \cdot e^{\delta_{1,0}} + r_1 \cdot E_{0,1}^+ \quad (2.14)$$

$E_{1,3}^-$ and $E_{0,1}^+$ are needed in our calculation because they present our input vector. The output vector is formed by $E_{0,2}^-$ and $E_{1,4}^+$. Thus we have to eliminate $E_{1,2}^+$ by substituting Equations (2.8), (2.9) and (2.10) into Equation (2.11). Thereafter, the terms are grouped together and rearranged so that $E_{1,2}^+$ is on the left side and we obtain:

$$\begin{aligned}
 E_{1,2}^+ &= \frac{t_1}{1 - r_1 \cdot r_2 \cdot e^{\delta_{0,1} + \delta_{1,0}}} \cdot E_{0,1}^+ \cdot e^{\delta_{0,1}} \\
 &+ \frac{r_1 \cdot t_2}{1 - r_1 \cdot r_2 \cdot e^{\delta_{0,1} + \delta_{1,0}}} \cdot E_{1,3}^- \cdot e^{\delta_{0,1} + \delta_{1,0}}
 \end{aligned} \quad (2.15)$$

Then we substitute Equation (2.15) into (2.14) and group again the terms together so that we obtain:

$$\begin{aligned}
 E_{0,2}^- &= \left\{ \frac{r_1 + r_2 \cdot t_1^2 \cdot e^{\delta_{0,1} + \delta_{1,0}}}{1 - r_1 \cdot r_2 \cdot e^{\delta_{0,1} + \delta_{1,0}}} \right\} \cdot E_{0,1}^+ \\
 &+ \left\{ \frac{t_1 \cdot t_2 \cdot e^{\delta_{1,0}}}{1 - r_1 \cdot r_2 \cdot e^{\delta_{0,1} + \delta_{1,0}}} \right\} \cdot E_{1,3}^-
 \end{aligned} \quad (2.16)$$

Equation (2.16) can also be stated as:

$$E_{0,2}^- = a_{11} \cdot E_{0,1}^+ + a_{12} \cdot E_{1,3}^- \quad (2.17)$$

The two coefficients of the electric fields in Equation (2.16) are the definitions of a_{11} and a_{12} and they are required to specify the transfer matrix. We need two other coefficients, designated a_{21} and a_{22} to be incorporated within the matrix. Generally, it is the same type of calculation with other equations. Therefore, we do not state every Equation and only describe the procedure and the final results. Equation (2.9) and (2.13) are used as the initial equations and the input and output vectors are the same. $E_{1,3}^-$ and $E_{0,1}^+$ are known, so we substitute every other term that appears in the equations by the other equations, (2.6) – (2.13). Thereafter, the equations are rearranged as before so that Equation (2.9) can be substituted into (2.13). Thus we obtain:

$$\begin{aligned}
 E_{1,4}^+ &= \left\{ \frac{t_1 \cdot t_2 \cdot e^{\delta_{0,1}}}{1 - r_1 \cdot r_2 \cdot e^{\delta_{0,1} + \delta_{1,0}}} \right\} \cdot E_{0,1}^+ \\
 &+ \left\{ \frac{t_2 + r_1 \cdot t_2^2 \cdot e^{\delta_{0,1} + \delta_{1,0}}}{1 - r_1 \cdot r_2 \cdot e^{\delta_{0,1} + \delta_{1,0}}} \right\} \cdot E_{1,3}^-
 \end{aligned} \quad (2.18)$$

Equation (2.19) can also be stated as:

$$E_{1,4}^+ = a_{21} \cdot E_{0,1}^+ + a_{22} \cdot E_{1,3}^- \quad (2.19)$$

We now have calculated a_{21} and a_{22} and therefore all the expressions that are needed for the matrix for a single ring resonator. In general, we have the matrix:

$$\begin{bmatrix} E_{0,2}^- \\ E_{1,4}^+ \end{bmatrix} = \begin{bmatrix} a_{11} & a_{12} \\ a_{21} & a_{22} \end{bmatrix} \cdot \begin{bmatrix} E_{0,1}^+ \\ E_{1,3}^- \end{bmatrix} \quad (2.20)$$

The mathematics is slightly complicated by the need for complex numbers, which give us the ability to account for phase as well as amplitude changes. Even for

a single ring resonator it is not straightforward and multiple ring structures become yet more demanding.

2.6 Extension to Multiple Rings

In order to achieve better filtering functions we want to model multiple ring resonators because we assume that they will give us more design possibilities to find our desired “box-like” functions. They provide coupled resonances and, being more complicated structures, they have more independently adjustable parameters, giving greater design flexibility. We use matrices because they simplify the calculations of our linear equations and we have done this in two ways. The first is an extension of the formulation that leads to Equation (2.20) to be applied to two or more rings, in which all of the constituent parameters, such as ring circumferences and coupler ratios can have individually adjustable values. Further details are provided in Chapters 3 and 4. The second extension is to a special case in which all of the rings are identical and therefore we need repeated application of the transfer matrix for each of the constituent rings. This issue is addressed further in Chapter 5. The matrix methodology used for resonators of N identical rings is called “diagonal decomposition”. It provides us with a computationally efficient means of raising a matrix to a power. Every matrix models one ring. As we can see from the Equations (2.16) and (2.19), which show the matrix for the single ring, the algebra is very demanding. Therefore, we avoid the direct multiplication of matrices for ring numbers in excess of three and instead we use the “diagonal decomposition”.

2.7 Diagonal Decomposition

We do not explain underlying the theory of “diagonal decomposition” (DD) in great detail but the reader is referred to numerous linear algebra texts, such as References [8][9]. The DD is used to raise a non-singular square matrix to a power. It is an important constraint that we only can raise pairs of rings to the power of N . Figure 2-4 depicts a multiple ring resonator for N rings showing the alternating clockwise and counter-clockwise optical propagation. We always obtain such alternating circuits if we use more than one ring. Different matrices are required for the two propagation directions and we can designate them A_R (“right”) and A_L (“left”). Given that DD operates on identical matrices, we must use the technique on the

product matrix $A = A_L \cdot A_R$ for an adjacent pair of rings. DD allows us to calculate $A^N = (A_L \cdot A_R)^N$, for an integer N.

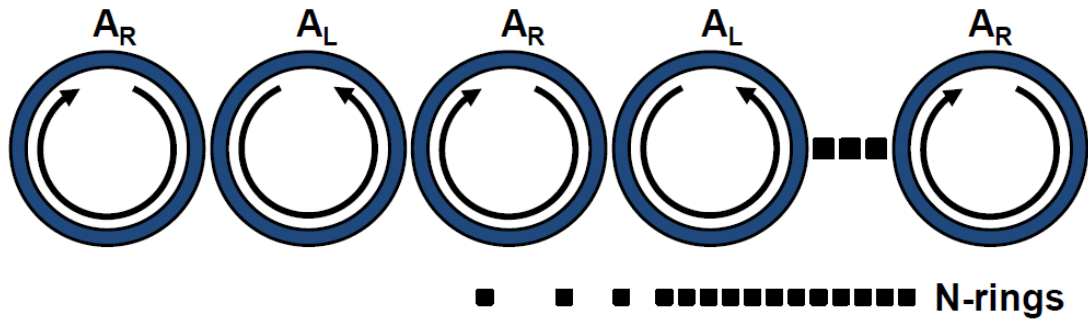


Figure 2-4 Multiple ring resonators with N-rings; although the rings are identical, the guided waves circulate alternately, which is why we need two types of matrices, A_R and A_L .

By using the DD we raise the matrices representing a two-ring resonator structure to the power of N, which means we can calculate the transfer matrix for 2^N rings. We now describe in general terms how to raise the square matrix A to the power of N. At first, the concept of “similar matrices” is needed. The matrices A and D, which are non-singular square matrices, are similar if another non-singular square matrix P can be found so that we obtain:

$$D = P^{-1} \cdot A \cdot P \tag{2.21}$$

We select D to be a diagonal matrix, which is one where all elements that are not on the leading diagonal are zero. P^{-1} is the inverse of P and it is also non-singular. Similar matrices have some advantageous properties, such as the same determinant, the same rank and the same eigenvalues. Our goal is to find a matrix P that makes Equation (2.21) is valid. We premultiply Equation (2.21) by P and postmultiply it by P^{-1} so that we have:

$$A = P \cdot D \cdot P^{-1} \tag{2.22}$$

Thus we can easily raise A to an integer power:

$$A^N = (P \cdot D \cdot P^{-1}) \cdot (P \cdot D \cdot P^{-1}) \dots (P \cdot D \cdot P^{-1}) \quad (2.23)$$

Then we factor out the diagonal matrix D:

$$A^N = P \cdot D \cdot (P^{-1} \cdot P) \cdot D \cdot (P^{-1} \cdot P) \cdot D \dots (P^{-1} \cdot P) \cdot D \cdot P^{-1} \quad (2.24)$$

And we identify $P^{-1} \cdot P$ as the identity matrix I, so that Equation (2.24) can be stated as:

$$A^N = P \cdot D^N \cdot P^{-1} \quad (2.25)$$

This result signifies that if a diagonal matrix similar to A is identified, together with a suitable non-singular matrix P, it is much simpler to raise A to the power of N. The reason is that a diagonal matrix can be raised to the power of N merely by raising all of the elements in the leading diagonal to the power of N.

We do not explain every step of the diagonal decomposition in detail. However, the basic ones are summarised in the Figure 2-5, which indicates the order in which they are most appropriately carried out. Figure 2-5 is really a “recipe”, the detailed justification for which can be obtained by consulting many text-books on linear algebra [10][11].

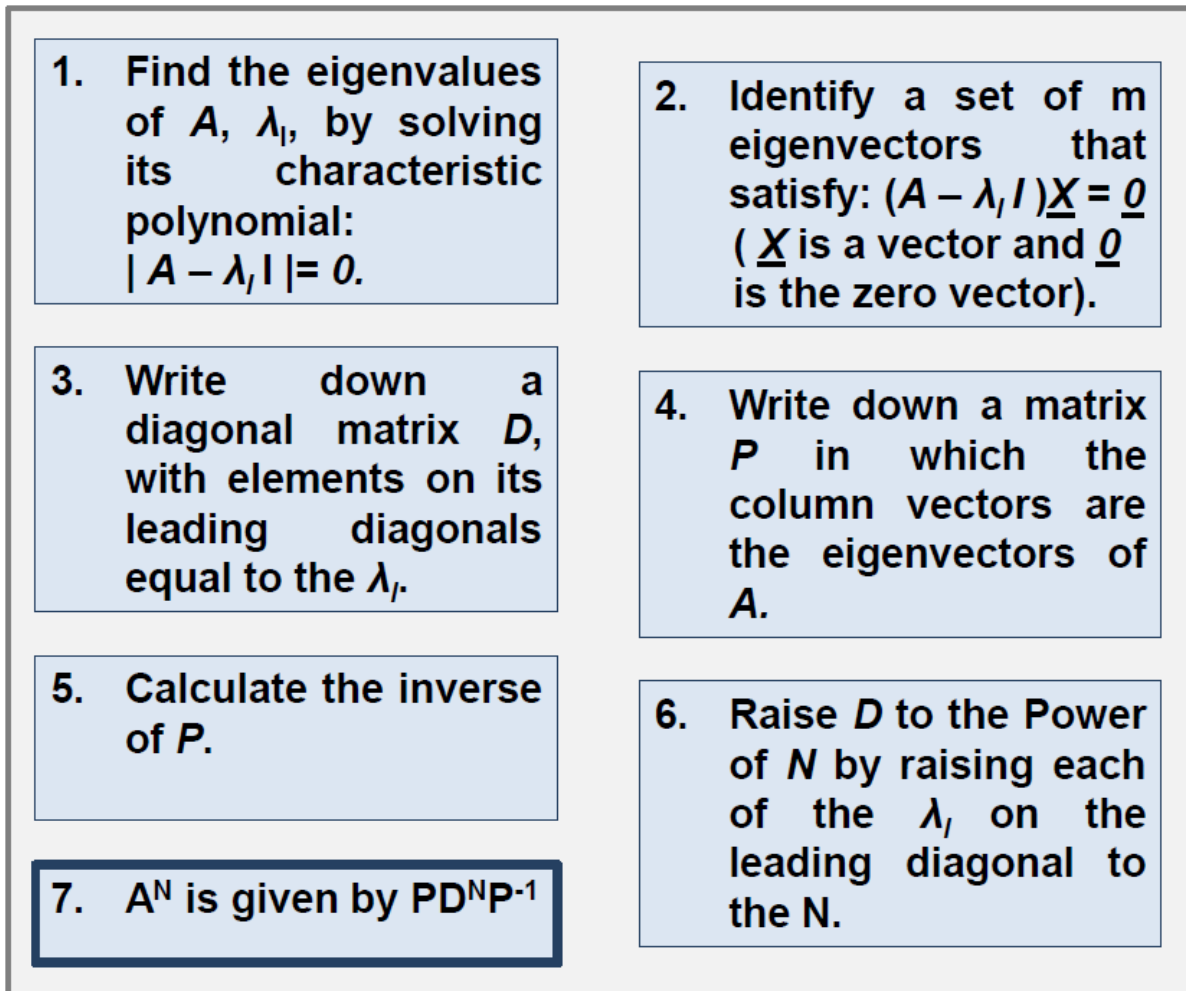


Figure 2-5 The diagonal decomposition algorithm for raising a matrix A to the power of N .

A brief summary of Figure 2-5 is as follows. When A is an $m \times m$ matrix, we have up to m eigenvalues $\lambda_1, \lambda_2, \dots, \lambda_m$ and for each one an eigenvector can be selected, where the m eigenvectors are linearly independent of each other. The eigenvalues are defined as λ_i , the eigenvectors are stated as \underline{X} and $\underline{0}$ is the zero vector. P is also an $m \times m$ matrix. As we can see in Figure 2-5, first of all the eigenvalues of matrix A are determined from the characteristic polynomial. By substituting λ_i in turn into the Equation from step 1, we find the suitable eigenvectors. In the third step the diagonal matrix is written down. Afterwards, we formulate matrix P and the inverse of matrix P in steps 4 and 5. In the following step we raise D to the power of N by raising each element on its leading diagonal to the power of N .

The technique summarised in Figure 2-5 will help us in Chapter 5 for raising a matrix to a power. It is worth all the effort because if we look at our equations for a

single ring resonator and we imagine raising it to the power of 4 or higher, we would have to solve prohibitively large equations. In addition, we have to calculate with complex numbers.

2.8 Figures of Merit: Finesse and Modulation Depth

Once we have determined the transfer function for a given design of resonator, we need to specify a number of figures of merit that quantify its filtering function. In doing this we assume that it has been possible to obtain a periodic transfer function in which there are single peaks that can in some sense be described as being “box-like”. The ideal means to provide such performance is via a closed-form analytical formula. However, owing to the complicated nature of the algebra, such formulas are not easily derived for resonators consisting of large numbers of rings. In that case, some form of numerical means is necessary to provide us with appropriate filtering performance. Thereafter, we need our figures of merit to decide how good the filter is for the various tasks that it might perform. Many figures of merit could be defined but the two that we use in this report, especially in Chapter 4, are (a) the finesse and (b) the depth of modulation.

The finesse is a measure of the resonator’s frequency selectivity. Generally, finesse is more commonly used in optics than in microwaves and electronic circuits, where the quality factor (“Q-value”) is preferred. The finesse is defined as the filter’s free spectral range (FSR) divided by the 3dB bandwidth of the peaks, as given by Equation (2.26), where $\Delta\nu$ and $\delta\nu_{1/2}$ are both frequency intervals (Hz).

$$F = \frac{\Delta\nu}{\delta\nu_{1/2}} \quad (2.26)$$

High values of F correspond to very narrow peaks. In many applications of single resonators, such as the Fabry-Pérot designs, it is preferable, to aim for the highest values of F in order to achieve very selective filters. However, as described in Chapter 1, high finesse operation can sometimes be a disadvantage. A quasi-rectangular pass-band with good rejection at other frequencies might be a more desirable attribute and this is what we mean by “box-like” performance.

The finesse can be determined mathematically for single resonant structures, where it is a function only of the reflectances (actual or effective) of the mirrors or couplers, as the case may be. High finesses are achieved by using reflectances that are as close as possible to unity and reducing all losses (both the reflectors and propagation medium between the reflectors) to being as close as possible to zero.

When we have obtained a transfer function with single, periodic and box-like peaks, we can easily define a depth of modulation, $M^{(dB)}$, in which the superscript signifies the fact that parameter is most conveniently specified in decibels. If we define the relative peak intensity of the transfer function to be Y_{max} and the relative minimum intensity to be Y_{min} , the depth of modulation is quite simply

$$M^{(dB)} = 10 \cdot \log_{10}[Y_{max} / Y_{min}] \quad (2.27)$$

$M^{(dB)}$ is useful for optical network design purposes because it specifies the out-of-band rejection and it is a number that should normally be as high as possible. When $M^{(dB)}$ is too low, adjacent optical channels are passed by the ring resonator and when they arrive at the receiver, together with the intended channels, they cause optical cross-talk. For this reason, the depth of modulation is a particularly important figure of merit. There is no simple guideline that specifies the minimum acceptable value of $M^{(dB)}$ because every optical telecommunications network is different. However, it would be unusual for values lower than 30dB to be tolerable and 40dB might be a more realistic design target.

3 Matrix Theory of Two- and Three-Ring Resonators

3.1 Introduction

This chapter explains the general matrix formulation for a single ring resonator and the complete matrix-method for two- and three-ring resonators. A matrix method was used to calculate the amplitude transfer function for multiple ring resonators. The matrix approach continues to use complex electric fields but it differs from that of Oscar Rautenberg; it is used to obtain the same results in another way. Losses were included in the formulation, as explained in Chapter 2. Solving equations for more than two rings becomes very complicated and therefore possibly subject to algebraic mistakes. This is why it was necessary to resort to a systematic matrix-based approach to regiment the algebra in a manner that reduces the likelihood of mistakes. By using our more extended technique, we learn about the different aspects of the two- and three-ring structure in order to be able to apply it to N-rings and to establish a general procedure.

The methodology explained in this chapter is necessary to calculate more than about four rings and we extend it in Chapter 5, where we explain how to multiply N identical matrices using “diagonal decomposition”. For two and three rings the diagonal decomposition technique is not worthwhile. However, it would be unrealistic to calculate the intensity transfer function for ten rings with the methodology used here. The equations would be too large and not practical without computer algebra. Therefore, in this Chapter we calculate the one, two and three-ring resonator with the simple technique, and in Chapter 5 we use the diagonal decomposition to calculate more than three-rings. This chapter forms a link with Chapter 4, in which we interpret the final results (the transfer functions) and explain how they can enable the design of filters for applications as wavelength demultiplexers.

In order to present the matrix formulation for a ring resonator, we made some assumptions, which are entirely consistent with both physical reasoning and the findings of Chapters 2 and 4. If we look at a ring resonator, we see that light propagates unidirectionally; it travels in each ring either clockwise or counter-clockwise and our equations simulate this behavior. However, our assumption depends on the absence of certain physical processes, the most important of which

are Raman, Brillouin and Rayleigh light scattering because they create backward-propagating waves. Furthermore, we assume that there is no gain due to the presence of rare earth ions, such as erbium. All lightwaves are taken to be randomly polarised and none of the waveguides or couplers demonstrate polarization anisotropy.

The general matrix formulation is explained in Section 3.2. Thereafter, we apply it to the two- and three-ring resonator in Sections 3.3 and 3.4, respectively.

3.2 Matrix Formulation

We consider a one-ring resonator and two couplers to determine the matrix for a single ring, as illustrated in Figure 3-1. Reference points m, n are marked on the rings in which m is the coupler number and n is the coupler’s input-output point: 1, 2, 3 or 4, going in a clockwise direction.

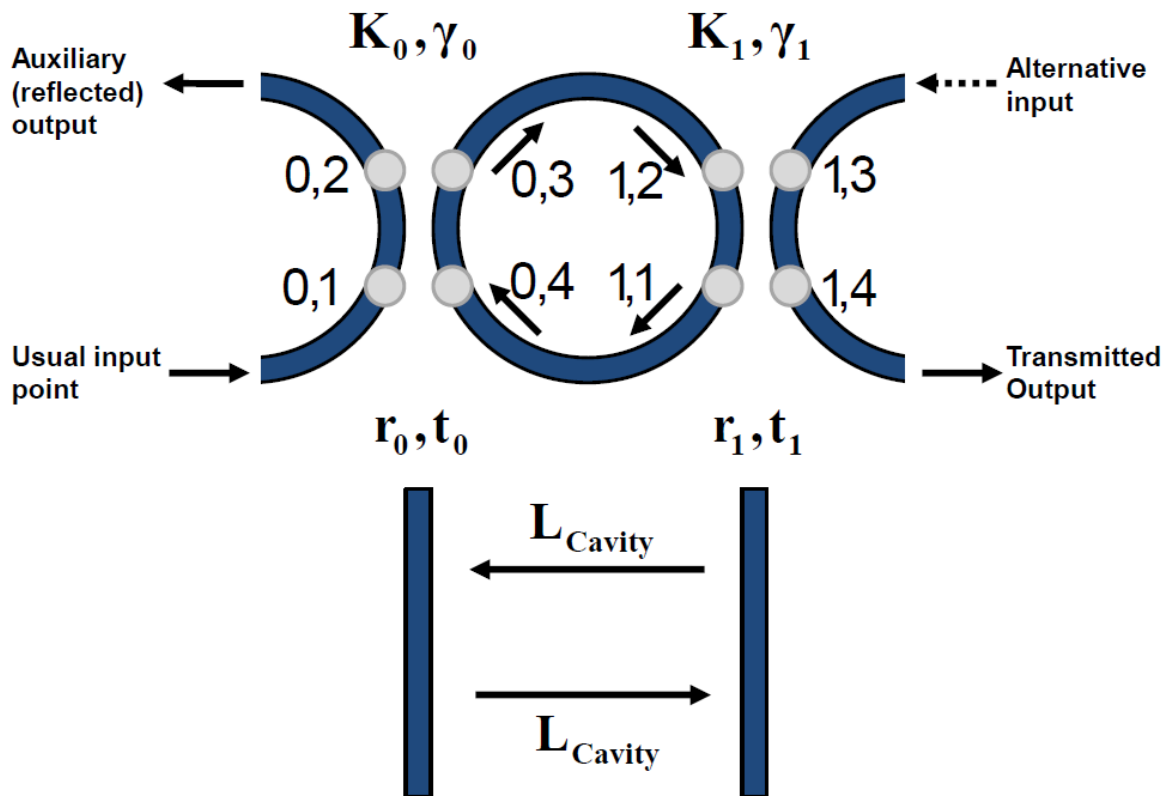


Figure 3-1 One ring resonator (top) and the equivalent two-mirror Fabry-Pérot resonator (below).

As defined in Section 2.4, K_m and γ_m are the coupling coefficient and the coupler excess loss, respectively. r_m and t_m are their equivalents in the FP theory, where r_m is the reflectance of the mirror and t_m is its transmittance [6]. Owing to the equivalence of the ring and FP resonators, we can refer to “effective” transmittances of couplers as defined in Section 2.4. One optical circuit in the ring is the equivalent of a double passage in the cavity of a FP resonator of length L . Two times the length of the cavity has the same role as the circumference of a ring. Therefore, the free spectral range, as defined in Section 2.2, is calculated using $L_{\text{Ring}} = 2 \cdot L_{\text{Cavity}}$. The indices shown in Figure 3-1 denominate the order of the couplers respective to the mirrors. Light is launched into the ring at the coupling point (0,1) shown in Figure 3-1 and we obtain the output at point (1,4). If we inject a signal into the device from point (0,1) on the ring resonator, there are two possible output points. On the one hand, we have the output from point (1,4), which is like the transmission transfer function of a Fabry-Pérot resonator. On the other hand, we have the output from point (0,2) which is like the reflection transfer function of a Fabry-Pérot resonator. In principle, there can also be an input at point (1,3), and in that case the light would also travel clockwise in the ring, exiting at both (0,2) and (1,4). However, we do not consider this case because, by symmetry considerations, it is mathematically identical to the analysis that we present, except for the change of subscripts on the electric field terms.

In order to calculate the matrix for one ring resonator, Equations (2.6) to (2.13) in Section 2.4 were used. From these, the following equations for the transfer between the points (0,1) & (0,2) and (1,1) & (1,2) are used:

$$E_{0,2}^- = r_0 \cdot E_{0,1}^+ + t_0 \cdot E_{1,1}^- \cdot e^{\delta_{1,0}} \quad (3.1)$$

$$E_{1,2}^+ = r_0 \cdot E_{1,1}^- \cdot e^{\delta_{0,1} + \delta_{1,0}} + t_0 \cdot E_{0,1}^+ \cdot e^{\delta_{0,1}} \quad (3.2)$$

$E_{0,1}$ is the known input. r_0 and t_0 are the effective reflectance and transmittance, respectively of coupler zero, as defined by Equations (2.4) and (2.5). Equations (3.1) and (3.2) need to be rearranged because we require the (0,1) and (0,2) terms

together and the (1,1) and (1,2) terms together. In this way we can establish a matrix-vector equation.

From Equation (3.1) we obtain:

$$E_{1,1}^- = \left(\frac{1}{t_0}\right) \cdot e^{-\delta_{1,0}} \cdot E_{0,2}^- - \left(\frac{r_0}{t_0}\right) \cdot e^{-\delta_{1,0}} \cdot E_{0,1}^+ \quad (3.3)$$

Then we substitute Equation (3.3) into (3.2) and achieve:

$$E_{1,2}^+ = \left(\frac{t_0^2 - r_0^2}{t_0}\right) \cdot e^{-\delta_{0,1}} \cdot E_{0,1}^+ + \left(\frac{r_0}{t_0}\right) \cdot e^{-\delta_{0,1}} \cdot E_{0,2}^- \quad (3.4)$$

By writing equation (3.3) and (3.4) in a matrix-vector format we obtain:

$$\begin{bmatrix} E_{1,1}^- \\ E_{1,2}^+ \end{bmatrix} = \begin{bmatrix} -\left(\frac{r_0}{t_0}\right) \cdot e^{-\delta_{1,0}} & \left(\frac{1}{t_0}\right) \cdot e^{-\delta_{1,0}} \\ \left(\frac{t_0^2 - r_0^2}{t_0}\right) \cdot e^{\delta_{0,1}} & \left(\frac{r_0}{t_0}\right) \cdot e^{\delta_{0,1}} \end{bmatrix} \cdot \begin{bmatrix} E_{0,1}^+ \\ E_{0,2}^- \end{bmatrix} \quad (3.5)$$

Equation (3.5) is the transfer function for a single ring in a matrix-vector format. We have to take care that in general $\delta_{1,0}$ and $\delta_{0,1}$ are not equal, because the couplers are not always positioned at the half-way points on the ring's circumference. They could be offset so that the lengths L_{01} and L_{10} are unequal. The matrix-vector equation can be stated as:

$$E_1 = M_{1,0} \cdot E_0 \quad (3.6)$$

The matrix in Equation (3.6) is for clockwise propagating light. It was also necessary to specify that light can propagate either clockwise or counter-clockwise in a ring, as depicted in Figure 3-2.

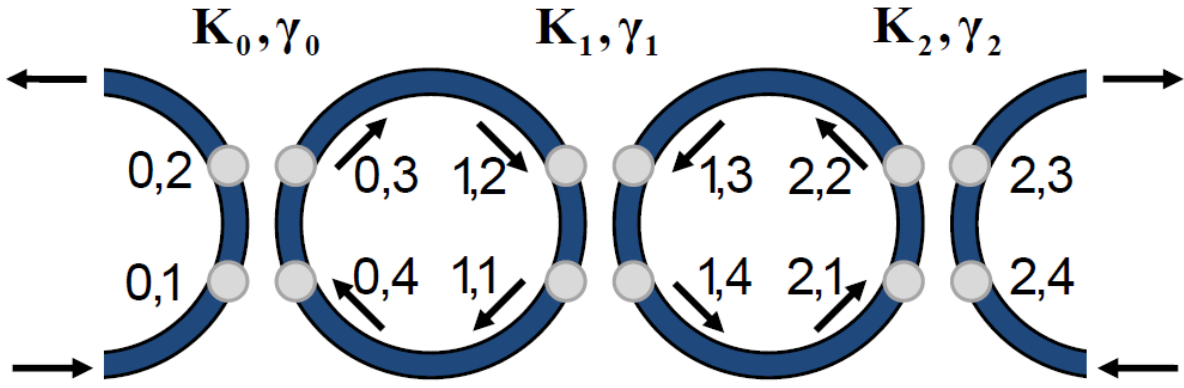


Figure 3-2 Two-ring resonator. Light propagates clockwise in the left ring and counter-clockwise in the right ring.

For this reason a second matrix for the counter-clockwise propagating light is needed, which is denoted as:

$$\begin{bmatrix} E_{2,1}^+ \\ E_{2,2}^- \end{bmatrix} = \begin{bmatrix} \left(\frac{r_1}{t_1}\right) \cdot e^{\delta_{1,2}} & \left(\frac{t_1^2 - r_1^2}{t_1}\right) \cdot e^{\delta_{1,2}} \\ \left(\frac{1}{t_1}\right) \cdot e^{-\delta_{2,1}} & -\left(\frac{r_0}{t_0}\right) \cdot e^{-\delta_{2,1}} \end{bmatrix} \cdot \begin{bmatrix} E_{1,1}^- \\ E_{1,2}^+ \end{bmatrix} \quad (3.7)$$

$$E_2 = M_{2,1} \cdot E_1 \quad (3.8)$$

We derived Equation (3.8) by performing nearly the same calculation; only the input- and output-points were different. If we compare Equations (3.7) and (3.8) with Equation (3.5), we see that the vector E_2 has the same type of elements as vector E_1 , but the elements are in different positions. The elements conform to a common format if we swap the subscripts “0” with “1” and “1” with “2”. Then we also have to exchange the elements on the diagonals. The physical reason is that light circulates clockwise in the left ring and counter-clockwise in the right ring.

Equations (3.7) and (3.8) show that the matrices do not connect the input with the output of the ring-structure. Therefore, we also need a coupler to provide a path from the last ring to the output, so we need to connect points (1,1) and (1,2) with points (1,3) and (1,4). Due to the fact that clockwise and counter-clockwise matrices are needed, we also obtain two different possible matrices for the last coupler; one

for a right-handed and one for a left-handed coupler. From Equations (2.10) and (2.13) we obtain:

$$E_{1,1}^- = r_1 \cdot E_{1,2}^+ + t_1 \cdot E_{1,3}^- \quad (3.9)$$

$$E_{1,4}^+ = r_1 \cdot E_{1,3}^- + t_1 \cdot E_{1,2}^+ \quad (3.10)$$

Equations (3.9) and (3.10) must be rearranged because the terms (1,1) and (1,2) are needed to be grouped together. Thus we achieve from Equation (3.8):

$$E_{1,3}^- = \left(\frac{1}{t_1}\right) \cdot E_{1,1}^- - \left(\frac{r_1}{t_1}\right) \cdot E_{1,2}^+ \quad (3.11)$$

We substitute Equation (3.11) into (3.10), to obtain:

$$E_{1,4}^+ = \left(\frac{r_1}{t_1}\right) \cdot E_{1,1}^- + \left(\frac{t_1^2 - r_1^2}{t_1}\right) \cdot E_{1,2}^+ \quad (3.12)$$

Equations (3.11) and (3.12) account for the actions of the right-hand coupler in the single ring resonator and they can be written in a matrix-vector format:

$$\begin{bmatrix} E_{1,3}^- \\ E_{1,4}^+ \end{bmatrix} = \begin{bmatrix} \left(\frac{1}{t_1}\right) & -\left(\frac{r_1}{t_1}\right) \\ \left(\frac{r_1}{t_1}\right) & \left(\frac{t_1^2 - r_1^2}{t_1}\right) \end{bmatrix} \cdot \begin{bmatrix} E_{1,1}^- \\ E_{1,2}^+ \end{bmatrix} \quad (3.13)$$

The matrix-vector equation can be also expressed as:

$$E_{out} = M_{out} \cdot E_1 \quad (3.14)$$

By doing the same calculation, only with different subscripts because of the changed direction of light propagation, we also derived the matrix-vector equation for the left-hand coupler, which is stated as:

$$\begin{bmatrix} E_{2,3}^+ \\ E_{2,4}^- \end{bmatrix} = \begin{bmatrix} \left(\frac{t_2^2 - r_2^2}{t_2}\right) & \left(\frac{r_2}{t_2}\right) \\ -\left(\frac{r_2}{t_2}\right) & \left(\frac{1}{t_2}\right) \end{bmatrix} \cdot \begin{bmatrix} E_{2,1}^+ \\ E_{2,2}^- \end{bmatrix} \quad (3.15)$$

$$E_{out} = M_{out} \cdot E_2 \quad (3.16)$$

When we compare Equations (3.13) and (3.15), we see that the matrix M_{out} has the same type of elements in both cases with a change of subscripts and the elements are in different positions. The reason is the same as before; light circulates clockwise or counter-clockwise. The coupler matrix to be used always depends on the number of rings. If we have an even number of rings and a counter-clockwise last ring, a left-hand coupler is used (Equation (3.15)), if we have an odd number of rings and the last ring is clockwise, a right-hand coupler is used (Equation (3.13)).

In order to obtain the complete amplitude transfer function for a single ring resonator, we now have to multiply the transfer matrix from Equation (3.5) by the coupler matrix from Equation (3.13), providing a connection between the input and the output. We have to take account for the order in which the matrices are multiplied:

$$E_{out} = M_{out} \cdot E_1 = M_{out} \cdot M_{1,0} \cdot E_0 \quad (3.17)$$

Equation (3.17) contains a right-hand coupler multiplied by a clockwise ring matrix. They are stated in reverse order with respect to the light propagation. E_0 is the input vector for the one-ring resonator. We do not state the whole matrix but we define it as matrix Q . Thus we obtain:

$$\begin{bmatrix} E_{1,3}^- \\ E_{1,4}^+ \end{bmatrix} = \begin{bmatrix} q_{1,1} & q_{1,2} \\ q_{2,1} & q_{2,2} \end{bmatrix} \cdot \begin{bmatrix} E_{0,1}^+ \\ E_{0,2}^- \end{bmatrix} \quad (3.18)$$

The q -elements that we derived are listed in Appendix A because they are complicated and provide little physical insight. $E_{0,1}^+$ and $E_{1,3}^-$ are either known input

signals or no input signals at all, which means that they can be zero. $E_{1,4}^+$ and $E_{0,2}^-$ are the corresponding output fields, which must be calculated. Therefore, we must write Equation (3.18) as a pair of equations and separate the terms to give us unknown quantities in terms of known quantities:

$$E_{1,3}^- = q_{1,1} \cdot E_{0,1}^+ + q_{1,2} \cdot E_{0,2}^- \quad (3.19)$$

$$E_{1,4}^+ = q_{2,1} \cdot E_{0,1}^+ + q_{2,2} \cdot E_{0,2}^- \quad (3.20)$$

We want to determine $E_{0,2}^-$ and $E_{1,4}^+$ and rearrange them on the left side in terms of known inputs $E_{0,1}^+$ and $E_{1,3}^-$. Thus:

$$E_{0,2}^- = \left(\frac{1}{q_{1,2}} \right) \cdot E_{1,3}^- - \left(\frac{q_{1,1}}{q_{1,2}} \right) \cdot E_{0,1}^+ \quad (3.21)$$

We substitute equation (3.21) into (3.20):

$$E_{1,4}^+ = \left(\frac{q_{1,2} \cdot q_{2,1} - q_{2,2} \cdot q_{1,1}}{q_{1,2}} \right) \cdot E_{0,1}^+ + \left(\frac{q_{2,2}}{q_{1,2}} \right) \cdot E_{1,3}^- \quad (3.22)$$

In most practical circumstances, where the ring resonator is being used as a simple filter either $E_{0,1}^+$ or $E_{1,3}^-$ is zero, but in most cases $E_{1,3}^-$ is zero because it is only an alternative input. In the present context we neglect it. Therefore, for the amplitude transfer function for a single ring resonator we obtain:

$$\left(\frac{E_{1,4}^+}{E_{0,1}^+} \right) = \left(\frac{q_{1,2} \cdot q_{2,1} - q_{2,2} \cdot q_{1,1}}{q_{1,2}} \right) \quad (3.23)$$

$(E_{1,4}^+/E_{0,1}^+)$ is the relation of the output to the input and of most interest for us. $(E_{0,2}^-/E_{0,1}^+)$ can also be calculated but it is of lesser use because it is the auxiliary output related to the input. The complete amplitude transfer function is stated in Appendix A.

3.3 Matrix Formulation of a Two-Ring Resonator

We derived two different matrix-vectors for a single-ring resonator and two different matrix-vectors for the last coupler. In this section we use these matrices to provide the transfer matrix for a two-ring resonator, as depicted in Figure 3-2. In the calculations great care was taken to account for the order in which the matrices are multiplied because matrix algebra is non-commutative, as stated before. From Equations (3.6) and (3.8) we obtain:

$$E_2 = M_{2,1} \cdot M_{1,0} \cdot E_0 \quad (3.24)$$

The vector E_2 in Equation (3.24) is not the output from the two-ring resonator. Therefore, we need the output vector E_{out} , which is defined by the left-hand coupler matrix. Thus from Equation (3.16) and (3.24) we obtain:

$$E_{out} = M_{out} \cdot E_2 = M_{out} \cdot M_{2,1} \cdot M_{1,0} \cdot E_0 \quad (3.25)$$

Equation (3.25) contains a left-hand coupler matrix multiplied by a counter-clockwise ring matrix and afterwards with a clockwise ring matrix. They are therefore stated in reverse order with respect to the light propagation. E_0 is the input vector for the two-ring resonator. Although the matrices are not particularly complicated, when we multiply them we obtain huge equations. Given that we now are modelling two rings, we must calculate with three effective reflectances and transmittances, which makes the calculations rather more demanding. For this reason we do not state the whole matrix. Instead, we define a matrix Q , which is given by:

$$Q = \begin{bmatrix} q_{1,1} & q_{1,2} \\ q_{2,1} & q_{2,2} \end{bmatrix} \quad (3.26)$$

Then for the two rings, including the output matrix M_{out} , we have:

$$\begin{bmatrix} E_{2,3}^+ \\ E_{2,4}^- \end{bmatrix} = \begin{bmatrix} q_{1,1} & q_{1,2} \\ q_{2,1} & q_{2,2} \end{bmatrix} \cdot \begin{bmatrix} E_{0,1}^+ \\ E_{0,2}^- \end{bmatrix} \quad (3.27)$$

The coefficients that we derived are listed in the Appendix A. Equation (3.27) shows that the output is equal to the overall transfer matrix for the two rings multiplied by the input vector. E_{01}^+ and E_{24}^- are either known input signals or no input signals at all, which means that they can be zero. E_{23}^+ and E_{02}^- are the corresponding output fields. Thus we obtain:

$$E_{2,3}^+ = q_{1,1} \cdot E_{0,1}^+ + q_{1,2} \cdot E_{0,2}^- \quad (3.28)$$

$$E_{2,4}^- = q_{2,1} \cdot E_{0,1}^+ + q_{2,2} \cdot E_{0,2}^- \quad (3.29)$$

E_{01}^+ and E_{24}^- are known quantities and we rearrange them to the right of the equation, but E_{23}^+ and E_{02}^- are the unknowns so we rearrange them on the left. This is given by:

$$E_{0,2}^- = \left(\frac{1}{q_{2,2}} \right) \cdot E_{2,4}^- - \left(\frac{q_{2,1}}{q_{2,2}} \right) \cdot E_{0,1}^+ \quad (3.30)$$

We substitute Equation (3.30) into (3.28):

$$E_{2,3}^+ = \left(\frac{q_{2,2} \cdot q_{1,1} - q_{1,2} \cdot q_{2,1}}{q_{2,2}} \right) \cdot E_{0,1}^+ + \left(\frac{q_{1,2}}{q_{2,2}} \right) \cdot E_{2,4}^- \quad (3.31)$$

As we can see, Equations (3.30) and (3.31) contain four unknown coefficients that need to be calculated. All of the coefficients include $1/q_{22}$, so we calculated it separately. We calculated $(q_{11}q_{22} - q_{12}q_{21})/q_{22}$, q_{12}/q_{22} and q_{21}/q_{22} by two methods. The first was the full expansion of all terms and the second was by using determinants and their properties. The use of both methods enabled us to crosscheck our results and to find out the easiest of the two, which is by determinants. We do not show these here because the equations for the Q matrix are very large and the coefficients in Equations (3.30) and (3.31) are even greater. The reader is referred to Appendix A for a listing of the terms and the complete amplitude transfer function.

We now have all of the information which is needed for the amplitude transfer function of a two-ring resonator and it is calculated using:

$$\left(\frac{E_{2,3}^+}{E_{0,1}^+}\right) = \left(\frac{q_{22} \cdot q_{11} - q_{12} \cdot q_{21}}{q_{22}}\right) \quad (3.32)$$

As in Section 3.2, $E_{2,4}^-$ is an alternative input and therefore neglected so that we achieve Equation (3.32). The final equations we obtained by calculating the four coefficients in Equations (3.30) and (3.31) are the same as the ones that Oscar Rautenberg derived with the non-matrix method. For this reason we can say that the matrix-method for a two-ring resonator works, even if in some respects it adds to the conceptual demands, compared with direct solution of twelve linear equations. However, there are two points to note: (a) the balance of difficulty shifts from the matrix approach to the direct algebraic solution as the number of rings is increased and (b) an important concern in this project is the possibility of algebraic mistakes because our calculations are complicated. The provision of identical end results, despite using different methodologies, gives us confidence in the validity of our work.

The design of practical filters requires transfer functions that are stated in terms of relative intensities, which are real numbers. In contrast, the terms stated in this section are all complex. The intensities can be obtained by multiplying the complex fields by their own complex conjugates. In most instances this is a lengthy calculation but it is a necessary final step in the formulation of a useful model of the filters. The details of this calculation are briefly stated in Appendix B and the appropriate end result is used in Chapter 4, where the filters' spectra are analysed in detail.

3.4 Matrix Formulation of a Three-Ring Resonator

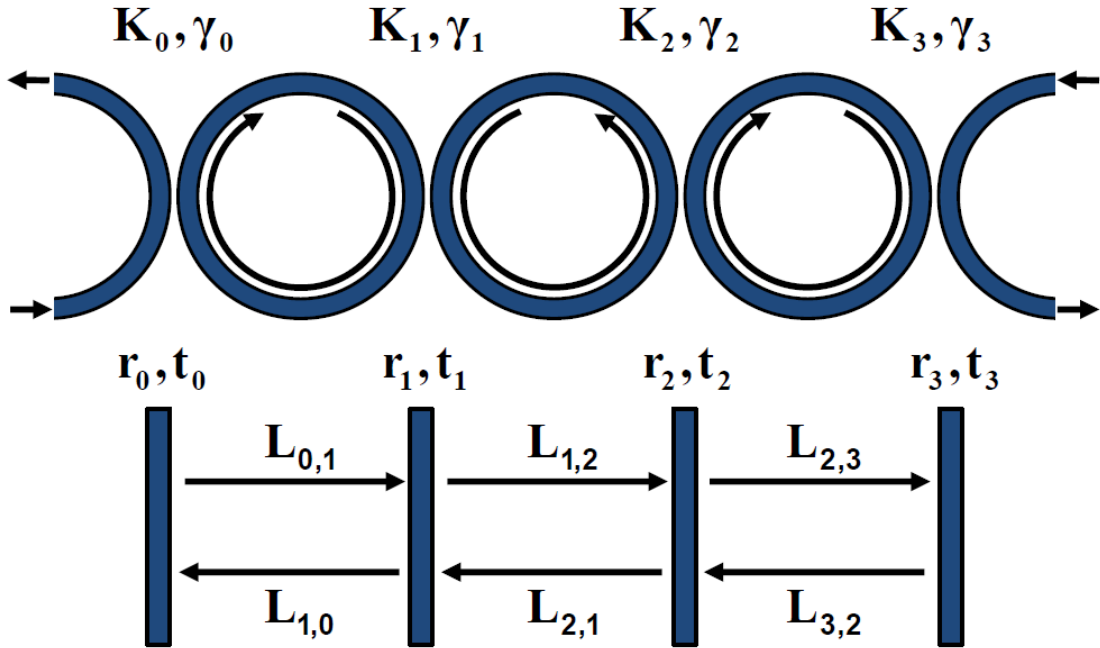


Figure 3-2 Three ring resonator (top) and the equivalent four-mirror Fabry-Pérot resonator (below). Light propagates clockwise in the left and right ring, counter-clockwise in the middle ring.

We use again the matrix method to formulate the total complex amplitude matrix for three rings. Therefore, the last coupler matrix (in that case a right-hand coupler) is multiplied by the three matrices for the constituent rings. Considering the order in which the matrices are multiplied, we start with the third ring, then the second and lastly the first ring.

The equation for the total complex amplitude matrix is:

$$E_{out} = M_{out} * M_{32} * M_{21} * M_{10} * E_0 \tag{3.33}$$

E_{out} and E_0 are (2x1) vectors, stating the output and the input on the compound resonator, respectively. M_{out} is the (2x2) matrix for the last coupler and M_{32} , M_{21} and M_{10} are the (2x2) transfer matrices for each ring, as described in Section 3.2. The indices relate to the ring for which they are used. The four M-matrices are given by:

$$M_{10} = \begin{bmatrix} -\left(\frac{r_0}{t_0}\right) \cdot e^{-\delta_{1,0}} & \left(\frac{1}{t_0}\right) \cdot e^{-\delta_{1,0}} \\ \left(\frac{t_0^2 - r_0^2}{t_0}\right) \cdot e^{\delta_{0,1}} & \left(\frac{r_0}{t_0}\right) \cdot e^{\delta_{0,1}} \end{bmatrix} \quad (3.34)$$

$$M_{21} = \begin{bmatrix} \left(\frac{r_1}{t_1}\right) \cdot e^{\delta_{1,2}} & \left(\frac{t_1^2 - r_1^2}{t_1}\right) \cdot e^{\delta_{1,2}} \\ \left(\frac{1}{t_1}\right) \cdot e^{-\delta_{2,1}} & -\left(\frac{r_1}{t_1}\right) \cdot e^{-\delta_{2,1}} \end{bmatrix} \quad (3.35)$$

$$M_{32} = \begin{bmatrix} -\left(\frac{r_2}{t_2}\right) \cdot e^{-\delta_{3,2}} & \left(\frac{1}{t_2}\right) \cdot e^{-\delta_{3,2}} \\ \left(\frac{t_2^2 - r_2^2}{t_2}\right) \cdot e^{\delta_{2,3}} & \left(\frac{r_2}{t_2}\right) \cdot e^{\delta_{2,3}} \end{bmatrix} \quad (3.36)$$

$$M_{out} = \begin{bmatrix} \left(\frac{1}{t_3}\right) & -\left(\frac{r_3}{t_3}\right) \\ \left(\frac{r_3}{t_3}\right) & \left(\frac{t_3^2 - r_3^2}{t_3}\right) \end{bmatrix} \quad (3.37)$$

As would be expected, the intensity transfer function is complicated and long. We calculate it with three different effective coupler reflectances and transmittances and six different inter-coupler fibre lengths are required. It is important to remember that in the general case the length L_{01} is not equal to L_{10} . As we have done in Section (3.2), we calculate with $\delta_{i,j}$, which includes complex numbers. The transfer matrix is long and complicated and so we only state the general matrix format which includes the transfer matrix Q in this Chapter. The constituent elements of Q are provided in Appendix A.

$$\begin{bmatrix} E_{3,3}^- \\ E_{3,4}^+ \end{bmatrix} = \begin{bmatrix} q_{1,1} & q_{1,2} \\ q_{2,1} & q_{2,2} \end{bmatrix} \cdot \begin{bmatrix} E_{0,1}^+ \\ E_{0,2}^- \end{bmatrix} \quad (3.38)$$

E_{01}^+ and E_{33}^- are known complex fields. E_{02}^- and E_{34}^+ are the unknown outputs, which must be calculated. Therefore, we rearrange the two equations from Equation (3.38) and obtain:

$$E_{0,2}^- = \left(\frac{1}{q_{1,2}}\right) \cdot E_{3,3}^- - \left(\frac{q_{1,1}}{q_{1,2}}\right) \cdot E_{0,1}^+ \quad (3.39)$$

We substitute Equation (3.39) into $E_{3,4}^+$ which we have from Equation (3.38):

$$E_{3,4}^+ = \left(\frac{q_{2,1} \cdot q_{1,2} - q_{1,1} \cdot q_{2,2}}{q_{1,2}}\right) \cdot E_{0,1}^+ + \left(\frac{q_{2,2}}{q_{1,2}}\right) \cdot E_{3,3}^- \quad (3.40)$$

Equations (3.39) and (3.40) incorporate four unknown terms, as we had in Section 3.3 for the two ring resonator. We calculated them by using the two methods: full expansion of all terms and by determinants and their properties. They are stated in the Appendix A because they are complicated and provide little physical insight into the resonator's operation, as well as the complete transfer function from Equation (3.41). However, they do provide all of the information needed for the final amplitude equation:

$$\begin{pmatrix} E_{3,4}^+ \\ E_{0,1}^+ \end{pmatrix} = \begin{pmatrix} q_{21} \cdot q_{12} - q_{11} \cdot q_{22} \\ q_{12} \end{pmatrix} \quad (3.41)$$

As in Sections 3.2 and 3.3, $E_{3,3}^-$ is an alternative input and we neglect it so that we achieve Equation (3.41). This result conforms to the complex amplitude equations using the non-matrix method of Oscar Rautenberg. We did not extend the calculation presented in this section to the intensity calculation that we would need to interpret the filter functions of our three-ring resonator. The necessary calculation can be performed by multiplying the fields $E_{0,2}^-$ and $E_{3,4}^+$ by their own complex conjugate, as described in Chapter 2 and they are given Appendix B. Our goal in the current chapter is merely to establish a matrix methodology and ensure that it provides results that are consistent with the non-matrix approach. Oscar Rautenberg has performed the intensity calculation for the two- and three-ring resonator with a non-matrix method and he provides the end result in Chapter 4. The calculation methodology is described in Appendix B.

4 Ring Transfer Functions and Their Interpretation

4.1 Introduction

The aim of this chapter is to interpret the (intensity) transfer functions of one-, two- and three-ring resonators. Our aim is to obtain filter functions which are progressively more “box-like” for potential application to a WDM system. A rectangle profile function is mathematically possible but we would need an infinite number of rings to realize it. Therefore, in the real world we have to make a compromise. Moreover, the calculation increases in difficulty (in a nonlinear manner) as we increase the number of rings. We achieved the intensity transfer function by multiplying the amplitude function with its own complex conjugate which is a huge calculation. So we decided to calculate the transfer functions for a maximum of three rings.

In this chapter we explain the properties and behaviour of one-, two- and three-ring resonators. We also obtain filter function that reach unity relative intensity at its resonant peaks in the zero loss limit. Our approach is to state and solve (by direct methods) a set of linear equations that establish relationships between the propagating electric fields and different points within the compound resonator. All the equations we use in this chapter are calculated by this non-matrix method and differ only by the effective reflectance, which we can simply replace by the equations for a coupler for a ring resonator as shown in Equation (2.4). The number of parameters in the transfer functions increases markedly with the number of rings because of the increasing number of constants, such as effective reflectances and because of the numerous possible wave interactions.

The ring circumferences are adjustable parameters so that we could have for every ring a separate length. However, as we explain in Section 4.5, our operational objectives are best achieved by ensuring that every ring has the same size. Therefore, most of our study is devoted to one value for every ring circumference. Another parameter is the loss coefficient α . In most of this chapter α is set to zero because it provides little physical insight into ring design for optimal performance. Moreover, it only appears in an exponential function and if we assume that the loss is zero, the exponential functions become one. Our approach is to optimise the filter

performance in the absence of loss and then to incorporate non-zero values of α to observe its effect. Throughout this chapter we plot graphs with “phase” (in radians) as the horizontal coordinate. The phase, Φ results from product from βL which are the arguments of the sinusoids within the transfer functions, as derived in Section 2.4.

4.2 Singe-Ring Resonator: Transfer Function

The transfer function for a one-ring resonator is derived in Section 3.2 and we obtain the same equation for the transfer function for a two-mirror Fabry-Pérot resonator if we replace the reflectances and transmittances with the substitutions from equation (2.4) and (2.5). When we assume that both couplers have the same coupling ratio which corresponds to two identical couplers, the transfer function is then given by

$$\left| \frac{E_{out}^+}{E_{in}^+} \right|^2 = \frac{T^2}{(1-R)^2 + 4 \cdot R \cdot \sin^2 \left[\frac{\Phi}{2} \right]} \quad (4.1)$$

with $R = r \cdot r = r^2$, $T = 1 - R$. We note that the r is the amplitude value for the effective reflectance and $\Phi = \beta \cdot L$. Where required, coupler and fibre losses can be included by using non-zero values of α and γ in Equations (2.2) and (2.4).

The transfer function is plotted in Figure 4-1 and 4-2, from which we can see that the one-ring resonator gives us a periodic function which repeats every 2π . A comparison of Figures 4-1 and 4-2 shows that narrow peaks with increased depth of modulation are obtained by using high values of the effective reflectances. Now we can see that we do not achieve a box-like function. The top of the peak does not become remotely rectangular merely by changing the effective reflectance value. Increased effective reflectances lead to narrower peaks, which means that the peak is no longer useful for high data rate communications channels because it is too narrow. With decreasing reflectance the peaks becomes wider but the disadvantage is that we achieve also a very bad rejection between the peaks as we can see for example at $\pi/2$ in Figure 4-1 where the relative intensity is 0.0625, a value which is only 12 dB down from the peaks and clearly unsuitable for telecommunications purposes.

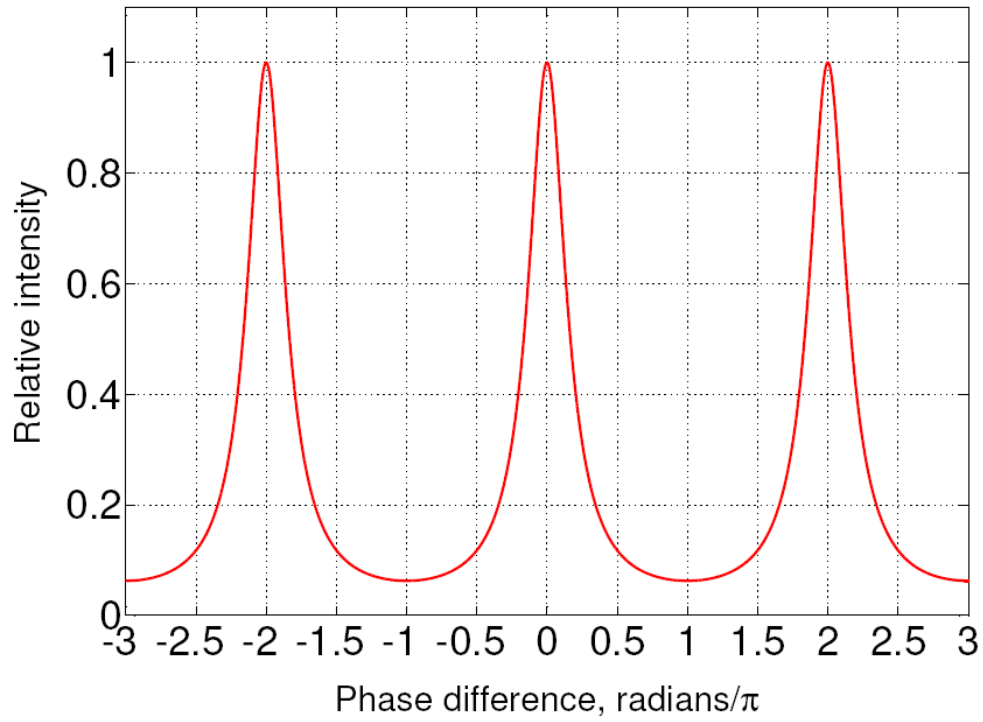


Figure 4-1 Transfer function of a one-ring resonator with effective reflectance $R = 0.6$. The coupling and fibre losses are assumed to be negligible.

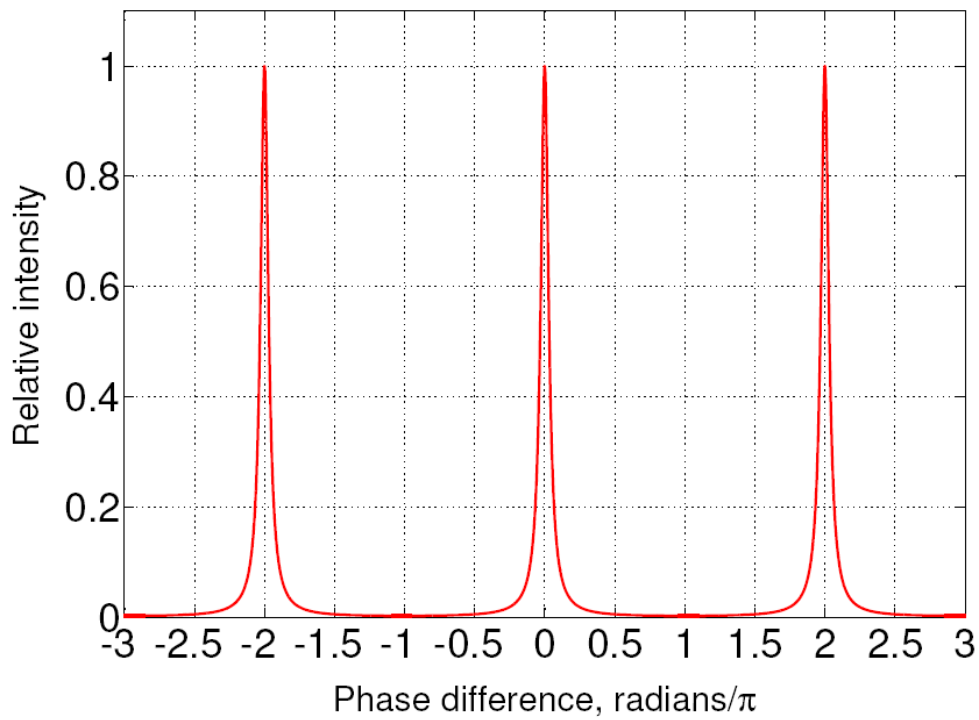


Figure 4-2 Transfer function of a one-ring resonator with effective reflectance $R = 0.9$. The coupling and fibre losses are assumed to be negligible.

Even in Figure 4-2, where the depth of modulation is 25.6dB, we are unlikely to achieve a filter that is sufficient for many applications. We could, of course, use values of R that are ever closer to unity and thereby obtain arbitrarily high values of $M^{(dB)}$ but it is clear from Figures 4-1 and 4-2 that we would pay the price of having peaks that are so narrow as to be unusable for high capacity WDM applications. Figures 4-3 and 4-4 are the direct equivalents of Figures 4-1 and 4-2, respectively but they are plotted on decibel scales to emphasise the out-of-band rejection that the filters offer. Consequently, by adjusting the parameters we have it is impossible to obtain a useful filter profile for our applications. What we can do is using more than one ring which means that the intensity transfer function becomes larger and more complicated.

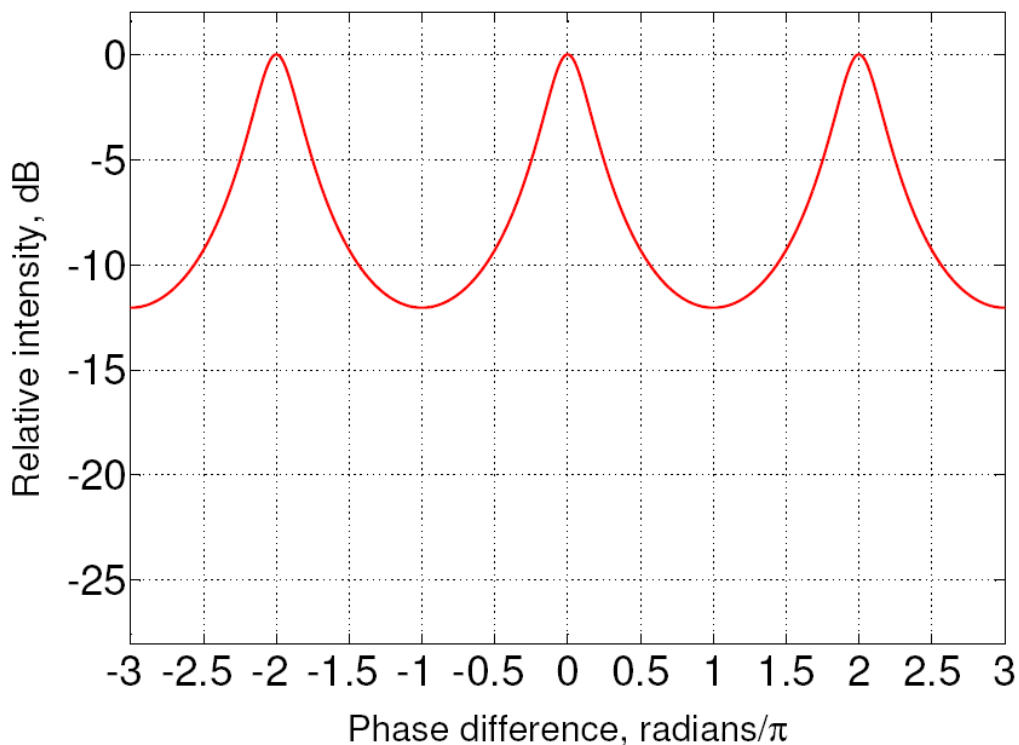


Figure 4-3 Equivalent plot to Figure 4.1 with a logarithmic vertical axis.

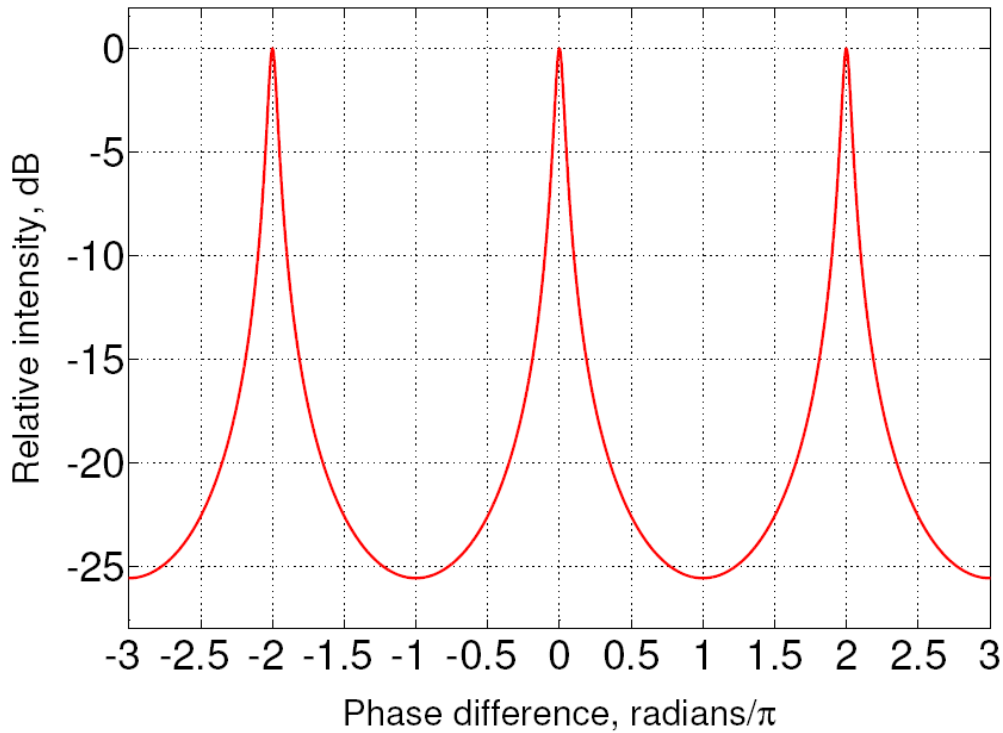


Figure 4-4 Equivalent plot to Figure 4.2 with a logarithmic vertical axis.

4.3 Single-Ring Resonator: Finesse

The concept of finesse is defined in Section 2.8: it is the ratio of the free spectral range to the full width at half maximum of the peaks. We assume that we have no losses so that $\alpha = 0$ and $t_j^2 + r_j^2 = 1$ with $j = 0, 1$. We know from Section 4.2 that the free spectral range appears at $\Phi = \pm 2\pi, \pm 4\pi, \pm 6\pi, \pm 8\pi$, and so on. Therefore, we can deduce that the free spectral range in phase space is $\Delta\Phi = 2\pi$ because it is a periodic function. So we need an expression for the full width at half maximum of the peaks $\delta\Phi_{1/2}$. We obtain the half of one peak which reaches unity, thus

$$\frac{T^2}{(1-R)^2 + 4 \cdot R \cdot \sin^2\left[\frac{\Phi}{2}\right]} = \frac{1}{2} \quad (4.2)$$

So we can use the fact of that $T^2 = 1 - R^2$ and transform Equation (4.2) to

$$\sin^2\left[\frac{\Phi}{2}\right] = \frac{(1-R)^2}{4 \cdot R} \quad (4.3)$$

which gives us Equation (4.4)

$$\sin \left[\frac{\Phi}{2} \right] = \pm \frac{(1-R)}{2 \cdot \sqrt{R}} \quad (4.4)$$

By using a approximation of Taylor series which says that for small argument $\sin[\Theta] \approx \Theta$, we obtain Equation (4.5).

$$\left[\frac{\Phi}{2} \right]_{\pm \frac{1}{2}} = \pm \frac{(1-R)}{2 \cdot \sqrt{R}} \quad (4.5)$$

Thus we have a plus sign term and a minus term for $\Phi/2$ which are defined in Equations (4.6) and (4.7).

$$\Phi_{+\frac{1}{2}} = + \frac{(1-R)}{\sqrt{R}} \quad (4.6)$$

$$\Phi_{-\frac{1}{2}} = - \frac{(1-R)}{\sqrt{R}} \quad (4.7)$$

The definition for $\delta\Phi_{1/2} = (\Phi_{+\frac{1}{2}} - \Phi_{-\frac{1}{2}})$ gives us Equation (4.8)

$$\delta\Phi_{\frac{1}{2}} = \frac{2 \cdot (1-R)}{\sqrt{R}} \quad (4.8)$$

Then we have the full width at half maximum and the free spectral range and can form Equation (4.9) for the finesse.

$$F = \frac{\Delta\Phi}{\delta\Phi_{\frac{1}{2}}} = \frac{\Delta\nu}{\delta\nu_{\frac{1}{2}}} = \frac{\pi \cdot \sqrt{R}}{(1-R)} \quad (4.9)$$

Now we have a formula for the finesse for a single-ring resonator, which assumed that we have negligible losses. The finesse is subject to the effective reflective $R = r^2$.

Figure 4-5 shows the finesse in decibels of a one-ring resonator. As expected, F becomes infinite in the limit as R tends to unity.

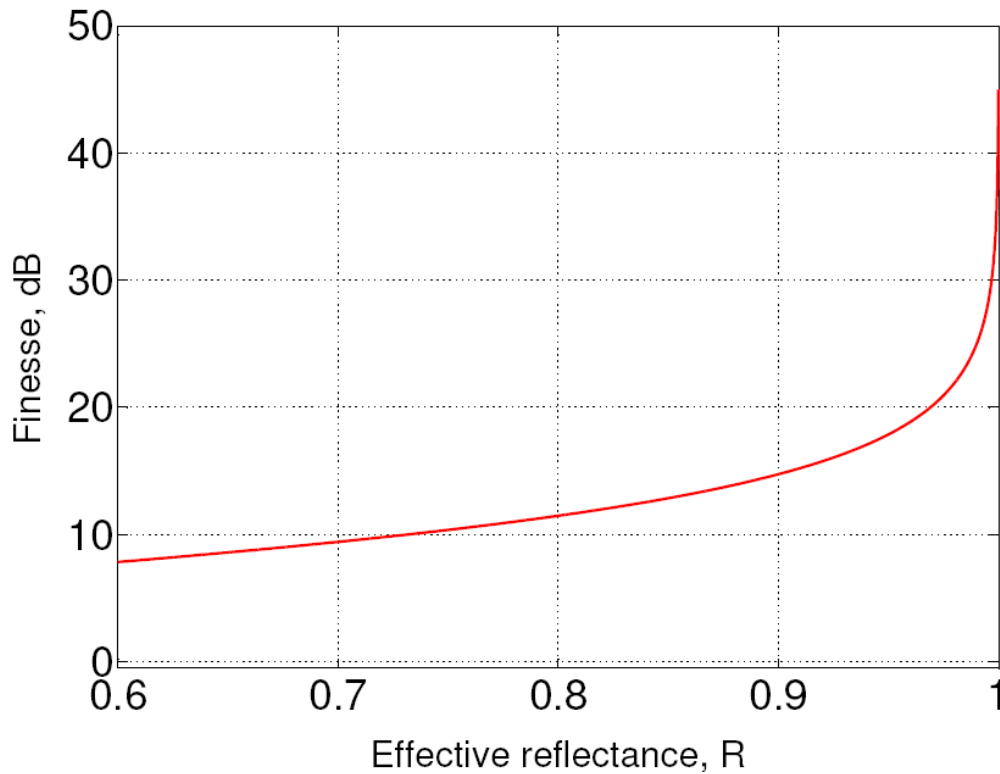


Figure 4-5 Variation of Finesse (in dB) as a function of effective reflectance R for a single-ring resonator with negligible losses.

4.4 Two-Ring Resonator: Transfer Function

As we have seen in Section 4.2, one ring is not sufficient to satisfy our needs. Now we explore the possibilities presented by a two-ring structure, the theory of which is derived in Section 3.3. As shown in Figure 4-6, there is one more coupler, creating one additional effective reflectance. The transfer function for a two-ring resonator is more complicated than that of a one-ring resonator. By replacing the effective reflectances using Equations (2.4) we obtain the equivalent intensity transfer function for the two-ring resonator.

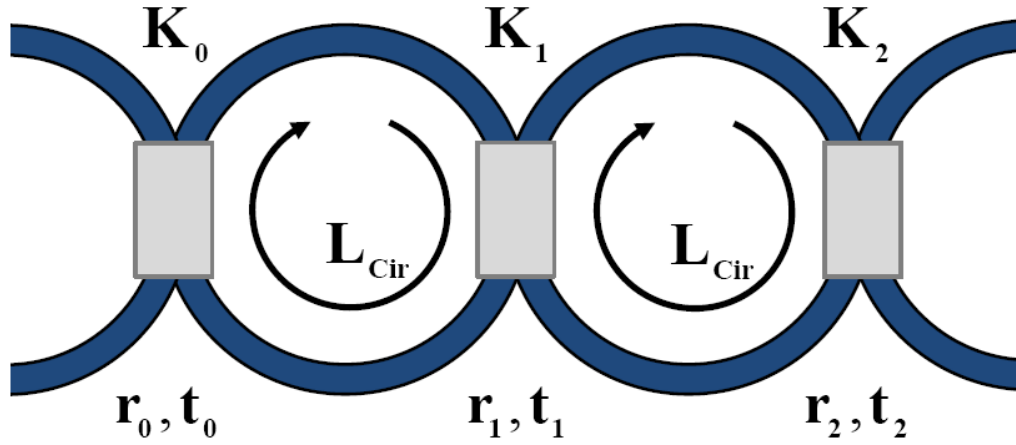


Figure 4-6 Two ring resonator with its parameters.

The intensity transfer function for a two-ring resonator is given by Equations (4.10) – (4.12), where the effective reflectances are defined in Equations (4.13) – (4.15). The Φ_1 and Φ_2 in Equation (4.16) and (4.17) are phase shifts in the first and second rings, respectively, where β is the waveguide's propagation constant and L_1 and L_2 are the ring circumferences. In the special case of zero losses $\alpha = 0$ and $t_1^2 + r_1^2 = 1$, so that $R_{01} = r_0 \cdot r_1$, $R_{12} = r_1 \cdot r_2$ and $R_{02} = r_0 \cdot r_2$.

$$\left| \frac{E_{out}^+}{E_{in}^+} \right|^2 = \frac{|T|^2}{|D|^2} \quad (4.10)$$

$$|T|^2 = t_0^2 \cdot t_1^2 \cdot t_2^2 \quad (4.11)$$

$$|D|^2 = (1 - R_{01} - R_{12} + R_{02})^2 \quad (4.12)$$

$$+4(R_{01} + R_{12} \cdot R_{02}) \cdot \sin^2 \left[\frac{\Phi_1}{2} \right]$$

$$+4(R_{12} + R_{01} \cdot R_{02}) \cdot \sin^2 \left[\frac{\Phi_2}{2} \right]$$

$$-4 \cdot R_{01} \cdot R_{12} \cdot \sin^2 \left[\frac{\Phi_1 - \Phi_2}{2} \right]$$

$$-4 \cdot R_{02} \cdot \sin^2 \left[\frac{\Phi_1 + \Phi_2}{2} \right]$$

$$R_{01} = r_0 \cdot r_1 \cdot \exp[-\alpha \cdot L_1/2] \quad (4.13)$$

$$R_{12} = r_1 \cdot r_2 \cdot \exp[-\alpha \cdot L_2/2] \quad (4.14)$$

$$R_{02} = r_0 \cdot (r_1^2 + r_2^2) \cdot r_1 \cdot \exp[-\alpha \cdot (L_1 + L_2)/2] \quad (4.15)$$

$$\Phi_1 = \beta \cdot L_1 \quad (4.16)$$

$$\Phi_2 = \beta \cdot L_2 \quad (4.17)$$

In order to visualise how the double-ring assembly influences the frequency response, we choose for r_0^2 and r_2^2 a value of 0.5 and for r_1^2 a value of 0.92. We use values of Φ_1 and Φ_2 in the ratio of 10:9, corresponding to two different ring circumferences. See Figure 4-7.

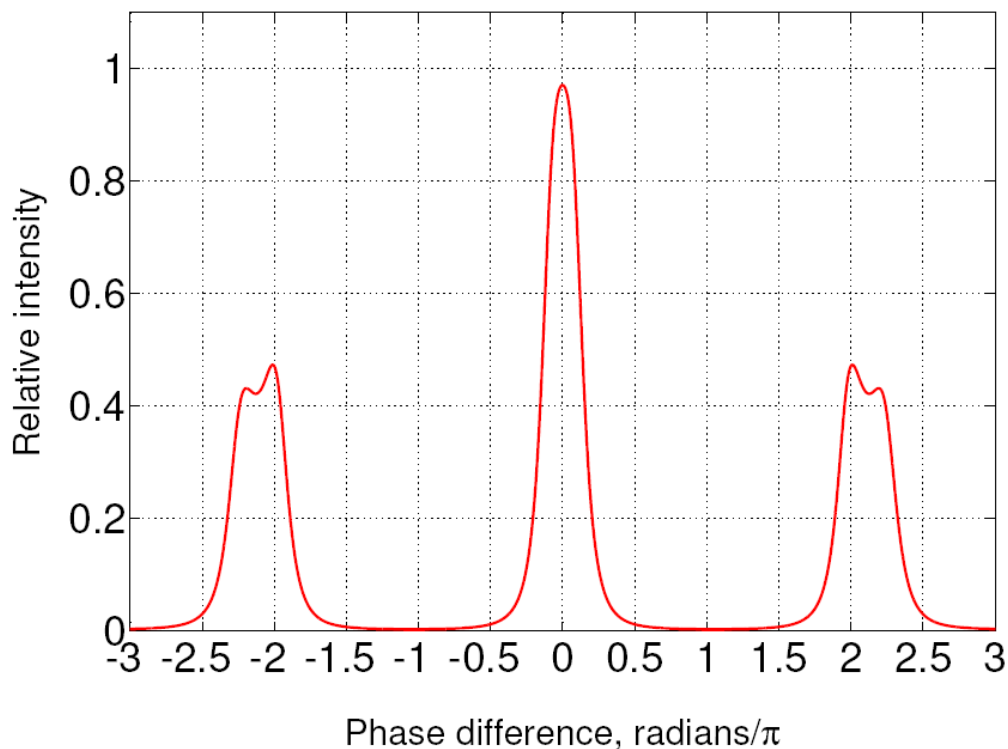


Figure 4-7 The transfer function of a two ring resonator with $r_0^2 = r_2^2 = 0.5$ and $r_1^2 = 0.92$. The ring lengths are in the ratio $L_1:L_2 = 10:9$ and losses due to imperfect coupling and waveguide transmission are ignored.

Figure 4-7 shows several significant features that are not suitable for filtering: The resonance peaks are unequal in magnitude, they do not reach 100% and they sometimes display double peaks. Inspection of the subsidiary peaks around $\pm 2\pi$ reveals that the form of the peak is divided into two smaller peaks; the larger one reaching 47,3% and the smaller with a relative intensity of 43,1%. Such behaviour is

not useful for our applications. We are not even approximating the 100% of intensity and so we do not have a useful filter profile. However, close inspection of Figure 4-7 shows that there is good out-of-band rejection at the frequencies mid-way between the peaks and this seems to be possible without the excessively narrow peaks that were discussed in Section 4.2. Consequently, we have grounds to hope that two-ring resonators might give us better performance than their single-ring counterparts, provided that we can select appropriate parameters.

4.5 Two-Ring Resonator: Equal Circumferences

In an attempt to ensure that all peaks are of equal magnitude, we have examined numerous combinations of effective reflectances and consistently found a means to prevent the unequal peaks that are displayed in Figure 4-7. We can achieve this with equal ring circumferences: $L_1 = L_2$. The reason is that both rings are simultaneously resonant at the same sets of frequencies. Figure 4-8 is an example with equal rings. We see that the peaks all reach unity but we also obtained double peaks, which is an unwanted feature that we have to try to avoid. The reason for the double peaks can be seen with reference to Equation (4.12). There is a $\sin^2[(\Phi_1 + \Phi_2)/2]$ term which is superimposed on $\sin^2[\Phi_1/2]$ and $\sin^2[\Phi_2/2]$ terms. (When $\Phi_1 = \Phi_2$ the $\sin^2[(\Phi_1 - \Phi_2)/2]$ term vanishes and we are left with two frequency modulations in the transfer function.) The different modulation frequencies Φ and $\Phi/2$ are superposed to give the twin peaks shown in Figure 4-8.

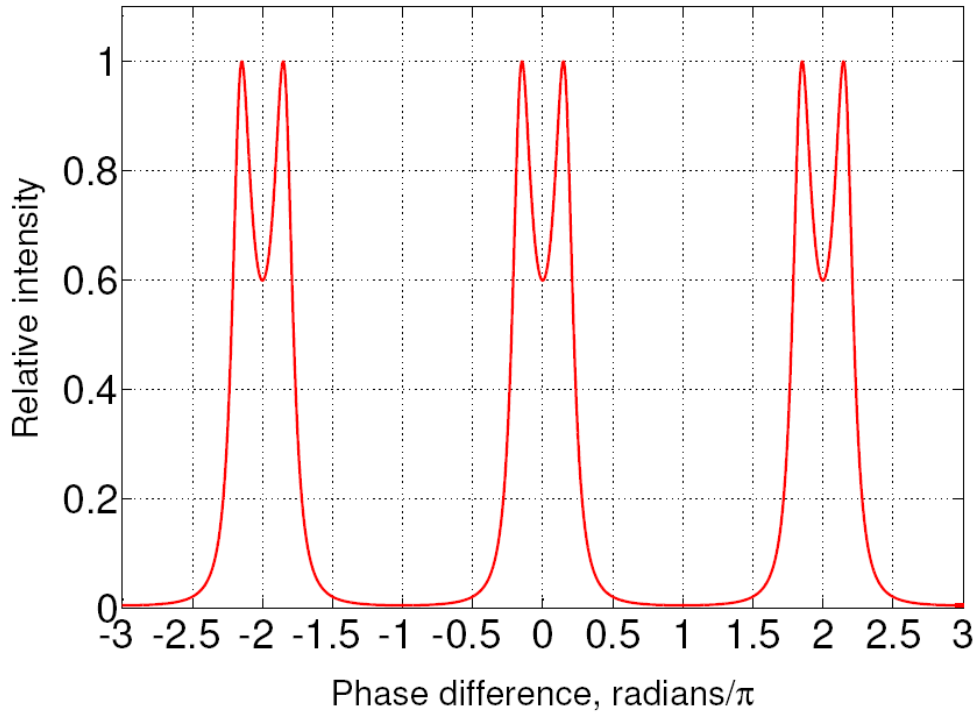


Figure 4-8 The transfer function of a two-ring resonator with identical ring circumferences, and effective reflectances of $r_0^2 = r_2^2 = 0.6$ and $r_1^2 = 0.75$. All losses are assumed to be negligible.

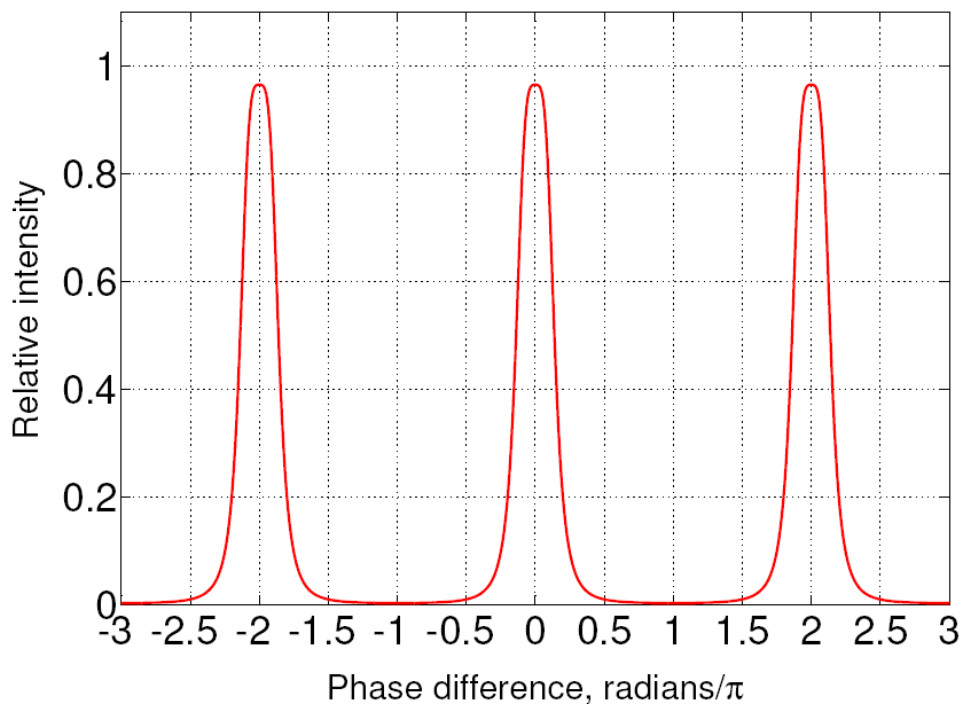


Figure 4-9 Transfer function of a two-ring resonator with equal ring circumferences, zero losses and effective reflectances of $r_0^2 = 0.7$, $r_2^2 = 0.4$ and $r_1^2 = 0.89$.

We have explored many values of the effective reflectances r_0^2 , r_1^2 and r_2^2 with the aim of eliminating the dual peaks shown in Figure 4-8. Our objective can be achieved with reasonable ease and an example is illustrated in Figure 4-9, where r_0^2 is equal to 0.7, r_2^2 is equal to 0.4 and r_1^2 has a value of 0.89. Now we have values but which satisfy our needs of a periodic filter profile with the same maximum values and always single peaks. It was found out by trying values, but not in a structured way. Unfortunately, as Figure 4-9 shows, the transfer function does not reach unity. We have not been able to obtain unity at the peaks when there are different outer couplers, that is when $r_0^2 \neq r_1^2 \neq r_2^2$. Therefore, we aim to explore solutions in which the outer couplers are equal so that $r_0^2 = r_2^2 = r^2$ but r_1^2 has a distinct value. Figure 4-10 then illustrates the revised structure of a two-ring resonator.

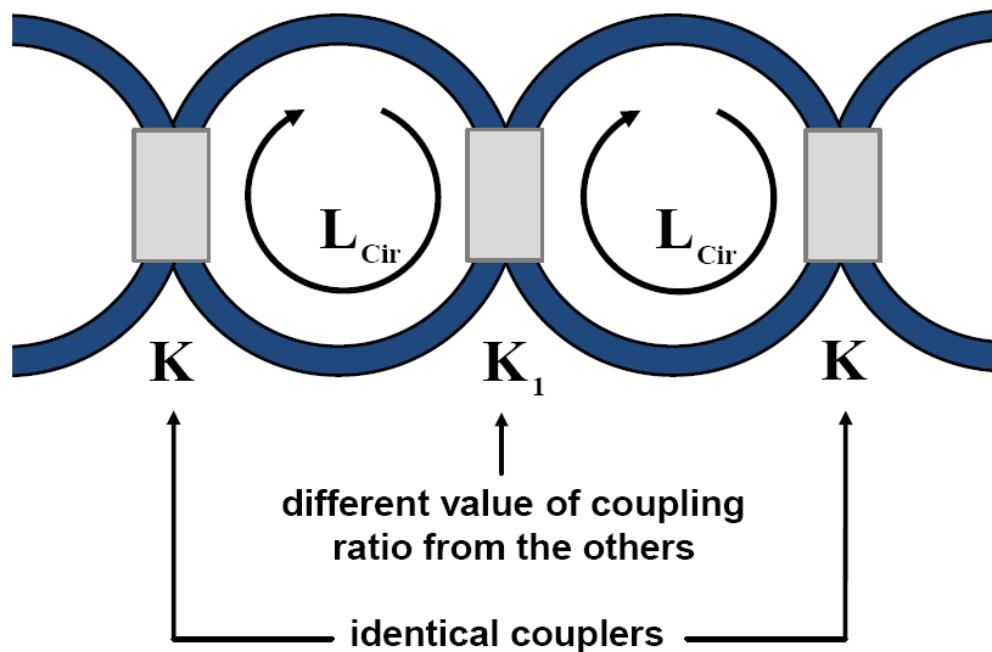


Figure 4-10 Two-ring resonator with equal ring circumferences and different outer coupling ratios, leading to the effective reflectances $r^2 = (1-K)$ and $r_1^2 = (1-K_1)$.

Until this point we have always chosen the values for the effective reflectances by trial and error. Now we know that we require equal ring circumferences and equal outer couplers to obtain equal peak heights, where every peak reaches unity. However, the two conditions are not sufficient to ensure that we also obtain a single peak. We tried many plots by satisfying both conditions of equal ring circumferences and outer coupler but it is not at all straightforward to achieve single peaks with many

effective reflectance values merely by guessing. A systematic computer search algorithm could be devised but it would always be less satisfactory than an analytical formula.

We want to make the choice for the effective reflectances more structured and to do this we start with Equations (4.11) to (4.17) with $\Phi_1 = \Phi_2 = \Phi$. We also consider zero transmission and coupler losses so that $\alpha = 0$ and $t_j^2 + r_j^2 = 1$, where $j = 0,1,2$. We define $Y(\Phi)$:

$$\left| \frac{E_{out}^+}{E_{in}^+} \right|^2 = \frac{|T|^2}{|D|^2} = Y(\Phi) \quad (4.18)$$

where the numerator is a constant in Φ

$$|T|^2 = t^4 \cdot t_1^2 \quad (4.19)$$

and the denominator is

$$\begin{aligned} |D|^2 = & (1 - 2 \cdot R + R_{02})^2 \\ & + 8R(1 + R_{02}) \cdot \sin^2 \left[\frac{\Phi}{2} \right] \\ & - 4 \cdot R_{02} \cdot \sin^2[\Phi] \end{aligned} \quad (4.20)$$

The effective reflectances are now

$$R = R_{01} = R_{12} = r \cdot r_1 \quad (4.21)$$

$$R_{02} = r_0 \cdot r_2 = r^2 \quad (4.22)$$

and the phase is is

$$\Phi = \Phi_2 = \Phi_1 \quad (4.23)$$

We must first calculate what makes the function $Y(\Phi)$ reach unity (at least, when the loss can be ignored). Our approach is to differentiate the whole transfer function, where its “extrema” are located; they occur when the derivative is equal to zero. We define the constants A, B and C to make the calculations easier and we

also use for the transfer function the expression $Y(\Phi)$ as we show in Equations (4.24) to (4.27).

$$Y(\Phi) = \frac{T^2}{\left[A + B \cdot \sin^2\left[\frac{\Phi}{2}\right] - C \cdot \sin^2[\Phi]\right]} \quad (4.24)$$

$$A = (1 - 2 \cdot R + R_{02})^2 \quad (4.25)$$

$$B = 8R(1 + R_{02}) \quad (4.26)$$

$$C = 4 \cdot R_{02} \quad (4.27)$$

Then, the derivative is

$$\frac{dY}{d\Phi} = \frac{-T^3 \cdot \{B \cdot \sin\left[\frac{\Phi}{2}\right] \cdot \cos\left[\frac{\Phi}{2}\right] - 2 \cdot C \cdot \sin[\Phi] \cdot \cos[\Phi]\}}{\left[A + B \cdot \sin^2\left[\frac{\Phi}{2}\right] - C \cdot \sin^2[\Phi]\right]^2} \quad (4.28)$$

$dY/d\Phi$ is zero if its numerator is zero and with the aid of standard trigonometric relations,

$$(B - 4 \cdot C \cdot \cos[\Phi]) \cdot \sin[\Phi] = 0 \quad (4.29)$$

So we have two conditions to bring Equation (4.29) to zero. The first one is that the \sin -term goes to zero and the second is that the bracketed term becomes zero. In both cases we satisfy our requirement for a vanishing first derivative, where the function exhibits its extrema. The two conditions can be summarised as: Condition a) $\sin(\Phi) = 0$ and Condition b) $B - 4 \cdot C \cdot \cos[\Phi] = 0$. By the use of standard trigonometric identities condition b) is the same as $\sin^2[\Phi/2] = \frac{1}{2} [1 - B/4C]$.

In Equation (4.18), which is the transfer function, we have two terms which are squares of sinusoids. One has the argument $\Phi/2$ and the other has the argument Φ . If we consider condition a) we recognize that we have two cases, which means

$$\text{when } \Phi = \pm\pi, \pm3\pi, \pm5\pi, \pm7\pi, \dots \quad Y(\Phi) = Y_{min} = \frac{T^2}{[1 + 2 \cdot R + R_{02}]} \quad (4.30)$$

$$\text{when } \Phi = 0, \pm2\pi, \pm4\pi, \pm6\pi, \pm8\pi, \dots \quad Y(\Phi) = Y_{max} = \frac{T^2}{[1 - 2 \cdot R + R_{02}]} \quad (4.31)$$

Equation (4.30) specifies the minima of the transfer function. Equation (4.31) can specify the maxima under certain circumstances (which is the reason for the terminology Y_{max}) but it always provides the value when the two rings are individually on resonance.

By substituting Condition b) we can transform the denominator from Equation (4.28) into a term which looks like

$$A + (B - 4 \cdot C) \cdot \sin^2 \left[\frac{\Phi}{2} \right] + 4 \cdot C \cdot \sin^4 \left[\frac{\Phi}{2} \right] \quad (4.32)$$

Equation (4.32) made use of standard trigonometric substitutions to obtain the \sin^4 -term. Thus by using condition b) and substituting Equation (4.25) to (4.27) for A, B and C, we obtain:

$$Y(\Phi) = Y_{peak} = \frac{T^3 \cdot R_{02}}{(R_{02} - R^2)(1 - R_{02})^2} \quad (4.33)$$

It should be remembered that we do not have loss and we have chosen to make the outer couplers equal. That means that we have $R_{01} = R_{12} = R = r_0 \cdot r_1$ and $R_{02} = r^2$ also shown in Equation (4.21) and (4.22). Also we have effective transmittances in the numerator which we can easily replace because, when the coupler losses are negligible, $r_j^2 = 1 - t_j^2$, shown in Section 2.4. So we have a T^2 -term in the numerator which is

$$T^3 = t^4 \cdot t_1^2 = (1 - r^2)^2(1 - r_1^2) \quad (4.34)$$

If we replace the terms in Equation (4.33) with the appropriate effective reflectances we obtain the transfer function shown in Equation (4.35).

$$Y_{peak} = \frac{(1-r^2)^2(1-r_1^2) \cdot r^2}{[r^2 - (r \cdot r_1)^2] \cdot [1-r^2]^2} = \frac{(1-r_1^2) \cdot r^2}{r^2[1-r_1^2]} = 1 \quad (4.35)$$

Equation (4.35) shows that the transfer function reaches unity when we have no loss and we have

$$\sin^2 \left[\frac{\Phi}{2} \right] = \frac{1}{2} \cdot \left[1 - \frac{B}{4C} \right] \quad (4.36)$$

which we obtain if we change condition b) with the help of standard trigonometric identities. We can therefore find an expression for Φ where this condition is applies. With the use of Equations (4.25) to (4.27) for the A-, B- and C-terms, we obtain Equation (4.37).

$$\Phi_{peak} = \frac{1}{2} \cdot \sin^{-1} \left[\pm 16 \cdot \sqrt{2} \cdot r^2 \cdot (2 \cdot r - r_1 \cdot (1 + r^2)) \right] \quad (4.37)$$

Equation (4.37) specifies the phase values where periodic peaks appear. It contains a “ \pm ” sign, which indicates where there are the double peaks as illustrated in Figure 4-11. In Figure 4-11 we have an enlargement of Figure 4-8 at round $\Phi = 0$, showing the value Φ_{peak} where the double peaks appear. The inverse sinusoid is a periodic function and so such double peaks occur at every $0, \pm 2\pi, \pm 4\pi, \pm 6\pi$, plus or minus Φ_{peak} and so on.

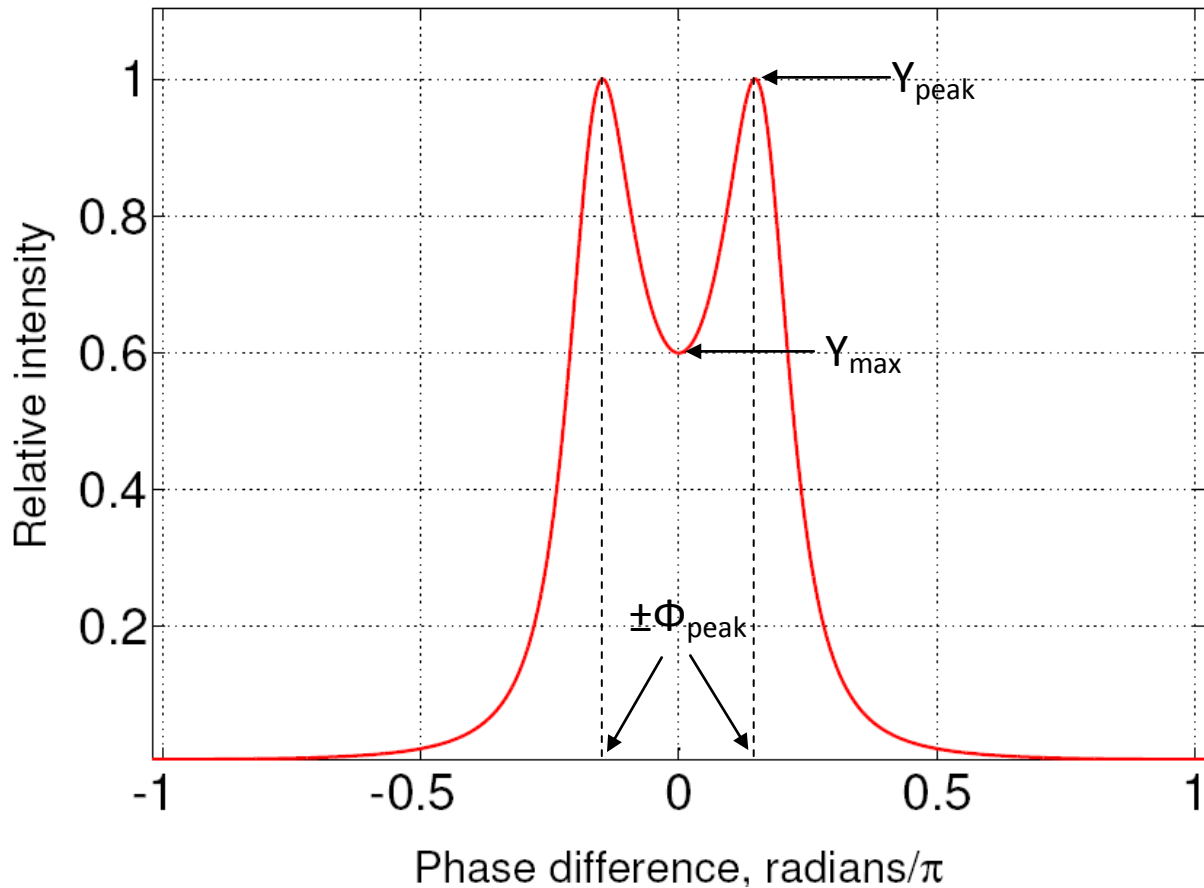


Figure 4-11 Enlargement of Figure 4-8 over range $-\pi \leq \Phi \leq +\pi$, showing Y_{max} from Equation (4.31) and Y_{peak} from Equation (4-35).

4.6 Two-Ring Resonator: Degeneracy Condition

We now make a further calculation to obtain what we believe to be one of the most important derived parameters in this report. It is what we designate the “degeneracy condition” for the two-ring resonator with equal ring circumferences. Our starting point is Equation (4.31) which applies when $\Phi = 0, \pm 2\pi, \pm 4\pi, \pm 6\pi$, etc. Equation (4.34) can be substituted for the numerator, giving

$$Y_{max} = \frac{T^3}{[1 - 2 \cdot R + R_{02}]} = \frac{(1-r^2)^2(1-r_1^2)}{[1 - 2 \cdot r \cdot r_1 + r^2]^2} = 1 \quad (4.38)$$

In Equation (4.38) we consider that the numerator and the denominator have to be the same to make the whole equation equal to unity. Therefore, we obtain Equation (4.39).

$$(1 - r^2)^2(1 - r_1^2) = [1 - 2 \cdot r \cdot r_1 + r^2]^2 \quad (4.39)$$

Now we have to solve this equation, which leads us to

$$r_1 = \frac{2 \cdot r}{(1+r^2)} \quad (4.40)$$

If we square this term we obtain an intensity value for the effective reflectance r_1^2 .

$$r_1^2 = \frac{4 \cdot r^2}{(1+r^2)^2} \quad (4.41)$$

Equation (4.41) states an important effective reflectance that allows us to specify the coupler ratio of the middle coupler, as shown in Figure 4-10. It is a value that guarantees unity relative intensity as long as we have zero losses, so that $\alpha = 0$, $t^2 = 1 - r^2$, $t_1^2 = 1 - r_1^2$ and equal ring circumferences $L_1 = L_2 = L$. Moreover, this little formula for the middle coupler simultaneously guarantees single peaks. The double peaks occur every $\pm \Phi_{peak}$ at every $0, \pm 2\pi, \pm 4\pi, \pm 6\pi$ and so on. We have also a formula for Φ_{peak} . The r_1 term from Equation (4.40) can be substituted into Equation (4.37) to provide Equation (4.42), which then becomes zero, as we can see in Equation (4.43).

$$\Phi_{peak} = \frac{1}{2} \cdot \sin^{-1} \left[\pm 16 \cdot \sqrt{2} \cdot r^2 \cdot \left(2 \cdot r - \frac{2 \cdot r}{(1+r^2)} \cdot (1 + r^2) \right) \right] \quad (4.42)$$

$$\Phi_{peak} = \frac{1}{2} \cdot \sin^{-1}[0] = 0 \quad (4.43)$$

Equation (4.43) means that we have a single peak at every $0, \pm 2\pi, \pm 4\pi, \pm 6\pi$, and so on and every peak reaches unity simultaneously. Therefore we call Equation (4.41) for the middle effective reflectance r_1^2 the “degeneracy condition”. With this condition we predict that both peaks, at $\pm \Phi_{peak}$, merge into each other and become to one single peak which reaches unity at the same time. Our terminology “degeneracy” is with reference to ionic and atomic spectra, where certain energy levels provide single or multiple emitted wavelengths, according to the external environment within which

the emitting species resides. It is also used in the context of optical polarisation phenomena

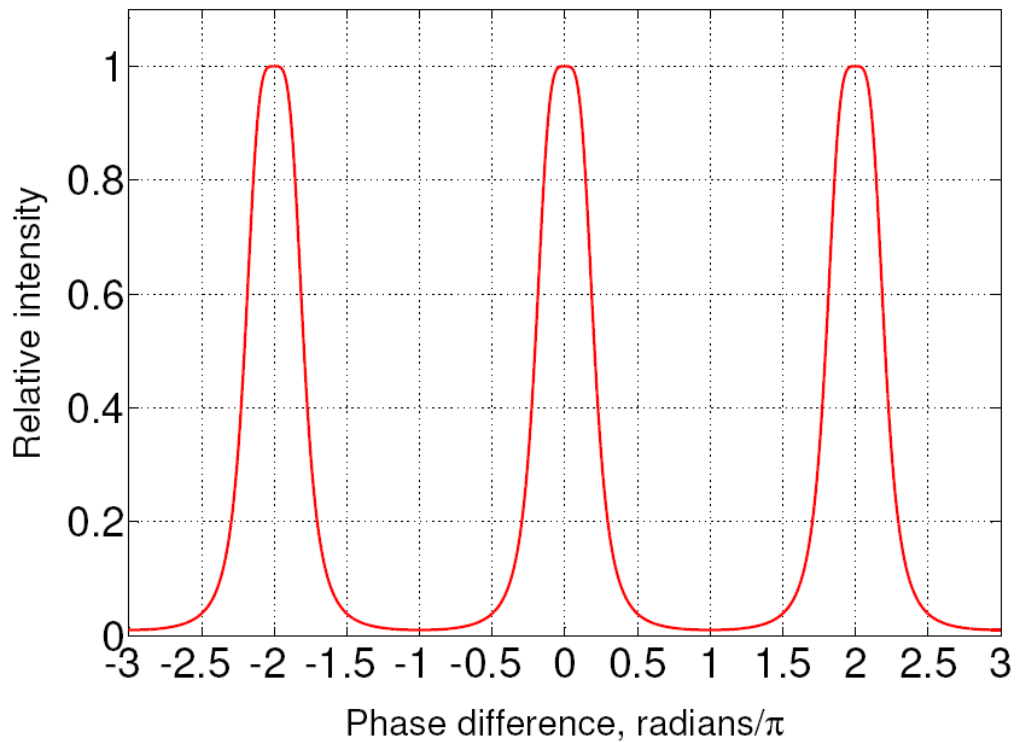


Figure 4-12 Transfer function for a two-ring resonator with equal outer couplers, effective reflectances of $r_1^2=0.818$ and $r^2=0.402$ and zero losses. The reflectances conform to the degeneracy condition. The depth of modulation is 20dB.

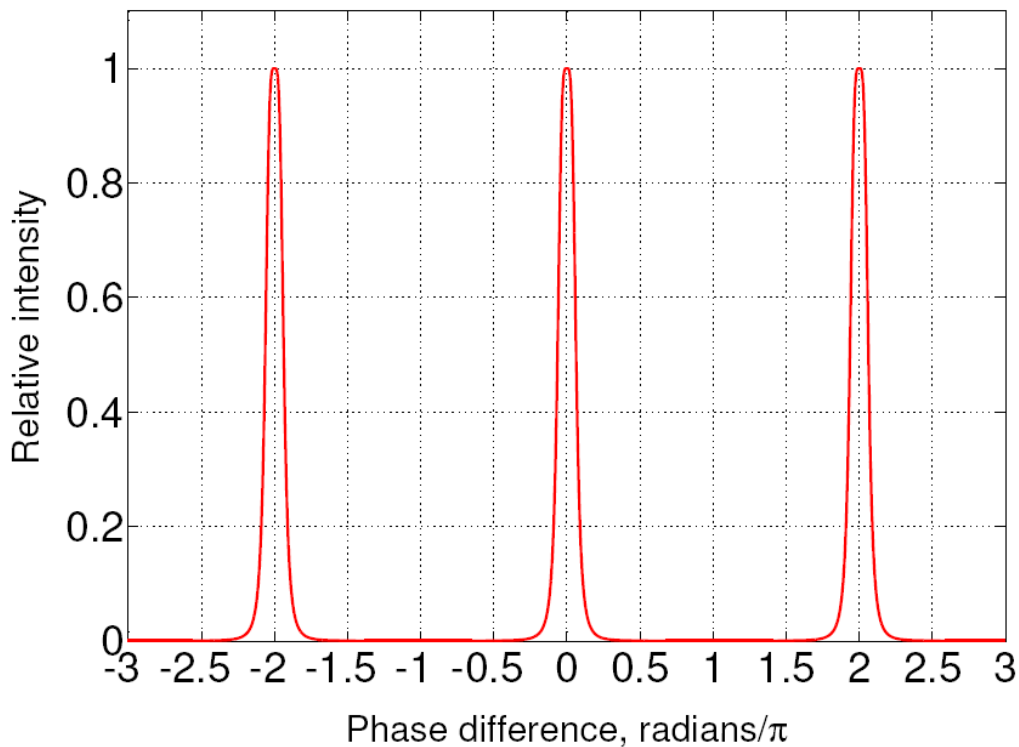


Figure 4-13 Transfer function for a two-ring resonator with equal outer couplers, effective reflectances of $r_1^2=0.98$ and $r^2=0.753$ and zero losses. The reflectances conform to the degeneracy condition. The depth of modulation is 40dB.

Figures 4-12 and 4-13 are plots of the transfer function for two-ring resonators that conform to the degeneracy condition. As required, there are no double peaks, every peak has the same height and they all reach unity at $\Phi = 0, \pm 2\pi, \pm 4\pi, \pm 6\pi, \dots$.

4.7 Two-Ring Resonator: Depth of Modulation

In a DWDM system we need an optical filter which passes through only one (modulated) signal channel with all its spectral components and rejects all of the others. The rejection of the channels that we do not need is also very important in order to avoid unwanted superposition at the receiver, which is known as “cross-talk”. Therefore, as explained in Section 2.8 the intensity transfer function between our selected channels should be zero, as far as possible. Figure 4-14 is for the same ring design as Figure 4-12 but the vertical axis is logarithmic to exaggerate the features at very low relative intensities. Unfortunately, the depth of modulation is 20dB and this is unlikely to be sufficient for many optical fibre transmission systems. Figure 4-15 is the equivalent plot to Figure 4-13 and it displays a depth of modulation of 40dB. This is a

good out-of-band rejection that corresponds to one part in ten thousand of the transmitted power at the peaks. Such performance is much more suitable for modern WDM communications.

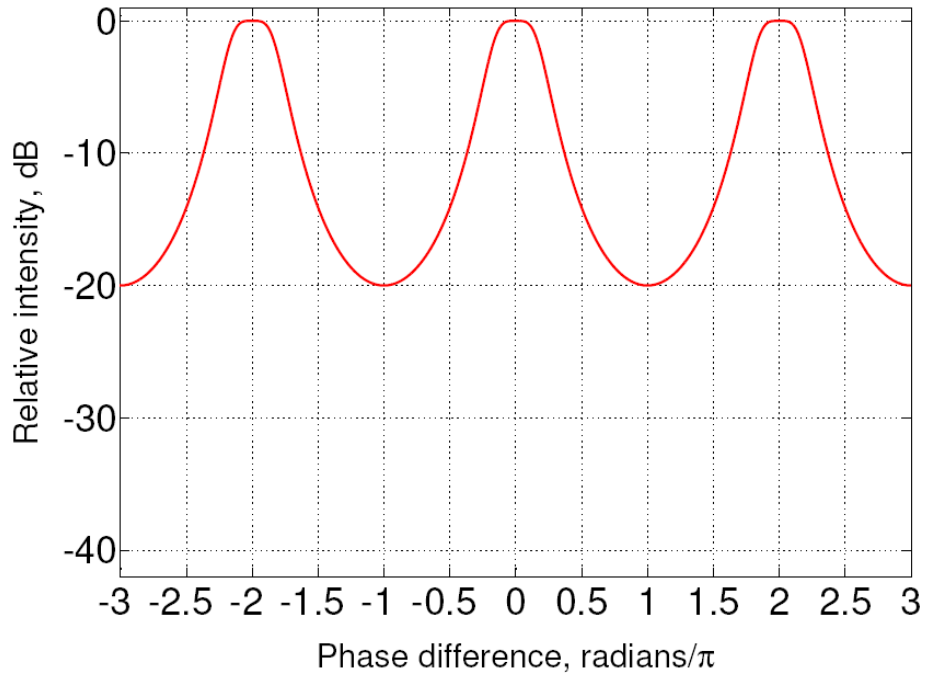


Figure 4-14 *Transfer function for a two-ring resonator with equal outer couplers, effective reflectances of $r_1^2=0.818$ and $r^2=0.402$ and zero losses. The reflectances conform to the degeneracy condition. The depth of modulation is 20dB in a logarithmic scale.*

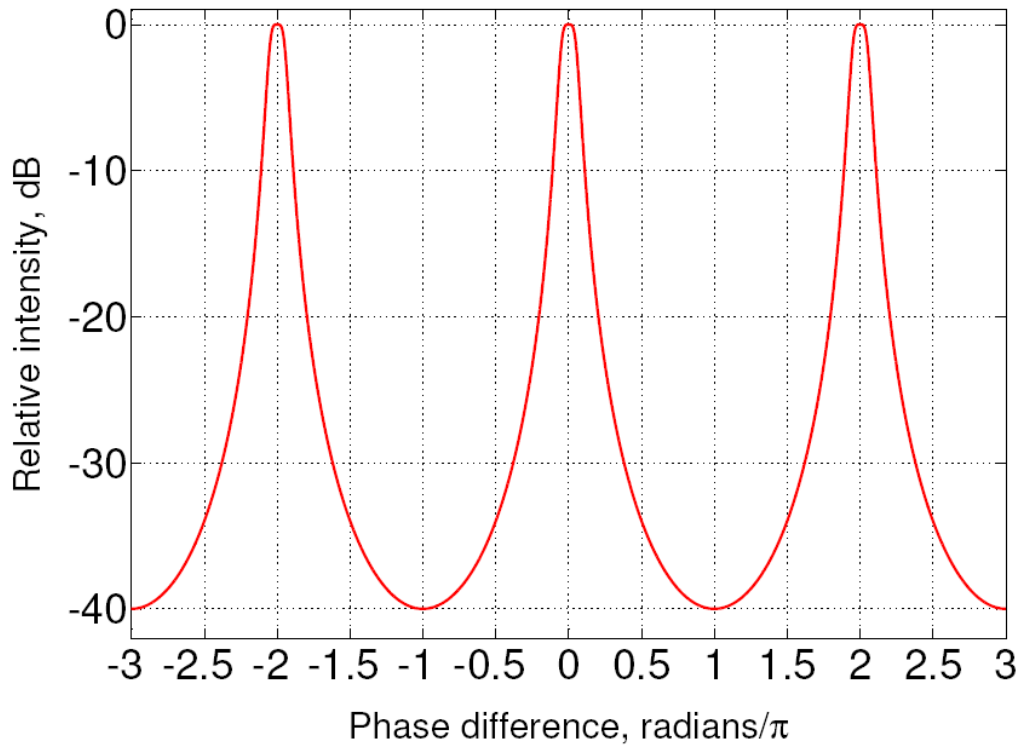


Figure 4-15 Transfer function for a two-ring resonator with equal outer couplers, effective reflectances of $r_1^2=0.980$ and $r^2=0.753$ and zero losses. The reflectances conform to the degeneracy condition. The depth of modulation is 40dB in a logarithmic scale.

Although we have shown that the degeneracy condition for r_1^2 (Equation 4.41) gives us good characteristics for the peaks, it does not predict the rejection between the peaks. We therefore need another expression to specify the minima of $Y(\Phi)$ when our degeneracy condition applies and we use it to determine the depth of modulation, as defined in Section 2.8. In order to do this we continue to assume equal ring circumferences for the rings, $L_1=L_2=L$, and zero losses $\alpha=0$. Therefore, we use all of the results we achieved until now for our next steps.

We have shown that the minima occur $\Phi = \pm\pi, \pm3\pi, \pm5\pi, \pm7\pi$, and so on, and for this the transfer function obeys Equation (4.30). We also have to consider Equation (4.41), which is our degeneracy condition for the effective reflectance for the middle coupler, r_1^2 . The T^2 term, with its associated effective reflectances, which are shown in Equation (4.34), are also substituted and we replace the denominator with Equation (4.21) and (4.22). So we obtain Equation (4.44).

$$Y_{min} = \frac{(1-r^2)^2(1-r_1^2)}{[1+2r \cdot r_1 + r^2]} \quad (4.44)$$

In order to keep our goal of no double peaks and full intensity we have to include our degeneracy condition, by replacing r_1 with Equation (4.40) and we arrive at Equation (4.45).

$$Y_{min} = \frac{(1-r^2)^2 \left(1 - \left(\frac{4r^2}{(1+r^2)^2} \right) \right)}{\left[1 + 2r \cdot \left(\frac{2r}{1+r^2} \right) + r^2 \right]} \quad (4.45)$$

So we can change the subject of this formula until we obtain Equation (4.46).

$$r^4 + \left[\frac{2 \cdot (3 \cdot Y_{min}^{1/2} + 1)}{(Y_{min}^{1/2} - 1)} \right] \cdot r^2 + 1 = 0 \quad (4.46)$$

This equation is a quadratic in r^2 and so it can easily be solved to give Equation (4.47).

$$r^2 = \frac{(1+3 \cdot Y_{min}^{1/2}) \pm 2 \cdot \sqrt{2 \cdot Y_{min}^{1/2} \cdot (1+Y_{min}^{1/2})}}{(1-Y_{min}^{1/2})} \quad (4.47)$$

Equation (4.47) contains a \pm sign, which follows from the quadratic equation, giving two different values for r^2 . So we have to interpret which one provides useful values for r^2 . We have tried both possibilities and found values in excess of unity when incorporating the “+” sign, which is not possible for our passive optical filter. Clearly, this is a non-physical solution because r^2 must lie between zero and one. Consequently, we must use the minus sign and we have a final formula for the effective reflectance r^2 in terms of the minimum value of the transfer function, Y_{min} . See Equation (4.48).

$$r^2 = \frac{(1+3 \cdot Y_{min}^{1/2}) - 2 \cdot \sqrt{2 \cdot Y_{min}^{1/2} \cdot (1+Y_{min}^{1/2})}}{(1-Y_{min}^{1/2})} \quad (4.48)$$

This formula gives us the possibility to obtain a value for r^2 by choosing Y_{min} . Furthermore, inclusion of the degeneracy condition ensures single peaks that always reach unity. If we consider the formula for the depth of modulation, which is described in Section 2.8, we obtain Equation (4.49) because in the present circumstances the depth of modulation is $Y_{max}/Y_{min} = 1/Y_{min}$. Thus, we have

$$M_{dB} = -10 \cdot \log(Y_{min}) \quad (4.49)$$

$$Y_{min} = 10^{(-M_{dB}/10)} \quad (4.50)$$

We can now use Equation (4.50) in combination with Equation (4.48) to calculate a value for the effective reflectances r^2 for the outer couplers. A value for the middle effective reflectance r_1^2 is then determined using Equation (4.41). We thus have a design procedure to obtain valuable filtering responses from two-ring resonators that is very easy to implement.

We present an example that shows how all the equations work with each other. If the required depth of modulation is $M_{dB} = 38\text{dB}$ then we obtain for $Y_{min} = 1.58 \cdot 10^{-4}$. By substituting Y_{min} into Equation (4.48) we obtain the effective reflectances for r^2 that correspond to both outer couplers: $r^2 = 0.7276$. We can then use that value to calculate r_1^2 with help of Equation (4.41) which gives a value of 0.9751. The appropriate transfer function is plotted in Figure 4-16.

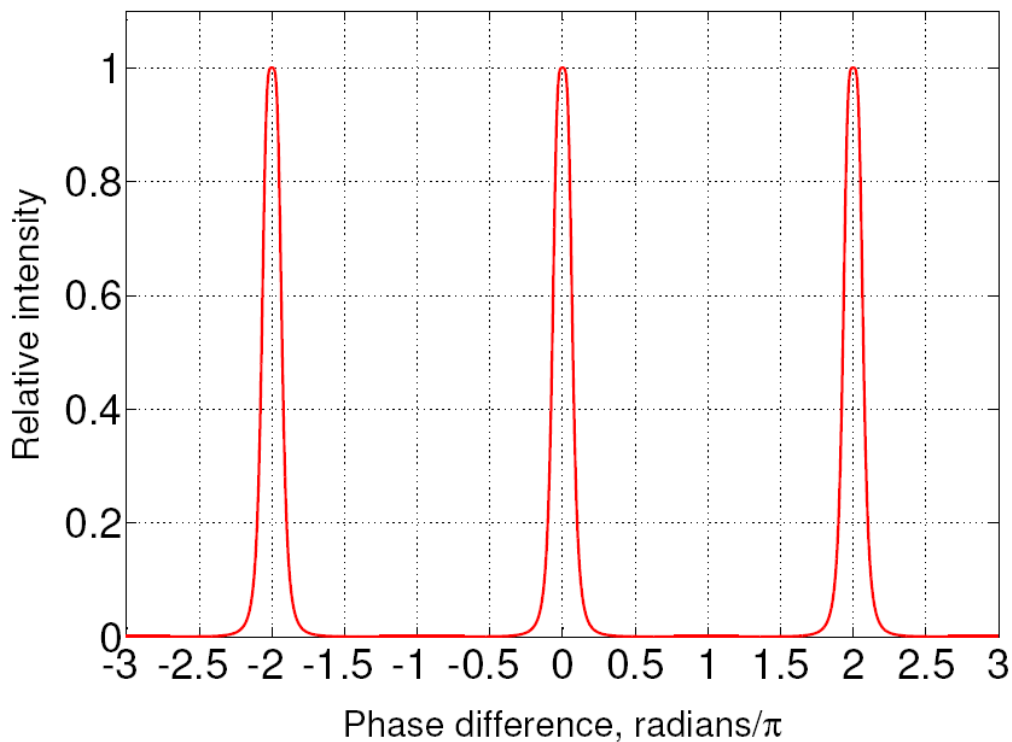


Figure 4-16 Transfer function for a two-ring resonator with equal outer couplers that is designed for single peaks of unity transmission and a depth of modulation of 38dB. The effective reflectances are $r^2 = 0.7276$ and $r_1^2 = 0.9751$. All losses were assumed to be zero.

In Figure 4-16 we achieved a transfer function for a two-ring resonator with a better profile than would be possible using single ring. Comparison with Figure 4-2, which is for a one-ring resonator, shows performance that is rather more box-like and therefore clearly superior. This invites the question of whether three-ring resonators will provide yet better results. The issue is addressed in Section 4.10.

4.8 Two-Ring Resonator: Finesse

The concept finesse is defined in Section 2.2: it is the ratio of the free spectral range to the full width at half maximum of the peaks. Finesse is not appropriate for use in multi-peaked transfer functions (such as Figures 4-7 and 4-8). However, it can be applied for two-ring resonators with $L_1 = L_2 = L$ and subject to the degeneracy condition. We continue to assume negligible losses so that $\alpha = 0$ and $t^2 + r^2 = 1$. We know from Section 2.2 that the free spectral range is the difference between any two

resonances. The peaks appear at $0, \pm 2\pi, \pm 4\pi, \pm 6\pi, \pm 8\pi, \dots$ and so $\Delta\Phi = 2\pi$, corresponding in frequency space to $\Delta\nu = c/(n_{\text{eff}} \cdot L)$

We require an expression for the full width at half maximum of the peaks $\delta\Phi_{1/2}$, which we obtain by starting with our intensity transfer function using Equations (4.19) and (4.32). The maximum of the transfer function is provided by Equation (4.31), in which T^2 is given by Equation (4.19). Equation (4.32) also includes the constants A, B and C, which are defined by Equations (4.25) – (4.27). The quantities that we require to calculate $\delta\Phi_{1/2}$ are the phases when the transfer function has the value of one half of the peak height and thus,

$$\frac{(1-r^2)^2(1-r_1^2)}{A+(B-4 \cdot C) \cdot \sin^2\left[\frac{\Phi}{2}\right]+4 \cdot C \cdot \sin^4\left[\frac{\Phi}{2}\right]} = \frac{(1-r^2)^2(1-r_1^2)}{2 \cdot A} \quad (4.51)$$

This then gives us

$$4 \cdot C \cdot \sin^4\left[\frac{\Phi}{2}\right] + (B - 4 \cdot C) \cdot \sin^2\left[\frac{\Phi}{2}\right] - A = 0 \quad (4.52)$$

Equation (4.52) is a quadratic equation in $\sin^2[\Phi/2]$ and its solution is provided in Equation (4.53).

$$\sin^2\left[\frac{\Phi}{2}\right] = \frac{(4 \cdot C - B) \pm \sqrt{(4 \cdot C - B)^2 + 16 \cdot A \cdot C}}{8C} \quad (4.53)$$

The constants A, B and C can be substituted to give:

$$(8 \cdot C) = 32 \cdot r^2 \quad (4.54)$$

$$(16 \cdot A \cdot C) = 64 \cdot r^2 \cdot \left[\frac{(1-r^2)^4}{(1+r^2)^2} \right] \quad (4.55)$$

$$(4 \cdot C - B) = 0 \quad (4.56)$$

We can then substitute Equations (4.54) to (4.56) into Equation (4.53) and achieve an expression for $\sin^2[\Phi/2]$. See Equation (4.57).

$$\sin^2 \left[\frac{\Phi}{2} \right] = \pm \frac{(1-r^2)^2}{4 \cdot r \cdot (1+r^2)} \quad (4.57)$$

This equation gives the possibility of imaginary values of Φ ($\sqrt{-1} = i$) from the argument of \sin^{-1} because of the square root. We ignore them because they do not seem to have a physical significance. Therefore, the half peak height occurs when

$$\Phi_{\frac{1}{2}} = 2 \cdot \sin^{-1} \left\{ \pm \left[\frac{(1-r^2)^2}{4 \cdot r \cdot (1+r^2)} \right]^{1/2} \right\} \quad (4.58)$$

Equation (4.58) gives us values which are placed on each side of every $0, \pm 2\pi, \pm 4\pi, \pm 6\pi, \pm 8\pi$ and so on. When the peaks are narrow, we have small values for the argument and thus to a first approximation from a Taylor series expansion $\sin^{-1}[\Theta] \approx \Theta$. We can thus simplify this Equation (4.58) and we obtain $\Phi_{\pm \frac{1}{2}}$, which is shown in Equation (4.59).

$$\Phi_{\pm \frac{1}{2}} = \pm \frac{(1-r^2)}{[r \cdot (1+r^2)]^{1/2}} \quad (4.59)$$

We achieve the bandwidth $\delta\Phi_{1/2}$ of the peak with $(\Phi_{+\frac{1}{2}} - \Phi_{-\frac{1}{2}})$ and we obtain Equation (4.60).

$$\delta\Phi_{\frac{1}{2}} = \frac{2 \cdot (1-r^2)}{[r \cdot (1+r^2)]^{1/2}} \quad (4.60)$$

We have the free spectral range $\Delta\Phi$ and the full width at half maximum $\delta\Phi_{1/2}$ and we can therefore calculate the finesse. See Equations (4.61) and (4.62)

$$F = \frac{\Delta\Phi}{\delta\Phi_{\frac{1}{2}}} = \frac{\Delta\nu}{\delta\nu_{\frac{1}{2}}} = \frac{2 \cdot \pi}{\frac{2 \cdot (1-r^2)}{[r \cdot (1+r^2)]^{1/2}}} \quad (4.61)$$

$$F = \frac{\pi \cdot [r \cdot (1+r^2)]^{1/2}}{(1-r^2)} \quad (4.62)$$

Finally, we have a function for the Finesse of a double-ring resonator with equal ring lengths, negligible losses and at the degeneracy condition. Figure 4-17 shows the finesse (expressed in dB) as a function to the effective reflectance r^2 , which are the effective reflectances for the outer couplers.

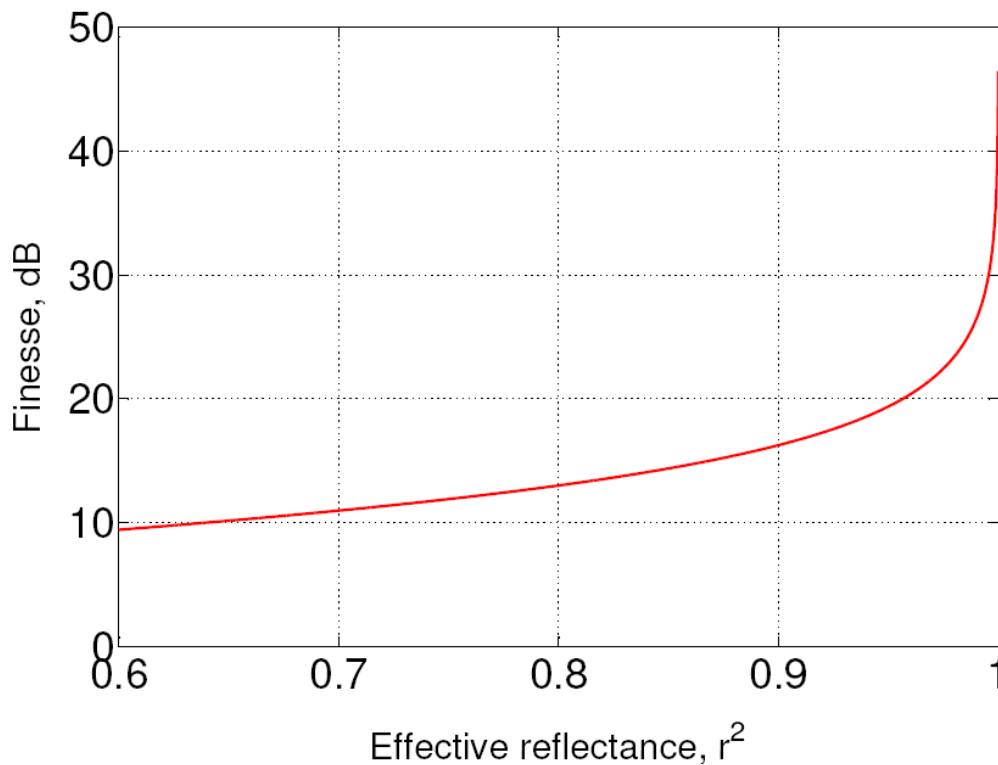


Figure 4-17 Variation of Finesse (in dB) as a function of effective reflectance of the outer couplers for a two-ring resonator with negligible losses and effective reflectances that obey the degeneracy condition.

Figure 4-17 shows that the finesse tends to infinity as r^2 becomes ever closer to unity. In this respect the behaviour is similar to that of a single resonator, be it a ring or a Fabry-Pérot design. (Figure 4-17 should be compared with Figure 4-5).

However, the functional form of Equation (4.62) is different from a single-ring resonator, which results from the (desirable) different peak shapes that a double ring can provide. In many applications of resonant structures, such as Fabry-Pérot filters for spectroscopy, the aim is to achieve very high values of F (for example over 1000). This is not the case in our present work, where we aim to achieve box-like pass-bands. For this reason, the finesse is a less important figure of merit in our current project that it would be in other applications of optical resonators.

4.9 Two-Ring-Resonator: The Influence of Loss

In the sections to this point we have ignored the losses that exist in integrated and fibre optical waveguides. We consider the influence of the loss coefficient α . Losses in integrated optical waveguides are most commonly quoted in a centimetre-gram-second (c.g.s.) system which has a unit of dB/cm, probably because its original usage was American. The European normally use the International System of units (SI units). Although coupler losses are also possible, their influence on the equations is very similar and, owing to limited time, we concentrate on the losses which appear in a waveguide. One reason for the loss is the absorption in the material of which the waveguide is constructed. Scattering losses often occur due to microscopic perturbations in the waveguide uniformity. However, the loss which is likely to be the greatest is the bending loss, especially with small-radius rings.

In our formulas we have $\exp[-\alpha \cdot L]$ and $\exp[-\alpha \cdot L/2]$ terms, where α is the intensity loss coefficient in m^{-1} and L is the length in meters. In the case of intensity we have

$$\frac{P_{out}}{P_{in}} = \exp[-\alpha \cdot L] \quad (4.63)$$

where

$$\alpha = -\left(\frac{1}{L}\right) \cdot \ln \left[\frac{P_{out}}{P_{in}} \right] \quad (4.64)$$

and “ln” is the natural logarithm. Now we have loss in dB/m, which gives us Equation (4.65).

$$x_{[m]} = 10 \cdot \log_{10} \left[\frac{P_{out}}{P_{in}} \right] \quad (4.65)$$

In Equation (4.65) the subscript “[m]” designates meters and it measured over a one meter length. We transform Equation (4.65) and obtain

$$\frac{P_{out}}{P_{in}} = 10^{\left(\frac{x_{[m]}}{10}\right)} \quad (4.66)$$

Substitute Equation (4.66) in Equation (4.64), and we arrive at

$$\alpha = -\left(\frac{1}{L}\right) \cdot \ln \left[10^{\left(\frac{x_{[m]}}{10}\right)} \right] \quad (4.67)$$

We form Equation (4.67) and obtain:

$$\alpha = 0.23026 \cdot \left(\frac{x_{[m]}}{L}\right) \quad (4.68)$$

We have defined $x_{[m]}$ so as to cancel out the negative sign. In a waveguide with losses we have $P_{out} < P_{in}$ and so $x_{[m]}$ is a negative number of decibels. We have a formula to translate the SI units to the loss coefficient in our formula but we need an expression for the c.g.s. units so we must convert $(x_{[m]}/L)$ to $(x_{[cm]}/L)$. It is given that $1\text{m} = 100\text{cm}$, so we must multiply $(x_{[m]}/L)$ by 100 and we have

$$\alpha = 23.026 \cdot \left(\frac{x_{[cm]}}{L}\right) \quad (4.69)$$

Equation (4.69) enables us to convert quoted loss values from research papers or manufactured products and convert them to a form that is suitable for our equations.

We give an example of how we can use Equation (4.69). We have a ring circumference of $200\mu\text{m}$, which corresponds to $2 \cdot 10^{-4}\text{m}$. Figure 4-16 shows an enlargement of three curves of the transfer function of a two-ring resonator. Its

effective reflectances were selected to conform to the degeneracy condition for a two ring resonator and a provide depth of modulation of 42dB when all losses are zero. We also assumed equal ring circumferences so that $L_1 = L_2 = L$ and equal outer couplers so that the corresponding effective reflectances are $r_0^2 = r_2^2 = r^2$. We kept these values constant and observe the behaviour of the transfer profile when using losses greater than zero, $\alpha \geq 0$. So that the top curve in red has no loss, $\alpha = 0$. We chose a loss of 3dB/cm for the centre curve (blue), corresponding to $\alpha = 69,078\text{m}^{-1}$, and 6dB/cm for the bottom curve (black), corresponds to $\alpha = 138,156\text{m}^{-1}$.

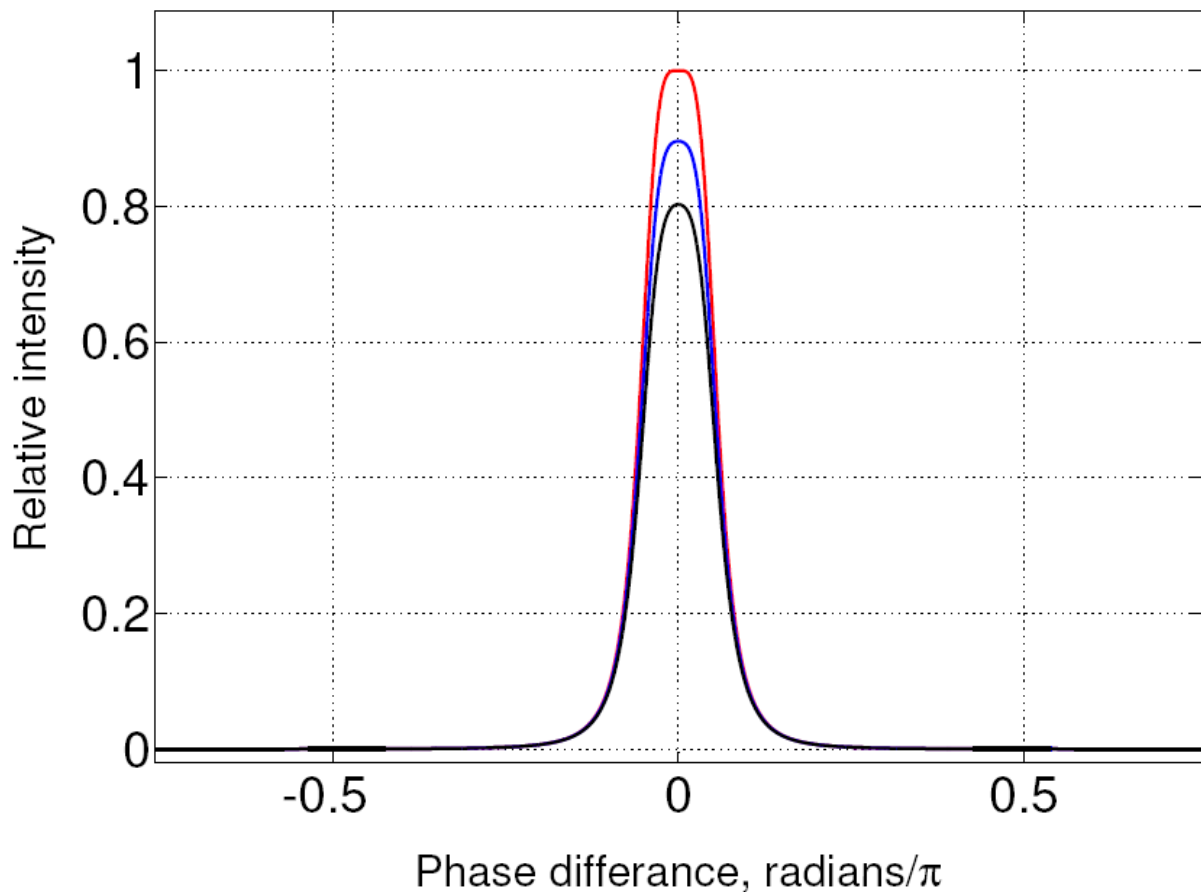


Figure 4-18 One peak of the transfer functions of a two-ring resonator, which has equal outer coupler and ring circumferences $L_1 = L_2 = L = 200\mu\text{m}$. Each curve has the same effective reflectances of $r^2 = 0.777$ and $r_1^2 = 0.984$. Loss coefficients: 0dB/cm (top curve, red), 3dB/cm (centre curve, blue), 6dB/cm (bottom curve, black).

As Figure 4-18 shows loss reduces the performance of the two-ring resonator. The peak height is reduced from 100%, in the zero loss limit to 89,6% and 80,3% with 3dB/cm and 6dB/cm, respectively. Careful observation of the graph also reveals a

slight change in shape; there is a small reduction in the flattening very close to $\Phi = 0$ radians. Nevertheless, there are positive aspects to be emphasised. First, there is no evidence of double peaks, as shown, for example, in Figure 4-8. Second, there does not appear to be a marked influence on the peak's full width at half maximum. Third, when we have examined the depth of modulation, it remains very close to 42dB, the zero loss value. Although waveguide loss reduces the transmitted power at the resonant frequencies, it has very little effect at $\pm\pi$, $\pm3\pi$, $\pm5\pi$, etc, where the transfer function is a minimum. The reason is that there is very little energy stored in the cavities at the frequencies mid-way between the resonances.

4.10 Three-ring resonator

As we have seen, the two-ring resonator gives us a better profile response than the one-ring resonator and so investigation of the three-ring structure is the logical next step. The intensity transfer function becomes correspondingly larger, as indicated in Equations (4.70) – (4.78), with respect to circumferences L_1 , L_2 and L_3 .

$$\left| \frac{E_{out}^+}{E_{in}^+} \right|^2 = \frac{|T|^2}{|D|^2} \quad (4.70)$$

Where the numerator term is

$$|T|^2 = t_0^2 \cdot t_1^2 \cdot t_2^2 \cdot t_3^2 \quad (4.71)$$

and the denominator is

$$\begin{aligned} |D|^2 = & [1 - R_{01} - R_{12} - R_{23} + R_{02} + R_{13} - R_{03} + R_{01} \cdot R_{23}]^2 \quad (4.72) \\ & + 4 \cdot [R_{01}(1 + R_{23}^2) + R_{12} \cdot R_{02} + R_{13} \cdot R_{03}] \cdot \sin^2 \left[\frac{\Phi_1}{2} \right] \\ & + 4 \cdot [R_{12} + R_{01} \cdot R_{02} + R_{23} \cdot R_{13} + R_{01} \cdot R_{23} \cdot R_{03}] \cdot \sin^2 \left[\frac{\Phi_2}{2} \right] \\ & + 4 \cdot [R_{23}(1 + R_{01}^2) + R_{12} \cdot R_{13} + R_{02} \cdot R_{03}] \cdot \sin^2 \left[\frac{\Phi_3}{2} \right] \end{aligned}$$

$$\begin{aligned}
 & -4 \cdot [R_{02} + R_{23} \cdot R_{03}] \cdot \sin^2 \left[\frac{(\Phi_1 + \Phi_2)}{2} \right] \\
 & -4 \cdot [R_{13} + R_{01} \cdot R_{03}] \cdot \sin^2 \left[\frac{(\Phi_2 - \Phi_3)}{2} \right] \\
 & -4 \cdot [R_{01} \cdot R_{23} + R_{12} \cdot R_{03}] \cdot \sin^2 \left[\frac{(\Phi_1 + \Phi_3)}{2} \right] \\
 & -4 \cdot R_{01} \cdot [R_{12} + R_{23} \cdot R_{13}] \cdot \sin^2 \left[\frac{(\Phi_1 - \Phi_2)}{2} \right] \\
 & -4 \cdot R_{23} \cdot [R_{12} + R_{01} \cdot R_{02}] \cdot \sin^2 \left[\frac{(\Phi_2 - \Phi_3)}{2} \right] \\
 & -4 \cdot [R_{01} \cdot R_{23} + R_{02} \cdot R_{13}] \cdot \sin^2 \left[\frac{(\Phi_1 - \Phi_3)}{2} \right] \\
 & +4 \cdot [R_{23} \cdot R_{02}] \cdot \sin^2 \left[\frac{(\Phi_1 + \Phi_2 - \Phi_3)}{2} \right] \\
 & +4 \cdot [R_{01} \cdot R_{13}] \cdot \sin^2 \left[\frac{(-\Phi_1 + \Phi_2 + \Phi_3)}{2} \right] \\
 & +4 \cdot [R_{01} \cdot R_{12} \cdot R_{23}] \cdot \sin^2 \left[\frac{(\Phi_1 - \Phi_2 + \Phi_3)}{2} \right] \\
 & +4 \cdot R_{03} \cdot \sin^2 \left[\frac{(\Phi_1 + \Phi_2 + \Phi_3)}{2} \right]
 \end{aligned}$$

The effective reflectances are given by

$$R_{01} = r_0 \cdot r_1 \cdot \exp[-\alpha \cdot L_1/2] \quad (4.73)$$

$$R_{12} = r_1 \cdot r_2 \cdot \exp[-\alpha \cdot L_2/2] \quad (4.74)$$

$$R_{23} = r_2 \cdot r_3 \cdot \exp[-\alpha \cdot L_3/2] \quad (4.75)$$

$$R_{02} = r_0 \cdot (t_1^2 + r_1^2) \cdot r_2 \cdot \exp[-\alpha \cdot (L_1 + L_2)/2] \quad (4.76)$$

$$R_{13} = r_1 \cdot (t_2^2 + r_2^2) \cdot r_3 \cdot \exp[-\alpha \cdot (L_1 + L_3)/2] \quad (4.77)$$

$$R_{03} = r_0 \cdot (t_1^2 + r_1^2) \cdot (t_2^2 + r_2^2) \cdot r_3 \cdot \exp[-\alpha \cdot (L_1 + L_2 + L_3)/2] \quad (4.78)$$

The phase shifts for individual ring transits are

$$\Phi_1 = \beta \cdot L_1 \quad (4.79)$$

$$\Phi_2 = \beta \cdot L_2 \quad (4.80)$$

$$\Phi_3 = \beta \cdot L_3 \quad (4.81)$$

All of the phase components of Equation (4.72) are in the \sin^2 -format, in which there is a complicated collection of constituents. We can observe components that result from (a) Φ_1 , Φ_2 and Φ_3 , the resonances of the individual cavities, (b) all possible pairs such as $(\Phi_1 + \Phi_2)$, which are resonances of double cavities within the entire structure, (c) every possible combination of difference frequency terms, such as $(\Phi_1 - \Phi_2)$, (d) hybrid terms, such as $(\Phi_1, \Phi_2 - \Phi_3)$, which results from the greatest possible resonant path through the entire compound assembly. Although the analogy is not exact, it is interesting to compare the terms in Equation (4.72) with the sum and difference frequencies which are observed in nonlinear optical processes, such as four-wave mixing and other parametric effects [12]. Many possible interactions take place within a three-ring structure, leading to potentially complicated spectra.

The three-ring resonator clearly has a much more complicated behaviour than the two-ring resonator and in particular there is a tendency to display triple – peak feature. Given that we require single peak resonances with unity throughput, we have targeted our investigation at equal ring circumferences, as shown in Figure 4-19: $L_1 = L_2 = L_3 = L$. In Figure 4-19 we also show how we chose the inner coupling coefficients to be equal so that $r_1^2 = r_2^2 = r_b^2$ and the outer coupler $r_0^2 = r_3^2 = r_a^2$.

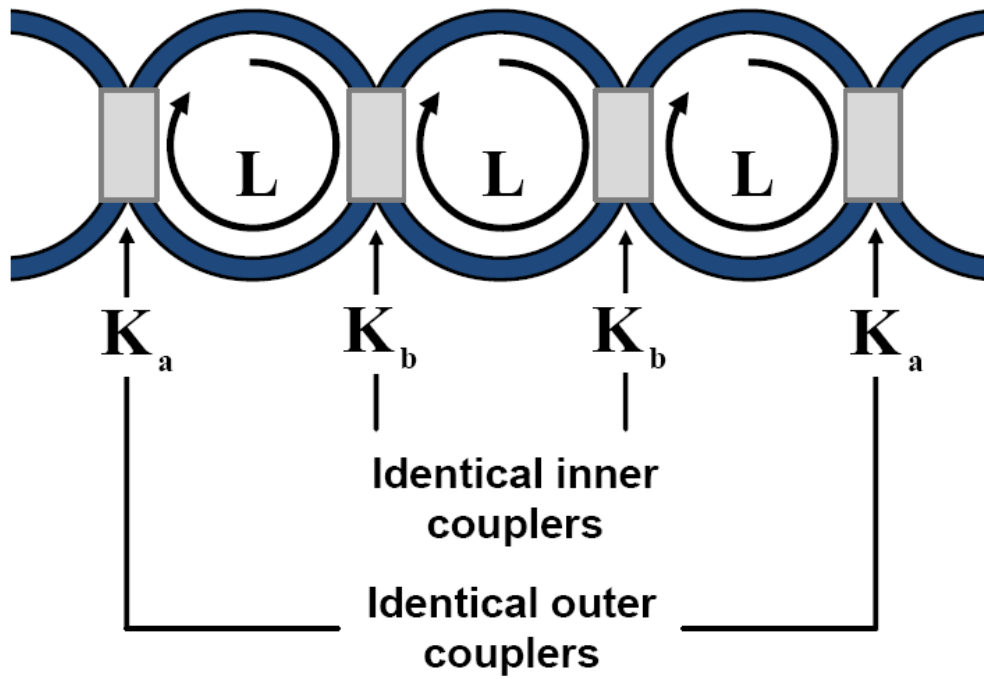


Figure 4-19 Three-ring resonator with equal ring circumferences and effective reflectances that conform to $r_a^2=(1-K)$ and $r_b^2=(1-K_b)$.

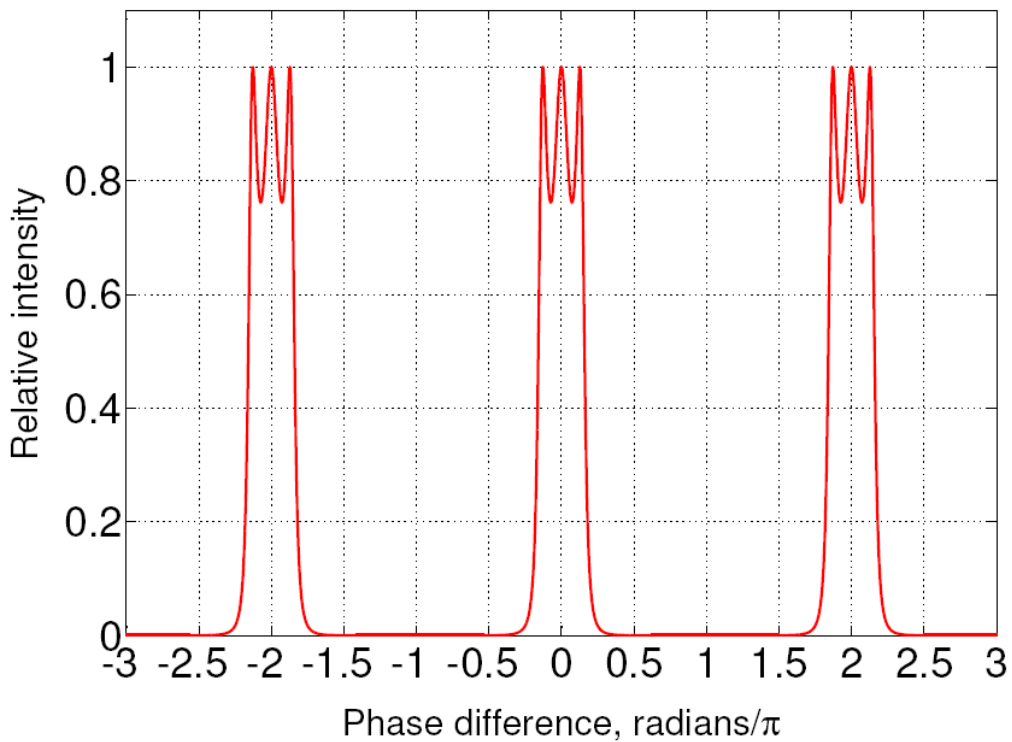


Figure 4-20 Three-ring resonator with equal ring circumferences and different but equal outer coupler and effective reflectances $r_a^2=0.65$ and $r_b^2=0.9$.

In Figure 4-20 is pictured the intensity function of the three-ring resonator as illustrated of Figure 4-19. There are resonances centred on $0, \pm 2\pi, \pm 4\pi, \pm 6\pi, \dots$, as in the two-ring resonator theory but we now see that each one has three symmetrical peaks. Nevertheless, the relative intensity is very low at $\pm\pi, \pm 3\pi, \pm 5\pi, \dots$, where we expect the global minima to be and the triple maxima on Figure 4-20 appear to reach 100% transmission. We therefore have grounds to believe that appropriate filtering performance can be obtained with careful selection of the effective reflectances. To reach our goal of having a box-like function at every peak and reaching full magnitudes, we have to find a “degeneracy condition” as we did for the two-ring resonator in Section 4.6. We have done this; the calculation used the same method that we previously presented. We do not state the intermediate steps in what turned out to be a lengthy calculation but the formula that we obtained is:

$$r_b = \frac{[r_a^4 + 14 \cdot r_a^2 + 1]^{1/2} - (r_a^2 + 1)}{2 \cdot r_a} \quad (4.82)$$

The effective reflectance for the inner coupling ratio r_b^2 is then given by

$$r_b^2 = \frac{\{[r_a^4 + 14 \cdot r_a^2 + 1] - (r_a^2 + 1)\}^2}{4 \cdot r_a^2} \quad (4.83)$$

Equation (4.83) provides a relationship between the inner and the outer effective reflectances that we must satisfy in order to achieve degenerate operation. In Figure 4-21 we have an example for the three-ring resonator where we included the degeneracy condition. The values that we used are $r_a^2 = 0.61$ and $r_b^2 = 0.97$. We assumed negligible losses, so that $\alpha = 0$ and $t_j^2 + r_j^2 = 1, j = a, b$. There are no triple peaks and the relative intensity on the resonances at $0, \pm 2\pi, \pm 4\pi, \pm 6\pi, \dots$.

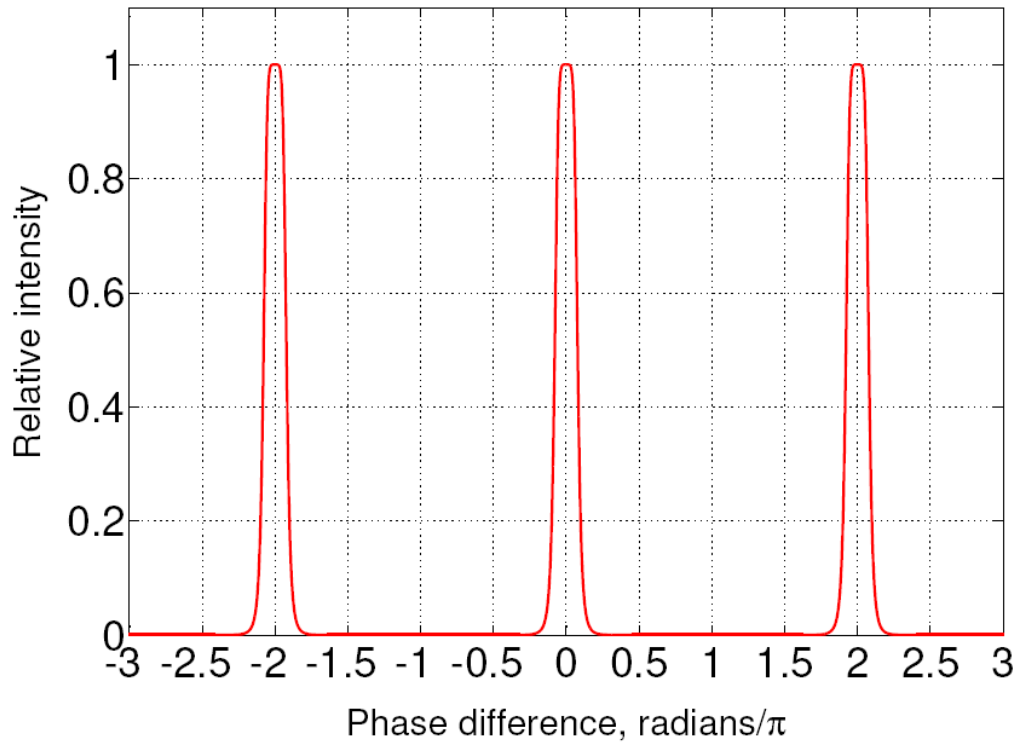


Figure 4-21 Transfer function of a three-ring resonator with equal ring circumferences and effective reflectances $r_a^2 = 0.61$ and $r_b^2 = 0.97$. All losses were neglected

The value for the outer effective reflectance, r_a^2 that we used to obtain Figure 4-21 was chosen by trial and error. Thereafter, the degeneracy condition, Equation (4.83), enables us to select r_b^2 . Just as in Section 4.7, we would like to design the rings to obtain a predetermined out-of-band rejection and therefore depth of modulation. Unfortunately, owing to the limited time for the project, it was not possible to derive an equivalent formula to Equation (4.48) for application to a three-ring resonator. Nevertheless, we are optimistic that such an equation can be obtained, as it does not appear to demand advanced mathematical techniques. Once available, it could be used in conjunction with Equation (4.83) to ensure the combined desirable features of single peak resonances, which reach unity relative intensity in the zero loss limit, together with a depth of modulation that is no less than some prior specification.

4.11 Comparison of Optimised Ring Transfer Functions

The previous sections have described how to optimise the spectral profile of one-, two- and three-ring resonators. We now compare them on a decibel scale in one plot. Each one is designed to ensure single peaks of unity relative intensity and

to have a depth of modulation of 42dB. The values for the three-ring resonator were found by trial and error to achieve our required depth of modulation. In the two- and three-ring structures, we assume equal ring circumferences, $L_1 = L_2 = L_3$ and equal outer couplers, which differed from the outer ones. Losses were neglected. The values of effective reflectance that we used to obtain Figure 4-22 are stated in Table 4-1.

Number of Rings	r_0^2	r_1^2	r_2^2	r_3^2
1	0.98424	0.98424	x	x
2	0.77692	0.98424	0.77692	x
3	0.448945	0.92273	0.92273	0.448945

Table 4-1 Values of effective reflectances used to obtain the curves shown on Figure 4-22.

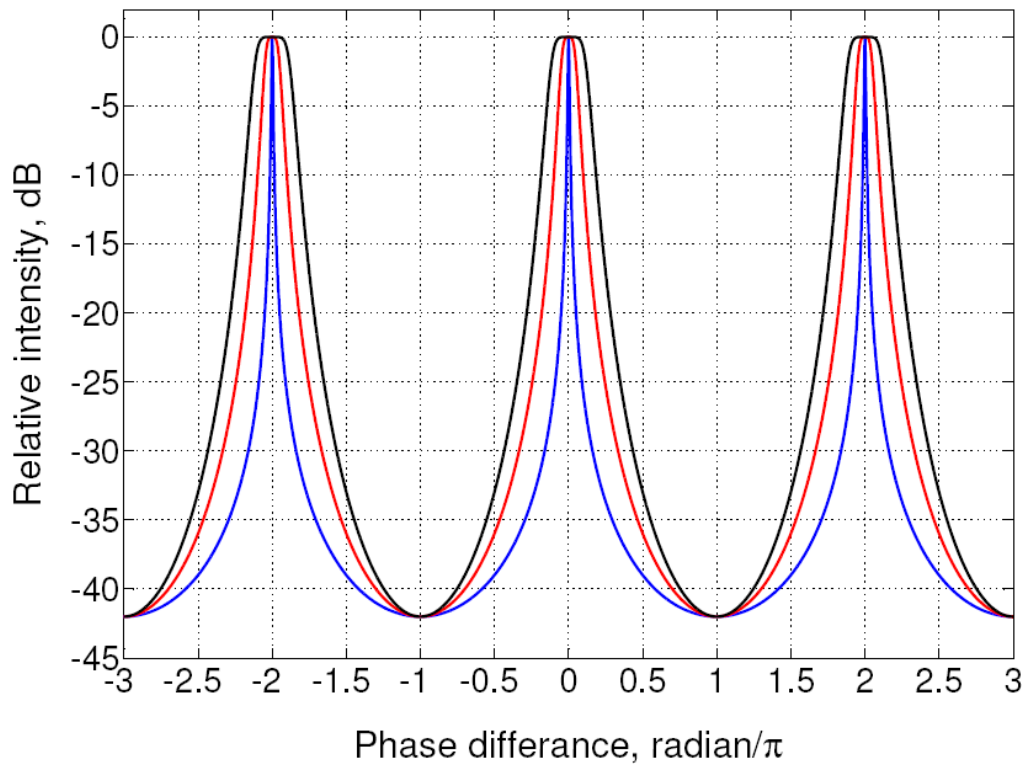


Figure 4-22 Transfer function of one-, two- and three-ring resonators on a decibel scale. Each one has a depth of modulation of 42 dB. The effective reflectances are listed on Table 4-1. Inner curve(blue): one ring, centre curve(red): two rings, outer curve(black): three rings.

Figure 4-23 shows the different profiles of the three curves, each with a depth of modulation of 42dB. There is a progressive broadening of the pass band's and the peaks at around 0dB become progressively flatter as we increase the number of rings. It is interesting to observe the pass-band in greater detail, as we do on a linear scale in Figure 4-23 for the phase difference at $\Phi = 0$. There is a clear progression towards our desired “box-like” profile.

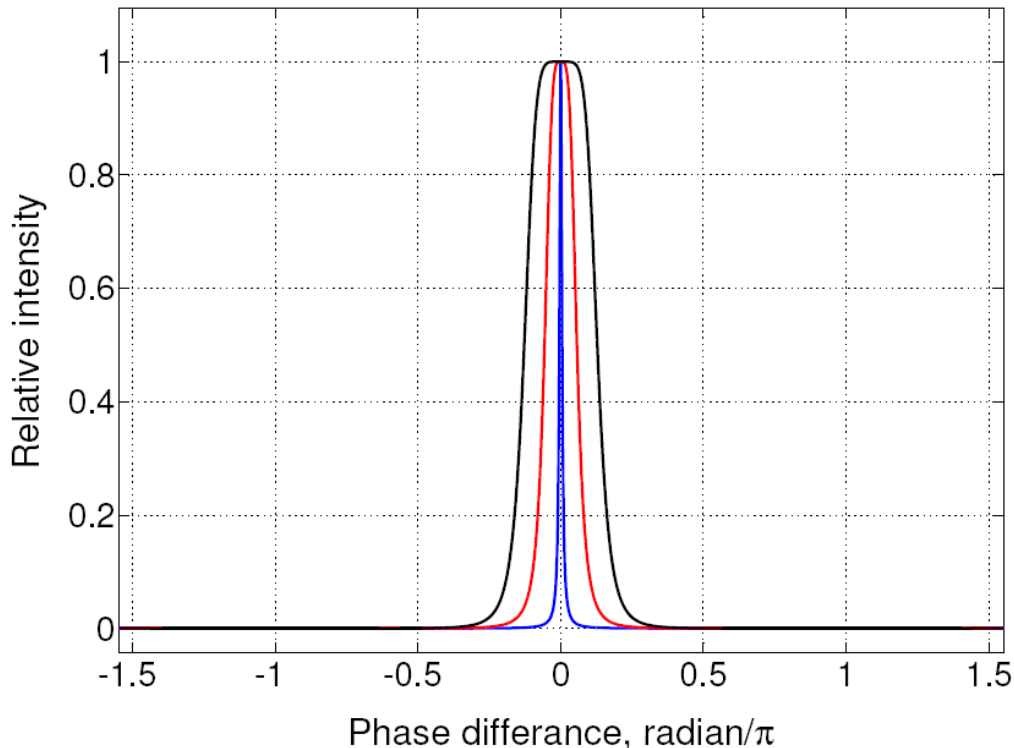


Figure 4-23 Transfer function of one-, two- and three-ring resonators on a linear scale. Each one has a depth of modulation of 42 dB. The effective reflectances are listed on Table 4-1. Inner curve(blue): one ring, centre curve(red): two rings, outer curve(black): three rings.

Our main goal is to create a box-like filter profile, which has broad and flat peaks. Figure 4-24 is an enlargement of Figure 4-23 at around $\Phi = 0$, which clearly illustrates how we can obtain an impressively flattened peak with three optimally designed rings. If the outer curve should have a bandwidth that is too broad there is not necessarily a problem. Quite simply, we can re-design it to have a very high depth of modulation (such as over 60dB) and in this way the peak will become narrower. Figure 4-23 is a vivid illustration that the single-ring resonator does not necessarily satisfy our needs because of its very small bandwidth. The two-ring resonator has a much better filter profile and it might be useful for some network

applications but it is very obvious that the three-ring resonator gives us greatest design freedom.

Figures 4-22 to 4-24 give us a very clear message: Increasing the number of rings improves our ability to achieve “box-like” spectra. We continue our study of multiple-ring structures in Chapter 5 with the aid of a more advance matrix computational technique.

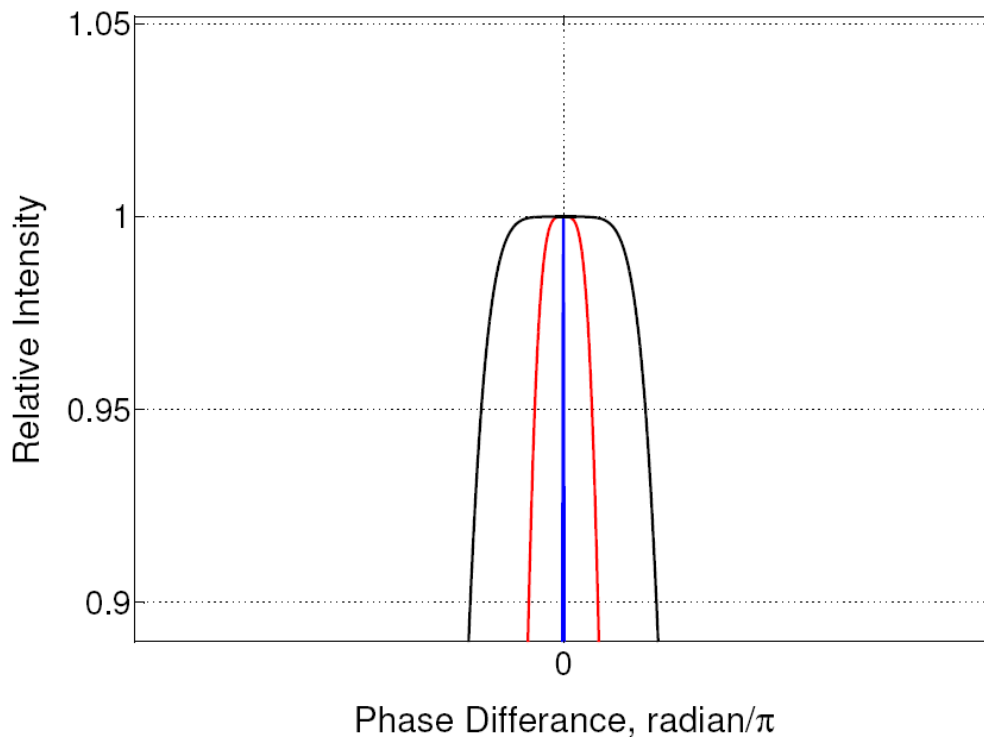


Figure 4-24 *Enlargement of Figure close to $\Phi = 0$ with its associated effective reflectances for every ring structure. Inner curve(blue): one ring, centre curve(red): two rings, outer curve(black): three rings*

5 Extension to N-ring resonators

In this chapter we extend our resonator formulation to N rings by using the matrix methodology explained in Chapter 3. Our results in Chapter 4 provide evidence that the filter functions can be improved by increasing the number of rings. Therefore, we suppose that resonators with more than three rings, such as 4, 5, 6 or more, let us obtain yet better performance. Chapter 4 also made clear that the equations for a three-ring resonator are huge. Therefore, in order to calculate more than three rings, a more advanced matrix technique called “diagonal decomposition” is used. The use of matrices is easier because they organize equations in a structured way that can be handled. Furthermore, it is an important issue for us to formulate the transfer function for N rings in general so that we obtain the function for a different number of rings by changing one value, the number of rings.

The “diagonal decomposition” (DD) is used to raise a matrix to a power but there is one slight limitation because it works only for repeated structures, which causes us some design constraints. Specifically, we cannot raise the matrix for one ring to a power, because light propagates clockwise or counter-clockwise, according to the launch point. Instead we have to raise the matrix for a pair of rings to a power, which is more complicated. Moreover, we note that all rings must have the same ring circumferences so that we do the calculation with one ring size, L.

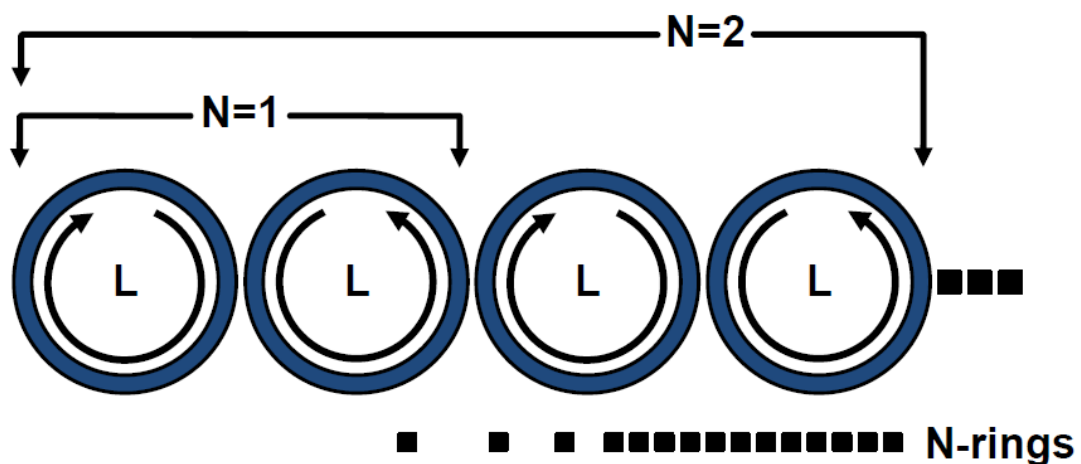


Figure 5-1 Multiple N-ring resonator; the matrices for pair rings are raised to a power, so that we can calculate all even numbers of ring resonators: The ring circumferences and coupling ratios are always the same.

In the following calculations, the effective reflectances of all couplers are identical because the calculations would be much more complicated if they were different. (However, performing the calculation with alternating effective reflectances for the “left” and “right” rings could be an interesting topic for a future project). First of all we define a matrix that states the transfer matrix for a two-ring resonator, the last coupler not included. Therefore, we multiply the Equations (3.5) and (3.7) from Chapter 3. These Equations are for the two different rings, one “right” and one “left”, as we called them in Chapter 2. We multiply these in general terms, which means that the effective reflectance r and transmittance t have no index numbers because the two rings have equal values. Thus we obtain:

$$A = \begin{bmatrix} a_{11} & a_{12} \\ a_{21} & a_{22} \end{bmatrix} = \begin{bmatrix} -\left(\frac{r}{t}\right)^2 + \frac{(t^2 - r^2)^2}{t^2} \cdot e^{2 \cdot \delta} & \left(\frac{r}{t^2}\right) + \frac{r \cdot (t^2 - r^2)}{t^2} \cdot e^{2 \cdot \delta} \\ -\left(\frac{r}{t^2}\right) \cdot e^{-2 \cdot \delta} - \frac{r \cdot (t^2 - r^2)}{t^2} & \left(\frac{1}{t^2}\right) \cdot e^{-2 \cdot \delta} - \left(\frac{r^2}{t^2}\right) \end{bmatrix} \quad (5.1)$$

This 2x2 matrix is called matrix A. As we observe, all terms have a factor of $(1/t^2)$. We also have terms such as $e^{2 \cdot \delta}$, which appear because of the same repeated ring circumferences. Now we factor out $(1/t^2)$ to achieve a simpler matrix B to calculate with which is $B = (t^2) \cdot A$. From Chapter 2, we have this formula for the DD: $A^N = PD^N P^{-1}$. The matrix B^N should be equal to $(t^{2N}) \cdot A^N$. Our goal is to find the matrices P, D^N and P^{-1} which provide, when multiplied together, the same matrix as A^N . First of all, the eigenvalues $\lambda_{1,2}$ of matrix B are to be determined by calculating:

$$|B - \lambda \cdot I| = 0 \quad (5.2)$$

where I is the (2x2) identity matrix. Thus we obtain:

$$\lambda = \frac{1}{2} \cdot \{(t^2 - r^2)^2 \cdot e^{2\cdot\delta} + e^{-2\cdot\delta} - 2 \cdot r^2\}$$

$$\pm \frac{1}{2} \left\{ [(t^2 - r^2)^2 \cdot e^{2\cdot\delta} + e^{-2\cdot\delta} - 2 \cdot r^2]^2 - 4 \cdot t^4 \right\}^{1/2}$$
(5.3)

As we see, two eigenvalues are derived. λ_1 is for the “+” term in Equation (5.3) and λ_2 is for the “-” term. The eigenvalues are unique and correspond to the eigenvectors X_1 and X_2 , respectively. The single steps of the calculation are not shown because the mathematics is very large. The detailed justifications for the general procedure can be obtained in text-books for linear algebra [10,11]. Continuing, we now calculate two valid eigenvectors by using the matrix-vector equation:

$$[B - \lambda \cdot I] \cdot X = 0$$
(5.4)

Considering Equation (5.4), we derive 4 different eigenvectors for 2 different eigenvalues:

$$X^a = \begin{bmatrix} X_1^a \\ X_2^a \end{bmatrix}$$

$$= \begin{bmatrix} [1 - (t^2 - r^2) \cdot e^{2\cdot\delta}] - \left\{ [1 - (t^2 - r^2) \cdot e^{2\cdot\delta}]^2 - 4 \cdot r^2 \cdot e^{2\cdot\delta} \right\}^{1/2} \\ 2 \cdot r \end{bmatrix}$$
(5.5)

$$X^b = \begin{bmatrix} X_1^b \\ X_2^b \end{bmatrix}$$

$$= \begin{bmatrix} [1 - (t^2 - r^2) \cdot e^{2\cdot\delta}] + \left\{ [1 - (t^2 - r^2) \cdot e^{2\cdot\delta}]^2 - 4 \cdot r^2 \cdot e^{2\cdot\delta} \right\}^{1/2} \\ 2 \cdot r \end{bmatrix}$$
(5.6)

These two are the ones that we use to form Matrix P. We did the same calculation in another way, obtaining the Equations (5.7) and (5.8) but Equation (5.7) is linearly dependent on Equation (5.5) just as Equation (5.8) is linearly dependent on Equation (5.6). This is acceptable because eigen-vectors are never unique. Indeed, it is an advantage to us because it allowed us to perform the calculation in two different ways, which gave us confirmation of the validity of our results for quality control purposes.

$$\begin{aligned}
 X^c &= \begin{bmatrix} X_1^c \\ X_2^c \end{bmatrix} \\
 &= \begin{bmatrix} 2 \cdot r \cdot e^{2 \cdot \delta} \\ [1 - (t^2 - r^2) \cdot e^{2 \cdot \delta}] - \left\{ [1 - (t^2 - r^2) \cdot e^{2 \cdot \delta}]^2 - 4 \cdot r^2 \cdot e^{2 \cdot \delta} \right\}^{\frac{1}{2}} \end{bmatrix}
 \end{aligned}
 \tag{5.7}$$

$$\begin{aligned}
 X^d &= \begin{bmatrix} X_1^d \\ X_2^d \end{bmatrix} \\
 &= \begin{bmatrix} 2 \cdot r \cdot e^{2 \cdot \delta} \\ [1 - (t^2 - r^2) \cdot e^{2 \cdot \delta}] + \left\{ [1 - (t^2 - r^2) \cdot e^{2 \cdot \delta}]^2 - 4 \cdot r^2 \cdot e^{2 \cdot \delta} \right\}^{\frac{1}{2}} \end{bmatrix}
 \end{aligned}
 \tag{5.8}$$

Equations (5.5) and (5.6) are linearly independent of each other, which means that no factor can be found that multiplies one of them and gives the other.

The next step is to write down the diagonal matrix D, as described in Chapter 2. Therefore, we need our eigenvalues $\lambda_{1,2}$. The leading diagonal of D is equal to the eigenvalues and it is stated as:

$$D = \begin{bmatrix} \lambda_1 & 0 \\ 0 & \lambda_2 \end{bmatrix}
 \tag{5.9}$$

We further had to choose in each case one of the eigenvectors to set up the P matrix, as described in Chapter 2. We choose X^a and X^b from the Equations (5.5) and (5.6) for our following calculation because they appear to provide the simplest algebra. Every eigenvector is one column vector in the P matrix so we obtain:

$$P = \begin{bmatrix} X_1^a & X_1^b \\ X_2^a & X_2^b \end{bmatrix} \quad (5.10)$$

A very important point to note is that the column vectors that constitute P must be in the same order as the corresponding eigenvalues in D. The inverse of the matrix P is now needed. Therefore, we also have to calculate the determinant of P. We achieve the following equation:

$$P^{-1} = \frac{1}{|P|} \cdot \begin{bmatrix} X_2^d & -X_1^d \\ -X_2^b & X_1^b \end{bmatrix} \quad (5.11)$$

All matrices which give us the matrix B are calculated so that we can multiply the matrices together to derive the matrix equation for $B = PDP^{-1}$. We have to take account for the order in which the matrices are multiplied. First P and D are multiplied and then PD with P^{-1} is multiplied; this is crucial because matrix algebra is non-commutative. During these calculations we defined some variables to simplify the mathematics because we achieved huge matrices.

Due to the fact that we have rather complicated mathematics, we need a quality control. In order to check if the DD method works, we first calculated PDP^{-1} without raising D to a power, which is to be the same as the matrix B. By incorporating the factor $(1/t^{2N})$, we obtain the matrix A (Equation (5.1)), which is the expected matrix for a pair of two rings. Therefore, the diagonal decomposition has been performed correctly.

The matrix B can now be raised to the n^{th} power in the following way:

$$B^N = P \cdot D^N \cdot P^{-1} \quad (5.12)$$

We define a term W to simplify and to reduce the size of the matrices:

$$W = \frac{[1 - (t^2 - r^2) \cdot e^{2 \cdot \delta}]}{\{[1 - (t^2 - r^2) \cdot e^{2 \cdot \delta}]^2 - 4 \cdot r^2 \cdot e^{2 \cdot \delta}\}^{\frac{1}{2}}} \quad (5.13)$$

We express all of the terms in the matrices P and P^{-1} within the terms of W and obtain:

$$P = \begin{bmatrix} [1 - (t^2 - r^2) \cdot e^{2 \cdot \delta}] \cdot \left(\frac{W - 1}{W}\right) & [1 - (t^2 - r^2) \cdot e^{2 \cdot \delta}] \cdot \left(\frac{W + 1}{W}\right) \\ 2 \cdot r & 2 \cdot r \end{bmatrix} \quad (5.14)$$

$$P^{-1} = \frac{1}{2} \cdot \begin{bmatrix} \frac{-W}{[1 - (t^2 - r^2) \cdot e^{2 \cdot \delta}]} & \frac{1}{2 \cdot r} \cdot (W + 1) \\ \frac{W}{[1 - (t^2 - r^2) \cdot e^{2 \cdot \delta}]} & \frac{1}{2 \cdot r} \cdot (-W + 1) \end{bmatrix} \quad (5.15)$$

From now on, the key challenge is raising the diagonal matrix to the power of N . This is done by raising the eigenvalues λ_1 and λ_2 of matrix D , as shown in Equation (5.9), to the power of N . Unfortunately, as Equation (5.3) indicates λ_1 and λ_2 are not simple terms. We factorise the matrix D and also express all the terms as functions of W and so we have:

$$D^N = \frac{(W^2 - 1)^N}{(4 \cdot t^2)^N} \cdot \begin{bmatrix} (W + 1)^N \cdot \left(W + \left(\frac{2 \cdot r^2}{t^2} - 1\right)\right)^N & 0 \\ 0 & (W - 1)^N \cdot \left(W - \left(\frac{2 \cdot r^2}{t^2} - 1\right)\right)^N \end{bmatrix} \quad (5.16)$$

The matrix P is then multiplied by D^N , after which PD^N is multiplied by P^{-1} so that finally have $PD^N P^{-1}$. Now, to calculate the output from the entire ring resonator, we need the matrix $A^N = B^N / (t^2)^N$, as shown earlier in this Chapter, where B is given by $PD^N P^{-1}$. Thus A^N is:

$$A^N = \begin{bmatrix} a_{11} & a_{12} \\ a_{21} & a_{22} \end{bmatrix}^N \quad (5.17)$$

Moreover, the output from the entire N -ring resonator requires a final matrix for the output coupler M_{out} . The coupler we need is a left-handed one because we always have an even number of rings, as described in Chapter 3. Thus we multiply A by M_{out} from Equation (3.15), which is designated as matrix Q :

$$Q = M_{out} \cdot A^N = \left(\frac{1}{t^{2N}} \right) \cdot M_{out} \cdot B^N = \begin{bmatrix} q_{11} & q_{12} \\ q_{21} & q_{22} \end{bmatrix} \quad (5.18)$$

The four q -elements are not stated here because they are too large but the reader is referred to the Appendix for a listing. Now, Matrix Q is the total amplitude transfer matrix. In order to calculate the output of the ring resonator, we need the amplitude transfer terms, which are stated by Equations (3.23) and (3.24) from the two-ring resonator theory of Chapter 3:

$$E_{0,2}^- = \left(\frac{1}{q_{2,2}} \right) \cdot E_{2,4}^- - \left(\frac{q_{2,1}}{q_{2,2}} \right) \cdot E_{0,1}^+ \quad (5.19)$$

$$E_{2,3}^+ = \left(\frac{q_{2,2} \cdot q_{1,1} - q_{1,2} \cdot q_{2,1}}{q_{2,2}} \right) \cdot E_{0,1}^+ + \left(\frac{q_{1,2}}{q_{2,2}} \right) \cdot E_{2,4}^- \quad (5.20)$$

For the q -elements we now use Equation (5.18), the general amplitude matrix. The most important term of these equations is $(q_{22}q_{11} - q_{12}q_{21})/q_{22}$ because it gives the transmitted output, $(E_{2,3}^+ / E_{0,1}^+)$:

$$\left(\frac{E_{out}}{E_{in}}\right) = \left(\frac{E_{2,3}^+}{E_{0,1}^+}\right) = \frac{q_{22} \cdot q_{11} - q_{12} \cdot q_{21}}{q_{22}} \quad (5.21)$$

In most cases, $E_{2,4}^-$ is zero but it could be used as an alternative input (for example, when the multi-ring resonator is used as an optical add-drop multiplexer). In the present context we neglect it and consider it as zero so that we achieve Equation (5.21). $(E_{0,2}^-/E_{0,1}^+)$ can also be calculated but it is not of interest for us because this is the auxiliary output related to the input. In general the q-term $(q_{22}q_{11}-q_{12}q_{21})/q_{22}$ is multiplied by its complex conjugate to achieve intensity formulation for the transmitted output.

Now, we have derived the general amplitude transfer function for N-ring resonators. For example for N=1, 2 and 3 we achieve the amplitude transfer function for 2, 4 and 6 rings, respectively. However, we also want to obtain the intensity transfer function for N-ring resonators. Therefore, we have to multiply Equation (5.21) by its own complex conjugate. It follows from Equations (5.13) – (5.16) that the q-coefficients are huge and the formulation of $(q_{22}q_{11}-q_{12}q_{21})/q_{22}$ is correspondingly large. Owing to the cross-checking and quality control measures we have performed, we are confident in the validity of our results up to Equation (5.21) and those presented in Appendix A. We then proceeded towards the intensity expression by multiplying Equation (5.21) by its own complex conjugate. However, we do not have sufficient faith in their accuracy to report the results that we obtained. The timescale in which to do this part of the work was too short and so the likelihood of mistakes was too high. Nevertheless, we have a positive outcome because our amplitude transfer function is in a format that can be passed on to a future team of students for continuation. The way ahead is a known route, even if it is an arduous one.

6 Conclusion

We reported a design study of compound micro-ring resonators for application as spectral filters in DWDM optical systems. Our approach was theoretical, deriving analytical equations to predict spectral profiles. We started with the complex field equations for the couplers and waveguides, allowing the derivation of the amplitude transfer function of one-ring, two-ring and a three-ring resonator by a matrix method. Our matrices structure the algebra, which is particularly desirable in the case of multiple rings, especially when there are more than three. The equations derived are expressed in terms of ring circumferences, coupling coefficients, waveguide propagation constants and losses.

We have calculated the intensity transfer functions for one-ring, two-ring and three-ring resonators and we have analyzed the resulting spectral profile in detail with a view to obtaining optimised filter performance. For the two-ring resonator we made conditions which are very important for suitability of a filter: There must be no double peaks, every peak reaches unity and all the peaks have the same magnitude. For these condition we require that the ring circumferences be equal. We have also derived a formula for the middle effective reflectance r_1^2 , which we call the “degeneracy condition” where the conditions apply. Furthermore, we have the condition that the outer couplers have to be equal. Then we arrived at a formula for a value for the outer couplers which allow us to choose a pre-determined out-of-band-rejection (in dB). After making our choice of optimised coupler characteristics we achieve a filter profile that is better matched to our application than what is available using a single ring.

We have also studied the influence of loss for fear that it could markedly deteriorate the filter performance. We found the magnitudes of the peaks from an optimised filter design decrease as a result of losses and that is to be expected. However, we keep the single-peak-behaviour, which is very good for application in a DWDM system. Moreover, it does not have a significant influence on the out-of-band rejection between the peaks.

We have investigated the filter profiles of the three-ring resonator. In the absence of optimisation we obtain responses involving triple peaks, even when all

ring circumferences are equal. However, we have derived a three-ring degeneracy condition which enables single-peaked spectra with unity relative intensity. In this way the “box-like” profile that can be obtained is very encouraging. By selecting the effective reflectances by trial and error, we could also provide good modulation depths. We believe that it will be possible to derive an analytical formula for a three-ring resonator’s depth of modulation. We have compared the spectral filter profiles from one-, two- and three-ring resonators that are all optimised and all have the same depth of modulation. Our results show a marked widening of the pass-band with the number of rings. Moreover, the three-ring structure can provide impressively flat tops when the resonance condition is satisfied.

Our encouraging results from the three-ring resonator have prompted a desire to study the transfer function provided by yet larger numbers of rings. Unfortunately, the necessary algebra is likely to become very difficult to handle. Therefore, we have been motivated to find an alternate approach, which is a formula for N identical rings by using “diagonal decomposition”. The method enables with opposite propagation directions. The algebra required is very long but we have derived the amplitude transfer function, which has been the most demanding stage in the process. Thereafter, future workers can provide the intensity expression.

All the transfer functions that we have derived are general and they include loss mechanisms. We have used them to study an optimised two-ring resonator and understood how the performance is affected by loss. The main influence is on the peak height; the spectral profile remains single-peaked and by such behaviour.

The results that we have obtained in this project provide grounds for optimism. We believe that there are many possibilities for future studies. Obvious lines of investigation include a continuation of our study of N -ring structures, possibly ones that alternate in characteristics. They could be rings of identical circumferences but alternating effective reflectances. In this way one could provide yet better “box-like” characteristics. However, there is one other possibility, which we have not had time to explore. If we use rings of alternating circumferences we might be able to suppress some of the resonant orders by what is known as the Vernier effect. The ring circumferences are in the ratio of integers that do not have a common factor (such as

10:9) and in this way we have a number of suppressed resonances, followed by “super-resonances” where all of the constituent rings simultaneously provide a large transmission. The benefit of this strategy is that we can obtain an effective increase in free spectral range without having to use rings so small that they suffer from unacceptable bending loss.

In conclusion, we have studied compound optical resonators consisting of linear arrays of micro-rings, providing a theoretical framework to predict how such devices can be used as demultiplexing filters for DWDM optical communications.

7 Appendix A: Q-Coefficients for the Transfer Matrix

7.1 One-Ring Resonator

In Section 3.2 the amplitude transfer matrix for a single-ring resonator is shown. In order to calculate the intensity transfer function the q-coefficients are needed:

$$q_{11} = -\frac{r_0}{t_0 \cdot t_1} \cdot e^{(-\delta_{1,0})} - \frac{r_1 \cdot (t_0^2 - r_0^2)}{t_0 \cdot t_1} \cdot e^{(\delta_{0,1})}$$

$$q_{12} = +\frac{1}{t_0 \cdot t_1} \cdot e^{(-\delta_{1,0})} - \frac{r_0 \cdot r_1}{t_0 \cdot t_1} \cdot e^{(\delta_{0,1})}$$

$$q_{21} = -\frac{r_0 \cdot r_1}{t_0 \cdot t_1} \cdot e^{(-\delta_{1,0})} + \frac{(t_0^2 - r_0^2) \cdot (t_1^2 - r_1^2)}{t_0 \cdot t_1} \cdot e^{(+\delta_{0,1})}$$

$$q_{22} = +\frac{r_1}{t_0 \cdot t_1} \cdot e^{(-\delta_{1,0})} + \frac{r_0 \cdot (t_1^2 - r_1^2)}{t_0 \cdot t_1} \cdot e^{(\delta_{0,1})}$$

With these q-terms, we now can calculate the amplitude transfer function:

$$\left(\frac{E_{1,4}^+}{E_{0,1}^+} \right) = \left(\frac{q_{12} \cdot q_{21} - q_{22} \cdot q_{11}}{q_{12}} \right) = \frac{t_0 t_1 e^{(\delta_{0,1})}}{1 - r_0 r_1 e^{(\delta_{0,1} + \delta_{1,0})}}$$

7.2 Two-Ring Resonator

In Section 3.3 the amplitude transfer matrix for a two-ring resonator is shown. In order to calculate the intensity transfer function the q-coefficients are needed:

$$\begin{aligned}
 q_{11} = & -\frac{r_0 \cdot r_1 \cdot (t_2^2 - r_2^2)}{t_0 \cdot t_1 \cdot t_2} \cdot e^{(\delta_{1,2} - \delta_{1,0})} \\
 & + \frac{(t_0^2 - r_0^2) \cdot (t_1^2 - r_1^2) \cdot (t_2^2 - r_2^2)}{t_0 \cdot t_1 \cdot t_2} \cdot e^{(\delta_{1,2} + \delta_{0,1})} \\
 & - \frac{r_0 \cdot r_2}{t_0 \cdot t_1 \cdot t_2} \cdot e[-(\delta_{2,1} + \delta_{1,0})] \\
 & - \frac{r_1 \cdot r_2 \cdot (t_0^2 - r_0^2)}{t_0 \cdot t_1 \cdot t_2} \cdot e^{(\delta_{0,1} - \delta_{2,1})}
 \end{aligned}$$

$$\begin{aligned}
 q_{12} = & + \frac{r_1 \cdot (t_2^2 - r_2^2)}{t_0 \cdot t_1 \cdot t_2} \cdot e^{(\delta_{1,2} - \delta_{1,0})} \\
 & + \frac{r_0 \cdot (t_1^2 - r_1^2) \cdot (t_2^2 - r_2^2)}{t_0 \cdot t_1 \cdot t_2} \cdot e^{(\delta_{1,2} + \delta_{0,1})} \\
 & + \frac{r_2}{t_0 \cdot t_1 \cdot t_2} \cdot e[-(\delta_{2,1} + \delta_{1,0})] \\
 & - \frac{r_0 \cdot r_1 \cdot r_2}{t_0 \cdot t_1 \cdot t_2} \cdot e^{(\delta_{0,1} - \delta_{2,1})}
 \end{aligned}$$

$$\begin{aligned}
 q_{21} = & + \frac{r_0 \cdot r_1 \cdot r_2}{t_0 \cdot t_1 \cdot t_2} \cdot e^{(\delta_{1,2} - \delta_{1,0})} \\
 & - \frac{r_2 \cdot (t_0^2 - r_0^2) \cdot (t_1^2 - r_1^2)}{t_0 \cdot t_1 \cdot t_2} \cdot e^{(\delta_{1,2} + \delta_{0,1})} \\
 & - \frac{r_0}{t_0 \cdot t_1 \cdot t_2} \cdot e[-(\delta_{2,1} + \delta_{1,0})]
 \end{aligned}$$

$$\begin{aligned}
 & - \frac{r_1 \cdot (t_0^2 - r_0^2)}{t_0 \cdot t_1 \cdot t_2} \cdot e^{(\delta_{0,1} - \delta_{2,1})} \\
 q_{22} = & - \frac{r_1 \cdot r_2}{t_0 \cdot t_1 \cdot t_2} \cdot e^{(\delta_{1,2} - \delta_{1,0})} \\
 & - \frac{r_0 \cdot r_2 \cdot (t_1^2 - r_1^2)}{t_0 \cdot t_1 \cdot t_2} \cdot e^{(\delta_{1,2} + \delta_{0,1})} \\
 & + \frac{1}{t_0 \cdot t_1 \cdot t_2} \cdot e^{[-(\delta_{2,1} + \delta_{1,0})]} \\
 & - \frac{r_0 \cdot r_1}{t_0 \cdot t_1 \cdot t_2} \cdot e^{(\delta_{0,1} - \delta_{2,1})}
 \end{aligned}$$

With these q-terms, we now can calculate the amplitude transfer function:

$$\begin{aligned}
 \left(\frac{E_{2,3}^+}{E_{0,1}^+} \right) &= \left(\frac{q_{22} \cdot q_{11} - q_{12} \cdot q_{21}}{q_{22}} \right) \\
 &= \frac{t_0 t_1 t_2 e^{(\delta_{0,1} + \delta_{1,2})}}{1 - r_0 r_1 e^{(\delta_{0,1} + \delta_{1,0})} - r_1 r_2 e^{(\delta_{1,2} + \delta_{2,1})} - r_0 r_2 (t_1^2 - r_1^2) e^{(\delta_{0,1} + \delta_{1,0} + \delta_{1,2} + \delta_{2,1})}}
 \end{aligned}$$

7.3 Three-Ring Resonator

In Section 3.3 the amplitude transfer matrix for a three-ring resonator is shown. In order to calculate the intensity transfer function the q-coefficients are needed:

$$\begin{aligned}
 q_{11} = & + \frac{r_0 \cdot r_1 \cdot r_2}{t_0 \cdot t_1 \cdot t_2 \cdot t_3} \cdot e^{(\delta_{1,2} - \delta_{1,0} - \delta_{3,2})} \\
 & - \frac{r_0}{t_0 \cdot t_1 \cdot t_2 \cdot t_3} \cdot e[-(\delta_{1,0} + \delta_{2,1} + \delta_{3,2})] \\
 & - \frac{r_2 \cdot (t_0^2 - r_0^2) \cdot (t_1^2 - r_1^2)}{t_0 \cdot t_1 \cdot t_2 \cdot t_3} \cdot e^{(\delta_{0,1} + \delta_{1,2} - \delta_{3,2})} \\
 & - \frac{r_0 \cdot (t_0^2 - r_0^2)}{t_0 \cdot t_1 \cdot t_2 \cdot t_3} \cdot e[-(\delta_{2,1} + \delta_{3,2} - \delta_{0,1})] \\
 & + \frac{r_0 \cdot r_1 \cdot r_3 \cdot (t_2^2 - r_2^2)}{t_0 \cdot t_1 \cdot t_2 \cdot t_3} \cdot e^{(\delta_{1,2} + \delta_{2,3} - \delta_{1,0})} \\
 & + \frac{r_0 \cdot r_2 \cdot r_3}{t_0 \cdot t_1 \cdot t_2 \cdot t_3} \cdot e^{(\delta_{2,3} - \delta_{2,1} - \delta_{1,0})} \\
 & - \frac{r_3 \cdot (t_0^2 - r_0^2) \cdot (t_1^2 - r_1^2) \cdot (t_2^2 - r_2^2)}{t_0 \cdot t_1 \cdot t_2 \cdot t_3} \cdot e^{(\delta_{0,1} + \delta_{1,2} + \delta_{2,3})} \\
 & + \frac{r_1 \cdot r_2 \cdot r_3 \cdot (t_0^2 - r_0^2)}{t_0 \cdot t_1 \cdot t_2 \cdot t_3} \cdot e^{(\delta_{2,3} - \delta_{2,1} + \delta_{0,1})} \\
 \\
 q_{12} = & - \frac{r_1 \cdot r_2}{t_0 \cdot t_1 \cdot t_2 \cdot t_3} \cdot e^{(\delta_{1,2} - \delta_{1,0} - \delta_{3,2})} \\
 & + \frac{1}{t_0 \cdot t_1 \cdot t_2 \cdot t_3} \cdot e[-(\delta_{1,0} + \delta_{2,1} + \delta_{3,2})] \\
 & - \frac{r_0 \cdot r_2 \cdot (t_1^2 - r_1^2)}{t_0 \cdot t_1 \cdot t_2 \cdot t_3} \cdot e^{(\delta_{0,1} + \delta_{1,2} - \delta_{3,2})}
 \end{aligned}$$

$$\begin{aligned}
 & - \frac{r_0 \cdot r_1}{t_0 \cdot t_1 \cdot t_2 \cdot t_3} \cdot e^{[-(\delta_{2,1} + \delta_{3,2} - \delta_{0,1})]} \\
 & - \frac{r_1 \cdot r_3 \cdot (t_2^2 - r_2^2)}{t_0 \cdot t_1 \cdot t_2 \cdot t_3} \cdot e^{(\delta_{1,2} + \delta_{2,3} - \delta_{1,0})} \\
 & - \frac{r_2 \cdot r_3}{t_0 \cdot t_1 \cdot t_2 \cdot t_3} \cdot e^{(\delta_{2,3} - \delta_{2,1} - \delta_{1,0})} \\
 & - \frac{r_0 \cdot r_3 \cdot (t_1^2 - r_1^2) \cdot (t_2^2 - r_2^2)}{t_0 \cdot t_1 \cdot t_2 \cdot t_3} \cdot e^{(\delta_{0,1} + \delta_{1,2} + \delta_{2,3})} \\
 & + \frac{r_0 \cdot r_1 \cdot r_2 \cdot r_3}{t_0 \cdot t_1 \cdot t_2 \cdot t_3} \cdot e^{(\delta_{2,3} - \delta_{2,1} + \delta_{0,1})} \\
 q_{21} = & + \frac{r_0 \cdot r_1 \cdot r_2 \cdot r_3}{t_0 \cdot t_1 \cdot t_2 \cdot t_3} \cdot e^{(\delta_{1,2} - \delta_{1,0} - \delta_{3,2})} \\
 & - \frac{r_0 \cdot r_3}{t_0 \cdot t_1 \cdot t_2 \cdot t_3} \cdot e^{[-(\delta_{1,0} + \delta_{2,1} + \delta_{3,2})]} \\
 & - \frac{r_2 \cdot r_3 \cdot (t_0^2 - r_0^2) \cdot (t_1^2 - r_1^2)}{t_0 \cdot t_1 \cdot t_2 \cdot t_3} \cdot e^{(\delta_{0,1} + \delta_{1,2} - \delta_{3,2})} \\
 & - \frac{r_1 \cdot r_3 \cdot (t_0^2 - r_0^2)}{t_0 \cdot t_1 \cdot t_2 \cdot t_3} \cdot e^{[-(\delta_{2,1} + \delta_{3,2} - \delta_{0,1})]} \\
 & - \frac{r_0 \cdot r_1 \cdot (t_2^2 - r_2^2) \cdot (t_3^2 - r_3^2)}{t_0 \cdot t_1 \cdot t_2 \cdot t_3} \cdot e^{(\delta_{1,2} + \delta_{2,3} - \delta_{1,0})} \\
 & - \frac{r_0 \cdot r_2 \cdot (t_3^2 - r_3^2)}{t_0 \cdot t_1 \cdot t_2 \cdot t_3} \cdot e^{(\delta_{2,3} - \delta_{2,1} - \delta_{1,0})} \\
 & + \frac{(t_0^2 - r_0^2) \cdot (t_1^2 - r_1^2) \cdot (t_2^2 - r_2^2) \cdot (t_3^2 - r_3^2)}{t_0 \cdot t_1 \cdot t_2 \cdot t_3} \cdot e^{(\delta_{0,1} + \delta_{1,2} + \delta_{2,3})} \\
 & - \frac{r_1 \cdot r_2 \cdot (t_0^2 - r_0^2) \cdot (t_3^2 - r_3^2)}{t_0 \cdot t_1 \cdot t_2 \cdot t_3} \cdot e^{(\delta_{2,3} - \delta_{2,1} + \delta_{0,1})}
 \end{aligned}$$

$$\begin{aligned}
 q_{22} = & - \frac{r_1 \cdot r_2 \cdot r_3}{t_0 \cdot t_1 \cdot t_2 \cdot t_3} \cdot e^{(\delta_{1,2} - \delta_{1,0} - \delta_{3,2})} \\
 & + \frac{r_3}{t_0 \cdot t_1 \cdot t_2 \cdot t_3} \cdot e[-(\delta_{1,0} + \delta_{2,1} + \delta_{3,2})] \\
 & - \frac{r_0 \cdot r_2 \cdot r_3 \cdot (t_1^2 - r_1^2)}{t_0 \cdot t_1 \cdot t_2 \cdot t_3} \cdot e^{(\delta_{0,1} + \delta_{1,2} - \delta_{3,2})} \\
 & - \frac{r_0 \cdot r_1 \cdot r_3}{t_0 \cdot t_1 \cdot t_2 \cdot t_3} \cdot e[-(\delta_{2,1} + \delta_{3,2} - \delta_{0,1})] \\
 & + \frac{r_1 \cdot (t_2^2 - r_2^2) \cdot (t_3^2 - r_3^2)}{t_0 \cdot t_1 \cdot t_2 \cdot t_3} \cdot e^{(\delta_{1,2} + \delta_{2,3} - \delta_{1,0})} \\
 & + \frac{r_2 \cdot (t_3^2 - r_3^2)}{t_0 \cdot t_1 \cdot t_2 \cdot t_3} \cdot e^{(\delta_{2,3} - \delta_{2,1} - \delta_{1,0})} \\
 & + \frac{r_0 \cdot (t_1^2 - r_1^2) \cdot (t_2^2 - r_2^2) \cdot (t_3^2 - r_3^2)}{t_0 \cdot t_1 \cdot t_2 \cdot t_3} \cdot e^{(\delta_{0,1} + \delta_{1,2} + \delta_{2,3})} \\
 & - \frac{r_0 \cdot r_1 \cdot r_2 \cdot (t_3^2 - r_3^2)}{t_0 \cdot t_1 \cdot t_2 \cdot t_3} \cdot e^{(\delta_{2,3} - \delta_{2,1} + \delta_{0,1})}
 \end{aligned}$$

With these q-terms, we now can calculate the amplitude transfer function:

$$\begin{aligned}
 \left(\frac{E_{3,4}^+}{E_{0,1}^+} \right) &= \left(\frac{q_{21} \cdot q_{12} - q_{11} \cdot q_{22}}{q_{12}} \right) \\
 &= \frac{-t_0 t_1 t_2 t_3 e^{(\delta_{0,1} + \delta_{1,2} + \delta_{2,3})}}{D}
 \end{aligned}$$

Where D is the denominator:

$$\begin{aligned}
 D &= 1 - r_0 r_1 \cdot e^{(\delta_{0,1} + \delta_{1,0})} \\
 &\quad - r_1 r_2 \cdot e^{(\delta_{1,2} + \delta_{2,1})}
 \end{aligned}$$

$$\begin{aligned} & - r_2 r_3 \cdot e^{(\delta_{2,3} + \delta_{3,2})} \\ & - r_0 r_2 (t_1^2 - r_1^2) \cdot e^{(\delta_{0,1} + \delta_{1,0} + \delta_{1,2} + \delta_{2,1})} \\ & - r_1 r_3 (t_2^2 - r_2^2) \cdot e^{(\delta_{1,2} + \delta_{2,1} + \delta_{2,3} + \delta_{3,2})} \\ & - r_0 r_1 r_2 r_3 \cdot e^{(\delta_{0,1} + \delta_{1,0} + \delta_{2,3} + \delta_{3,2})} \\ & - r_0 r_3 (t_1^2 - r_1^2)(t_2^2 - r_2^2) \cdot e^{(\delta_{0,1} + \delta_{1,0} + \delta_{1,2} + \delta_{2,1} + \delta_{2,3} + \delta_{3,2})} \end{aligned}$$

7.4 N-Ring Resonator

In Chapter 5 the amplitude transfer matrix for a N-ring resonator is shown. In order to calculate the intensity transfer function the q-coefficients are needed:

$$\begin{aligned}
 q_{11} = & + \frac{(t^2 - r^2)}{t} \cdot \frac{(W^2 - 1)^N}{2 \cdot t^{2N} \cdot (4 \cdot t^2)^N} \\
 & \cdot [(W + 1) \cdot (W - 1)^N \cdot (W - c)^N - (W - 1) \cdot (W + 1)^N \cdot (W + c)^N] \\
 & \cdot \frac{2 \cdot r \cdot \left(\frac{r}{t}\right) \cdot (W^2 - 1)^N \cdot W}{[1 - (t^2 - r^2) \cdot e^{(2 \cdot \delta)}] \cdot 2 \cdot t^{2N} \cdot (4 \cdot t^2)^N} \\
 & \cdot [(W - 1)^N \cdot (W - c)^N - (W + 1)^N \cdot (W + c)^N] \\
 q_{12} = & + \frac{(t^2 - r^2)}{t} \cdot \frac{(W^2 - 1)^{N+1} \cdot [1 - (t^2 - r^2) \cdot e^{(2 \cdot \delta)}]}{4 \cdot r \cdot t^{2N} \cdot W \cdot (4 \cdot t^2)^N} \\
 & \cdot [(W + 1)^N \cdot (W + c)^N - (W - 1)^N \cdot (W - c)^N] \\
 & \cdot \left(\frac{r}{t}\right) \cdot \frac{(W^2 - 1)^N}{2 \cdot t^{2N} \cdot (4 \cdot t^2)^N} \\
 & \cdot [(W + 1)^{N+1} \cdot (W + c)^N - (W - 1)^{N+1} \cdot (W - c)^N] \\
 q_{21} = & - \frac{r \cdot (W^2 - 1)^N}{2 \cdot t^{3N} \cdot (4 \cdot t^2)^N} \\
 & \cdot [(W + 1) \cdot (W - 1)^N \cdot (W - c)^N - (W - 1) \cdot (W + 1)^N \cdot (W + c)^N] \\
 & \cdot \frac{2 \cdot r \cdot (W^2 - 1)^N \cdot W}{[1 - (t^2 - r^2) \cdot e^{(2 \cdot \delta)}] \cdot 2 \cdot t^{3N} \cdot (4 \cdot t^2)^N} \\
 & \cdot [(W - 1)^N \cdot (W - c)^N - (W + 1)^N \cdot (W + c)^N]
 \end{aligned}$$

$$\begin{aligned}
 q_{22} = & - \frac{r \cdot (W^2 - 1)^{N+1} \cdot [1 - (t^2 - r^2) \cdot e^{(2 \cdot \delta)}]}{4 \cdot r \cdot t^{3N} \cdot W \cdot (4 \cdot t^2)^N} \\
 & \cdot [(W + 1)^N \cdot (W + c)^N - (W - 1)^N \cdot (W - c)^N] \\
 & \cdot \frac{(W^2 - 1)^N}{2 \cdot t^{3N} \cdot (4 \cdot t^2)^N} \\
 & \cdot [(W + 1)^{N+1} \cdot (W + c)^N - (W - 1)^{N+1} \cdot (W - c)^N]
 \end{aligned}$$

The following terms are used in these Equations:

$$W = \frac{[1 - (t^2 - r^2) \cdot e^{2 \cdot \delta}]}{\{[1 - (t^2 - r^2) \cdot e^{2 \cdot \delta}]^2 - 4 \cdot r^2 \cdot e^{2 \cdot \delta}\}^{\frac{1}{2}}}$$

$$c = \left(\frac{2 \cdot r^2}{t^2} - 1 \right)$$

These terms give us the coefficients to calculate the amplitude transfer function for an N-ring resonator:

$$\begin{aligned}
 \left(\frac{E_{out}}{E_{in}} \right) &= \left(\frac{E_{2,3}^+}{E_{0,1}^+} \right) = \frac{q_{22} \cdot q_{11} - q_{12} \cdot q_{21}}{q_{22}} \\
 &= \frac{4 \cdot t^2 \cdot (W^2 - 1)^{2N} \cdot (W^2 - c^2)^N \cdot 2 \cdot W}{D}
 \end{aligned}$$

D states the denominator:

$$\begin{aligned}
 D = & (4t^2)^N 2t^{3N} \cdot \{2W(W + 1) - [1 - (t^2 - r^2)e^{(2 \cdot \delta)}](W^2 - 1)\} \\
 & \cdot (W + 1)^N \cdot (W + c)^N \\
 & - (4t^2)^N 2t^{3N} \cdot \{2W(W - 1) - [1 - (t^2 - r^2)e^{(2 \cdot \delta)}](W^2 - 1)\} \\
 & \cdot (W - 1)^N \cdot (W - c)^N
 \end{aligned}$$

8 Appendix B: Derivation of Intensity Transfer Functions

8.1 Two-ring resonator

The amplitude transfer function is given by Equation (3.22):

$$\left(\frac{E_{23}^+}{E_{01}^+}\right) = \left(\frac{q_{22} \cdot q_{11} - q_{12} \cdot q_{21}}{q_{22}}\right) =$$

Substitution of the terms defined in Appendix A gives us

$$\frac{t_0 \cdot t_1 \cdot t_2 \cdot e^{[\delta_{01} + \delta_{12}]}}{1 - r_0 \cdot r_1 \cdot e^{[\delta_{01} + \delta_{10}]} - r_1 \cdot r_2 \cdot e^{[\delta_{12} + \delta_{21}]} - r_0 \cdot (r_1^2 + t_1^2) \cdot r_2 \cdot e^{[\delta_{01} + \delta_{10} + \delta_{12} + \delta_{21}]}}$$

Definitions of terms of the transfer function.

$$\delta_{jk} = -\left(\frac{\alpha}{2} + i\beta\right) \cdot L_{jk} \quad \text{with } j,k = 0,1,2 \text{ and } i = \sqrt{-1}$$

$$\theta_1 = \delta_{01} + \delta_{10}$$

$$\theta_2 = \delta_{12} + \delta_{21}$$

$$R_{01} = r_0 \cdot r_1 \cdot e^{[-\alpha \cdot L_1/2]}$$

$$R_{12} = r_1 \cdot r_2 \cdot e^{[-\alpha \cdot L_2/2]}$$

$$R_{02} = r_0 \cdot (t_1^2 + r_1^2) \cdot r_1 \cdot e^{[-\alpha \cdot (L_1 + L_2)/2]}$$

$$\Phi_1 = \beta \cdot L_1$$

$$\Phi_2 = \beta \cdot L_2$$

$$t_j = iK_j^{1/2} (1 - \gamma_j)^{1/2} \quad \text{with } j = 0,1,2 \text{ and } i = \sqrt{-1}$$

$$\tau_j^2 = -t_j^2$$

We define the denominator as

$$D = 1 - R_{01} \cdot e^{[i\Phi_1]} - R_{12} \cdot e^{[i\Phi_2]} + R_{02} \cdot e^{[i(\Phi_1+\Phi_2)]}$$

The numerator is defined as

$$T = t_0 \cdot t_1 \cdot t_2 \cdot e^{[\delta_{01}+\delta_{12}]}$$

The square of the numerator is

$$|T|^2 = |t_0|^2 \cdot |t_1|^2 \cdot |t_2|^2 \cdot e^{[-\alpha(L_{01}+L_{12})]}$$

When we square the denominator we achieve a large equation which we can group to an equation which consists of a constant term and others that are multiplied by cosine of an angle.

$$\begin{aligned} |D|^2 = & (1 + R_{01}^2 + R_{12}^2 + R_{02}^2) - 2[R_{01} + R_{12}R_{02}] \cdot \cos[\Phi_1] \\ & - 2[R_{12} + R_{01}R_{02}] \cdot \cos[\Phi_2] + 2R_{01}R_{12} \cdot \cos[\Phi_1 - \Phi_2] \\ & + 2R_{02} \cdot \cos[\Phi_1 + \Phi_2] \end{aligned}$$

Now we substitute the cosine terms to obtain $\sin^2[\Phi/2]$ terms.

Note: $\cos[\theta] = 1 - 2 \cdot \sin^2\left[\frac{\theta}{2}\right]$

Thus

$$\begin{aligned} |D|^2 = & (1 + R_{01}^2 + R_{12}^2 + R_{02}^2) - 2R_{01} - 2R_{12}R_{02} - 2R_{12} \\ & - 2R_{01}R_{02} + 2R_{01}R_{12} + 2R_{02} \end{aligned}$$

$$\begin{aligned}
 &+4[R_{01} + R_{12}R_{02}] \cdot \sin^2[\Phi_1/2] \\
 &+4[R_{12} + R_{01}R_{02}] \cdot \sin^2[\Phi_2/2] \\
 &-4R_{01}R_{12} \cdot \sin^2[(\Phi_1 - \Phi_2)/2] \\
 &-4R_{02} \cdot \sin^2[(\Phi_1 + \Phi_2)/2]
 \end{aligned}$$

We factorise the constant terms and obtain the final form for the denominator:

$$\begin{aligned}
 |D|^2 &= (1 - R_{01} - R_{12} + R_{02})^2 \\
 &+4(R_{01} + R_{12} \cdot R_{02}) \cdot \sin^2 \left[\frac{\Phi_1}{2} \right] \\
 &+4(R_{12} + R_{01} \cdot R_{02}) \cdot \sin^2 \left[\frac{\Phi_2}{2} \right] \\
 &-4 \cdot R_{01} \cdot R_{12} \cdot \sin^2 \left[\frac{\Phi_1 - \Phi_2}{2} \right] \\
 &-4 \cdot R_{02} \cdot \sin^2 \left[\frac{\Phi_1 + \Phi_2}{2} \right]
 \end{aligned}$$

8.2 Three-ring resonator

The amplitude transfer function is given by Equation (3.41):

$$\left(\frac{E_{23}^+}{E_{01}^+}\right) = \left(\frac{q_{22} \cdot q_{11} - q_{12} \cdot q_{21}}{q_{22}}\right) = \left(\frac{T}{D}\right)$$

We define the numerator and the denominator of the resulting expression.

$$T = t_0 \cdot t_1 \cdot t_3 \cdot e^{(\delta_{01} + \delta_{12} + \delta_{33})}$$

and

$$\begin{aligned} D = & 1 - r_0 \cdot r_1 \cdot e^{(\delta_{01} + \delta_{10})} - r_1 \cdot r_2 \cdot e^{(\delta_{12} + \delta_{21})} - r_2 \cdot r_3 \cdot e^{(\delta_{23} + \delta_{32})} \\ & - r_0 \cdot r_1 \cdot (t_1^2 - r_1^2) \cdot e^{(\delta_{01} + \delta_{10} + \delta_{12} + \delta_{21})} \\ & - r_1 \cdot r_3 \cdot (t_2^2 - r_2^2) \cdot e^{(\delta_{12} + \delta_{21} + \delta_{23} + \delta_{32})} \\ & - r_0 \cdot r_3 \cdot (t_1^2 - r_1^2) \cdot (t_2^2 - r_2^2) \cdot e^{(\delta_{01} + \delta_{10} + \delta_{12} + \delta_{21} + \delta_{23} + \delta_{32})} \\ & + r_0 \cdot r_1 \cdot r_2 \cdot r_3 \cdot e^{(\delta_{01} + \delta_{10} + \delta_{23} + \delta_{32})} \end{aligned}$$

where

$$\delta_{jk} = -\left(\frac{\alpha}{2} + i\beta\right) \cdot L_{jk} \quad \text{with } j, k = 0, 1, 2, 3 \text{ and } i = \sqrt{-1}$$

$$\theta_1 = \delta_{01} + \delta_{10}$$

$$\theta_2 = \delta_{12} + \delta_{21}$$

$$\theta_3 = \delta_{23} + \delta_{32}$$

$$R_{01} = r_0 \cdot r_1 \cdot e^{(-\alpha \cdot L_1/2)}$$

$$R_{12} = r_1 \cdot r_2 \cdot e^{(-\alpha \cdot L_2/2)}$$

$$R_{23} = r_2 \cdot r_3 \cdot e^{(-\alpha \cdot L_3/2)}$$

$$R_{02} = r_0 \cdot (t_1^2 + r_1^2) \cdot r_1 \cdot e^{(-\alpha \cdot (L_1+L_2)/2)}$$

$$R_{13} = r_1 \cdot (t_2^2 + r_2^2) \cdot r_3 \cdot e^{(-\alpha \cdot (L_1+L_3)/2)}$$

$$R_{03} = r_0 \cdot (t_1^2 + r_1^2) \cdot (t_2^2 + r_2^2) \cdot r_3 \cdot e^{(-\alpha \cdot (L_1+L_2+L_3)/2)}$$

$$\Phi_1 = \beta \cdot L_1$$

$$\Phi_2 = \beta \cdot L_2$$

$$\Phi_3 = \beta \cdot L_3$$

$$t_j = iK_j^{1/2} (1 - \gamma_j)^{1/2} \text{ with } j = 0,1,2,3 \text{ and } i = \sqrt{-1}$$

$$\tau_j^2 = -t_j^2$$

When we multiply the quotient (T/D) by its own complex conjugate, we obtain the intensity transfer function of a three resonator by using the same methodology as in Section 8.1, which gives us large equations for the denominator. The intensity transfer function is then given by the numerator which is

$$|T|^2 = t_0^2 \cdot t_1^2 \cdot t_2^2 \cdot t_3^2$$

And the denominator is

$$|D|^2 = [1 - R_{01} - R_{12} - R_{23} + R_{02} + R_{13} - R_{03} + R_{01} \cdot R_{23}]^2$$

$$+ 4 \cdot [R_{01}(1 + R_{23}^2) + R_{12} \cdot R_{02} + R_{13} \cdot R_{03}] \cdot \sin^2 \left[\frac{\Phi_1}{2} \right]$$

$$+ 4 \cdot [R_{12} + R_{01} \cdot R_{02} + R_{23} \cdot R_{13} + R_{01} \cdot R_{23} \cdot R_{03}] \cdot \sin^2 \left[\frac{\Phi_2}{2} \right]$$

$$+ 4 \cdot [R_{23}(1 + R_{01}^2) + R_{12} \cdot R_{13} + R_{02} \cdot R_{03}] \cdot \sin^2 \left[\frac{\Phi_3}{2} \right]$$

$$\begin{aligned}
 & -4 \cdot [R_{02} + R_{23} \cdot R_{03}] \cdot \sin^2 \left[\frac{(\Phi_1 + \Phi_2)}{2} \right] \\
 & -4 \cdot [R_{13} + R_{01} \cdot R_{03}] \cdot \sin^2 \left[\frac{(\Phi_2 - \Phi_3)}{2} \right] \\
 & -4 \cdot [R_{01} \cdot R_{23} + R_{12} \cdot R_{03}] \cdot \sin^2 \left[\frac{(\Phi_1 + \Phi_3)}{2} \right] \\
 & -4 \cdot R_{01} \cdot [R_{12} + R_{23} \cdot R_{13}] \cdot \sin^2 \left[\frac{(\Phi_1 - \Phi_2)}{2} \right] \\
 & -4 \cdot R_{23} \cdot [R_{12} + R_{01} \cdot R_{02}] \cdot \sin^2 \left[\frac{(\Phi_2 - \Phi_3)}{2} \right] \\
 & -4 \cdot [R_{01} \cdot R_{23} + R_{02} \cdot R_{13}] \cdot \sin^2 \left[\frac{(\Phi_1 - \Phi_3)}{2} \right] \\
 & +4 \cdot [R_{23} \cdot R_{02}] \cdot \sin^2 \left[\frac{(\Phi_1 + \Phi_2 - \Phi_3)}{2} \right] \\
 & +4 \cdot [R_{01} \cdot R_{13}] \cdot \sin^2 \left[\frac{(-\Phi_1 + \Phi_2 + \Phi_3)}{2} \right] \\
 & +4 \cdot [R_{01} \cdot R_{12} \cdot R_{23}] \cdot \sin^2 \left[\frac{(\Phi_1 - \Phi_2 + \Phi_3)}{2} \right] \\
 & +4 \cdot R_{03} \cdot \sin^2 \left[\frac{(\Phi_1 + \Phi_2 + \Phi_3)}{2} \right]
 \end{aligned}$$

List of References

- [1] P. Urquhart, "Passive Components for Optical Communications", Lecture slides, Universidad Pública de Navarra, Pamplona, Spain, (2009)
- [2] P. Urquhart, "Compound Optical-Fiber-Based Resonators", Journal of the Optical Society of America –A, Vol. 5, (06), 803-812, (1988)
- [3] J. Zhang, J. W. Y. Lit, "Compound Fiber Ring Resonator: Theory", Journal of the Optical Society of America -A, Vol.11, (06), 1867-1873, (1994)
- [4] P. Urquhart, "Optical Fiber Transmission", 3rd Edition, Vol.2, G.Hill(Editor), Focal Press, (2009)
- [5] P. Urquhart, C. Millar, M. Brierley, "Fiber Fox-Smith Resonators: Application to Single-Longitudinal-Mode Operation of Fiber Lasers", Journal of the Optical Society of America –A, Vol.5, (08), 1339-1346, (1988)
- [6] H. van de Stadt, J. M. Muller, "Multimirror Fabry-Perot Interferometers", Journal of the Optical Society of America -A, Vol.02, (08), 1363-1370, (1985)
- [7] ITU-T Recommendation G.694.1, "Spectral Grids for WDM Applications: DWDM Frequency Grid"
- [8] K. Murota, Y. Kanno, M. Kojima, S. Kojima, "A Numerical Algorithm for Block-Diagonal Decomposition of Matrix - Algebras, Part I: Proposed Approach and Application to Semidefinite Programming"
- [9] T. Maehara, K. Murota, "A Numerical Algorithm for Block-Diagonal Decomposition of Matrix - Algebra, Part II: General Algorithm"
- [10] W. K. Nicholson, "Linear Algebra with Applications", 3rd Edition, PWS Publishing Company, Boston, (1990)
- [11] A. M. Tropper, "Linear Algebra", 4th Edition, Thomas Nelson and Sons, London, (1975)
- [12] G.P. Agrawal, "Nonlinear Fiber Optics", 3rd Edition, Academic Press, see Chapter 10, (2001)